

**Synergism of IL10R and TLR9 signaling affects
gene expression, proliferation and metabolism in B cells:**

**A comparative study of STAT3/NF- κ B
and c-Myc mediated effects**



Doctoral Thesis

In partial fulfillment of the requirements for the degree
“Doctor rerum naturalium (Dr. rer. nat.)“
in the Molecular Medicine Study Program
at the Georg-August University Göttingen

submitted by Maren Feist
born in Salzgitter-Bad

Göttingen, 2016

Members of the thesis committee

Supervisor

Name: Prof. Dr. Dieter Kube
 Institute: University Medical Center Göttingen
 Clinic for Hematology and Medical Oncology
 Robert-Koch-Straße 40
 37099 Göttingen
 Email: d.kube@med.uni-goettingen.de

Second member of thesis committee

Name: Prof. Dr. Detlef Doennecke
 Institute: University Medical Center Göttingen
 Department of Molecular Biology
 Humboldtallee 23
 37073 Göttingen
 Email: ddoenec@gwdg.de

Third member of thesis committee

Name Prof. Dr. Jörg Großhans
 Institute: University Medical Center Göttingen
 Institute of Developmental Biochemistry
 Justus-von-Liebig Weg 11
 37077 Göttingen
 Email: joerg.grosshans@med.uni-goettingen.de

Date of Disputation:

Affidavit

By this I declare that I independently authored the presented thesis:

“Synergism of IL10R and TLR9 signaling affects gene expression, proliferation and metabolism in B cells: A comparative study of STAT3/NF- κ B and c-Myc mediated effects“

and that I did not use other auxiliary means than indicated. Paragraphs that are taken from other publications, by wording or by sense, are marked in every case with a specification of the literary source.

Furthermore, I declare that I carried out the scientific experiments following the principles of Good Scientific Practice according to the valid “Richtlinien der Georg-August-Universität Göttingen zur Sicherung guter wissenschaftlicher Praxis“.

Maren Feist

Göttingen,

List of publications

EHRENTRAUT S., SCHNEIDER B., NAGEL S., POMMERENKE C., QUENTMEIER H., GEFERS R., FEIST M., KAUFMANN M., MEYER C., KADIN M. E., DREXLER H. G., MACLEOD R.A.F. 2016. Th17 cytokine differentiation and loss of plasticity after SOCS1 inactivation in a cutaneous T-cell lymphoma. *Oncotarget*.

SCHRADER A., MEYER K., WALTHER N., STOLZ A., FEIST M., HAND E., VON BONIN F., EVER M., KOHLER C., SHIRNESHAN K., VOCKERODT M., KLAPPER W., SZCZEPANOWSKI M., MURRAY P.G., BASTIANS H., TRÜMPER L., SPANG R., KUBE D.. 2016. Identification of a new gene regulatory circuit involving B cell receptor activated signaling using a combined analysis of experimental, clinical and global gene expression data. *Oncotarget*.

FEIST M., KEMPER J., TARUTTIS F., REHBERG T. , ENGELMANN J. C., GRONWALD W., HUMMEL M., SPANG R., KUBE D. . 2016. Synergy of Interleukin 10 and Toll-like receptor 9 signaling in B cell proliferation: implications for lymphoma pathogenesis. *International Journal of Cancer: in revision*.

SCHWARZFISCHER P., REINDERS J., DETTMER K., KLEO K., DIMITROVA L., HUMMEL M., FEIST M., KUBE D., SZCZEPANOWSKI M., KLAPPER W., TARUTTIS F., ENGELMANN J., SPANG R., GRONWALD W., OEFNER P. J.. 2016. Comprehensive metabolomics of Burkitt and diffuse large B-cell lymphoma cell lines and primary tumor tissues. *Journal of Proteome Research: in revision*.

TARUTTIS F., FEIST M., SCHWARZFISCHER P., GRONWALD W., KUBE D., SPANG R., ENGELMANN J. C.. 2016. Whole cell spike-ins calibrate RNA-seq and qPCR data to an external reference point and uncover unbalanced gene expression changes. *Submitted*.

FEIST M., SCHWARZFISCHER P., HEINRICH P., TARUTTIS F., PEREZ-RUBIO P., ENGELMANN J. C., KEMPER J., DUDEK J., SPANG R., HUMMEL M., DETTMER-WILDE K., GRONWALD W., KUBE D.. 2016. Metabolic shifts toward glutamine in lymphoma: context dependent expression of GOT2 and use of metabolic derivatives. *In preparation*.

Contents

List of publication	III
Acknowledgment	VII
Abstract	VIII
List of tables	IX
List of figures	XI
Nomenclature	1
1 Introduction	1
1.1 Germinal centers: sites of mature B cell activation and transformation	1
1.1.1 Germinal centers and mature B cell activation	1
1.1.2 Germinal centers and B cell transformation	2
1.2 Signaling pathways involved in normal and aberrant B cell activation	3
1.2.1 Canonical and non-canonical NF- κ B signaling	4
1.2.2 JAK/STAT signaling	6
1.2.3 PI3K/MAPK signaling	7
1.2.4 The proto-oncogene c-Myc	8
1.2.5 Myc as a global gene amplifier	8
1.2.6 Cooperation of signaling pathways	9
1.3 Regulation of cell cycle and metabolism	10
1.3.1 Cell cycle regulation	10
1.3.2 Metabolic regulation	11
1.4 Aim of the study	13
2 Material and Methods	14
2.1 Material, recipes and equipment	14
2.1.1 Biological material	14
2.1.2 Chemicals and consumable supplies	14
2.1.3 Buffers, solutions and media	16
2.1.4 Equipment	20
2.1.5 Cell culture supplements, inhibitors and siRNA	21
2.1.6 Antibodies	23
2.1.7 Oligonucleotides	25
2.1.8 Ready to use reaction systems	25
2.1.9 Software	26
2.2 Cell biology	26
2.2.1 Cell culture techniques	26
2.2.2 Respiratory analysis	29
2.2.3 Flow cytometry	31
	IV

2.3	Protein biochemistry	32
2.3.1	Preparation of lysates	32
2.3.2	SDS-PAGE	32
2.3.3	Immunoblotting	33
2.4	Molecular Biology	33
2.4.1	Spike-in for transcriptomic data	33
2.4.2	RNA Isolation	33
2.4.3	Reverse Transcription	34
2.4.4	qRT-PCR (quantitative Reverse-Transcriptase-Polymerase Chain Reaction)	34
2.4.5	RNA Sequencing	35
2.4.6	Chromatin Immunoprecipitation	36
2.5	Metabolomics	37
2.5.1	Sample preparation	37
2.5.2	NMR spectrometry	38
2.5.3	Mass spectrometry	38
2.6	Statistical and bioinformatic analyses	38
3	Results	40
3.1	A resting B cell model by Myc withdrawal in P493-6 cells	40
3.1.1	Simulating resting B cells by Myc withdrawal in P493-6	41
3.1.2	Factors of the B cell microenvironment activate P493-6 Myc ^{low} cells	41
3.2	Development of a cell spike-in to reveal global gene expression changes	43
3.2.1	<i>Drosophila melanogaster</i> is a suitable spike-in organism	43
3.2.2	<i>Drosophila</i> spike-in reliably detects global gene expression changes	44
3.2.3	Proof of principle: Spike-in cells reveal Myc induced global amplification	46
3.3	Analysis of combinatorial stimulation effects in Myc ^{low} cells	48
3.3.1	Stimuli combinations induce cooperative changes in Myc ^{low} cells	48
3.3.2	Stimulation induced cell cycle entry correlates with metabolic changes	50
3.3.3	S-phase entry of Myc ^{low} cells is mainly driven by combined IL10 and CpG stimulation	51
3.4	Comparison of IL10+CpG and Myc induced gene expression	52
3.5	Investigation of IL10R and TLR9 activation in B cell proliferation	56
3.5.1	Combined IL10 and CpG stimulation induces cell doubling in Myc ^{low} cells	56
3.5.2	IL10+CpG stimulation induces G1/S-phase entry in Myc ^{low} cells	57
3.5.3	Synergistic upregulation of G1/S cell cycle regulators in IL10+CpG stimulated cells	58
3.5.4	Synergistic effect of IL10+CpG stimulation on proliferation is Myc independent	60
3.5.5	IL10+CpG stimulation induced proliferation is NF-κB and STAT3 dependent	61
3.5.6	IL10 and CpG do not influence each other's STAT3 and p65 activation	63
3.5.7	STAT3 and NF-κB directly bind to the <i>CDK4</i> promoter	65
3.6	Effects of IL10R and TLR9 signaling on cell metabolism	67
3.6.1	IL10+CpG stimulation synergistically induces expression of metabolic genes	67

3.6.2	Proliferation of IL10+CpG stimulated Myc ^{low} and Myc ^{high} cells is strictly glutamine dependent	68
3.6.3	Glutamine is incorporated into TCA intermediates and amino acids	70
3.6.4	Myc ^{high} but not IL10+CpG stimulated cells use glutamine for aerobic respiration	72
3.6.5	Glutamine derived aKG is important for proliferation of Myc ^{high} cells	74
3.6.6	Proliferation of IL10+CpG stimulated Myc ^{low} cells depends on aspartate and nucleotides synthesis	75
3.6.7	GOT2 is important for aspartate and nucleotide synthesis in IL10+CpG stimulated Myc ^{low} cells	78
3.6.8	<i>GOT2</i> is a target of Myc and STAT3/NF-κB	79
3.7	Comparison of glutamine metabolism in lymphoma cell lines	81
3.7.1	B cell lymphoma cell lines dependent on different signaling pathways	81
3.7.2	Differential usage of GOT2 derived metabolites in B cell lymphoma cell lines	82
3.7.3	<i>GOT2</i> expression is upregulated in Burkitt and ABC DLBCL patients	84
3.7.4	High <i>GOT2</i> expression is a negative prognostic factor in DLBCL	86
4	Discussion	87
4.1	Global gene expression amplification is not limited to <i>MYC</i> overexpression	87
4.2	Synergy in gene expression changes by STAT3 and NF-κB pathway activity	88
4.2.1	Simultaneous binding of STAT3 and NF-κB to target gene promoters	88
4.2.2	Supposed gene regulatory mechanisms of STAT3 and NF-κB	90
4.3	Effects of gene expression changes on proliferation and metabolism	91
4.3.1	Overexpression of G1/S cell cycle regulator genes induces proliferation	91
4.3.2	Increased gene expression of glutaminolysis enzymes supports transformation processes	91
4.4	Different glutamine usage in B cell lymphoma	92
4.4.1	Using glutamine as a energetic fuel	92
4.4.2	The role of glutamine in aspartate and nucleotide synthesis	94
4.5	IL10R and TLR9 signaling in B cell lymphoma development and progression	95
4.5.1	The role of IL10 and CpG in B cell lymphoma	96
4.5.2	STAT3 and NF-κB are important factors in B cell lymphoma pathogenesis	96
5	Summary and conclusion	98
6	References	100
7	Appendix	114
8	Curriculum Vitae	120

Acknowledgment

First of all, I would like to thank Prof. Dieter Kube for supervising and supporting me during this thesis project. He always encouraged me to develop my own project ideas and find solutions for the problems I faced. I'm very thankful for the hours we spent discussing and his notes during writing this thesis and other manuscripts.

In addition, I am very thankful to Prof. Lorenz Trümper for the opportunity to accomplish this thesis in his department.

Furthermore, I would like to thank Prof. Detlef Doennecke und Prof. Jörg Großhans for their helpful comments and discussions during the thesis committee meetings.

I'm very grateful for the support of our cooperation partners from the MycSys consortium. My special thanks goes to Franziska Taruttis, Philipp Schwarzfischer and Paul Heinrich for the good cooperating work and friendly discussions during this project. I would also like to thank Julia Engelmann, Thorsten Rehberg and Paula Perez-Rubio for their bioinformatical and statistical support. I like to express my gratitude to Rainer Spang, Wolfram Gronwald, Katja Dettmer and Michael Hummel for the hours we spent discussing the design of this project and the expertise they shared. Thanks also to Jan Dudek for introducing me to the Seahorse measurements and cellular respiration.

I would like to thank Frederike von Bonin and Susanne Hengst for performing qRT or immunoblots for me whenever I was too busy to do them on my own. Special thanks to Susanne for being a good listener and proving that shakings hands aren't a major problem in the lab.

Naturally, deep thanks to my current and former colleagues who spent with me a lot of time working, laughing but also crying. I like to thank Elisabeth Hand, Juliane Lippert and Christina Stadler for the short time we spent together. Thanks to Sonja Eberth and Natalie Freytag who left the lab too early, but always tried to stay in contact. My special gratitude goes to Judith Kemper for not only doing a lot of knockdown experiments but also finding the time for joking (and dancing) with me. Last of all, a special thanks to Franziska Linke, Annekatrin Arlt and Isabel Rausch for enduring my varying moods during the last time and their helpful comments during the writing of this thesis. I'm sorry that I did not find the time to spent more coffee breaks with you. Of course, I would like to thank my friends and family for their patience and support during this thesis. It was not always easy to be neither at one place nor the other, but you all were very understanding and gave me a fixed place to come home for. Thanks to my dear friend Juliane Hobusch for the hours at the telephone discussing general Ph.D. student problems and her friendly comments on this thesis. I'm also very gratitude for my brother, sharing his little family with me and distracting me when it was necessary.

Last of all, I would dedicate this thesis to my parents and my husband, equally. The first taught me all I needed to become the person I am and ever since encouraged and support me in everything I do. Where my parents helped me shaping the past, my husband was always helping me to create the future with all he had to give. Thank you for all your love and trust in me!

Abstract

The interplay of different signaling pathways activated by factors of the cellular environment and expression of the proto-oncogene *c-Myc* (*MYC*) defines B cell fate in the germinal center (GC). Importantly, the same signaling networks are chronically active in different types of B-cell lymphoma. While the effects of aberrantly expressed *MYC* on cell proliferation and metabolism were intensively studied, less is known about the cross talk of pathways, like NF- κ B and JAK/STAT signaling, in the context of B cell proliferation and metabolic reprogramming. Therefore, the aim of the study was to analyze (i) how chronic active factors of the GC microenvironment and their interaction networks can reprogram global gene expression (gGE) and metabolism of resting B cells to support B cell proliferation, (ii) what is common with *MYC* overexpression and (iii) whether this is important for lymphoma. Thus the P493-6 B cell line, carrying a conditional *MYC* expression construct, was stimulated with random combinations of GC derived factors as α -IgM, CD40L, IGF1, CpG and IL10 to model different signaling pathway and Myc activation on the same genetic background. Linear regression analysis of gGE and metabolome changes in stimulated Myc depleted cells revealed qualitative similar but quantitative different changes on these parameters by the different stimulations. Thereby, greatest changes were observed after IL10+CpG stimulation due to a strong synergy on gGE and metabolome associated with sustained cell cycle entry and cell proliferation. Using small molecule inhibitors and RNAi mediated knockdown a dependency of IL10+CpG induced proliferation on NF- κ B and JAK/STAT3 signaling was revealed. Furthermore, simultaneous binding of STAT3 and p65 to proximal promoter of the cell cycle regulator *CDK4* but also the aspartate amino transaminase *GOT2* was detected by chromatin immunoprecipitation. The increase in gGE mediated by IL10+CpG stimulation resembled Myc induced gene expression changes accompanied by a comparable cell proliferation but different glutamine metabolism. Herein, *GOT2* was essential for cell proliferation of both conditions. However, glutamine tracing, respiration analysis and rescue experiments revealed distinct dependencies of proliferation on glutamine derived metabolites: In IL10+CpG treated cells a strong dependency of cell proliferation on glutamine derived aspartate and nucleotides was observed, whereas in *MYC* overexpressing cells α -ketoglutarate was most important for respiration and proliferation. Using CA-46, OCI-LY3 and L-428 lymphoma cell lines the important role of *GOT2* for Myc and STAT3/NF- κ B dependent proliferation but also the differences in glutamine usage in context of these pathways could be confirmed. Last of all, a high expression of *GOT2* in proliferating centroblasts but also primary B cell lymphoma could be shown. Thereby, activated B cell like diffuse large B cell lymphoma (DLBCL) were characterized by higher *GOT2* expression as germinal center like DLBCL. More importantly high *GOT2* expression was associated with a worse clinical outcome of R-CHOP treated DLBCL patients. Overall, a new role for IL10R and TLR9 signaling and the interaction of STAT3 and NF- κ B signaling in gGE, proliferation and metabolism of B cells was identified that might also be important for lymphomagenesis.

List of Tables

1	Cell lines	14
2	Chemicals	14
3	Consumables	16
4	Ready to use solutions/buffers	16
5	Buffer recipes	17
6	Media	19
7	Equipment	20
8	Stimulants	21
9	Metabolites	21
10	Inhibitors used in cell culture	22
11	Inhibitors used for respiratory analysis	22
12	siRNA	22
13	ChIP antibodies	23
14	Flow cytometry antibodies	23
15	Immunoblot antibodies	24
16	Oligonucleotides used for qRT PCR	25
17	Oligonucleotides used for ChIP analysis	25
18	Reaction Systems	25
20	Cell line specific transfection parameters	27
19	Matrix of stimuli combinations used for linear regression experiments	28
21	Injection order for measuring respiratory parameters	30
22	Injection order for measuring glutamine dependency	30
23	Mix and measuring cycle times for XF assay	30
24	cDNA master mix	34
25	cDNA cyler program	34
26	qRT PCR cycle program	34
27	Gene Set Enrichment in KEGG Pathways of only IL10+CpG stimulation regulated genes.	114
28	Gene Set Enrichment in KEGG Pathways of only Myc regulated genes.	114
29	Gene Set Enrichment in KEGG Pathways of IL10+CpG stimulation and Myc regulated genes.	115
30	Linear regression coefficients of stimuli and stimuli interactions on number of cells in S-phase	117
31	Distribution of cell cycle phases in BrdU labeled cells over time	117
32	Linear regression analysis of cell cycle regulator gene expression	118

List of Figures

1	Scheme of main signaling nodes activated by a set of microenvironmental factors . . .	5
2	Schematic presentation of selected metabolic pathways affected by high <i>MYC</i> expression.	12
3	Calculation of respiratory parameters	30
4	BrdU gating scheme	31
5	Validation of conditional <i>MYC</i> expression, proliferation and growth in P493-6 cells .	41
6	P493-6 <i>Myc</i> ^{low} cells respond to stimulation with single B cell activating factors . . .	42
7	Experimental design of drosophila spike-in experiment	45
8	Gene expression normalization on drosophila spike-in reveals true fold changes . . .	46
9	Normalization on drosophila spike-in reveals global gene up-regulation in <i>Myc</i> ^{high} cells	47
10	Linear regression analysis reveals cooperative effects of stimuli.	49
11	Extracellular turnover of metabolites correlates with cellular replication	50
12	Intracellular metabolites differentially correlate to cellular replication rates	51
13	IL10+CpG stimulation synergistically induce S-phase entry in <i>Myc</i> ^{low} cells	52
14	Comparison of IL10, CpG, IL10+CpG stimulation and <i>Myc</i> induced gene expression.	53
15	Comparison and functional annotation of IL10+CpG stimulation and <i>Myc</i> induced gene expression	55
16	IL10+CpG stimulation induces proliferation in <i>Myc</i> ^{low} cells comparable to <i>MYC</i> overexpression	56
17	IL10+CpG stimulation increases S-phase entry compared to single stimulations in <i>Myc</i> ^{low} cells.	57
18	IL10+CpG stimulation synergistically increases G1/S regulator gene expression . . .	58
19	IL10+CpG stimulation and <i>Myc</i> mediated proliferation is dependent on CDK4/6 activity	59
20	Endogenous <i>Myc</i> induction is dispensable for IL10+CpG stimulation induced proliferation	60
21	IL10+CpG stimulation synchronously activates STAT3 and NF-κB signaling	61
22	IL10+CpG stimulation mediated proliferation is NF-κB and JAK/STAT dependent	62
23	<i>CDK4</i> expression is STAT3 and p65/RELA dependent	63
24	Comparable time course of STAT3 and NF-κB activation after single and combined stimulation in <i>Myc</i> ^{low} cells	64
25	STAT3 and p65 bind to the proximal promoter of <i>CDK4</i>	66
26	Synergistic upregulation of metabolic genes in IL10+CpG stimulated <i>Myc</i> ^{low} cells . .	68
27	Increased glutamine consumption is important for proliferation of IL10+CpG stimulated <i>Myc</i> ^{low} and <i>Myc</i> ^{high} cells	69
28	IL10+CpG stimulation and <i>Myc</i> induced proliferation is dependent on GLS	70
29	IL10+CpG stimulation and <i>MYC</i> overexpression are associated with an increase of glutamine incorporation into TCA intermediates and amino acids.	71
30	More citrate is oxidatively derived from glutamine in <i>Myc</i> ^{high} cells	72
31	Acidification and respiration of <i>Myc</i> ^{high} but not IL10+CpG stimulated cells is glutamine dependent	73
32	Respiration of <i>Myc</i> ^{high} cells is dependent on glutaminolysis	74
33	Proliferation of <i>Myc</i> ^{high} cells but not IL10+CpG stimulated cells is aKG dependent .	75
34	IL10+CpG stimulation induced proliferation is dependent on glutamine derived aspartate	76
35	IL10+CpG stimulation induced proliferation depends on glutamine derived nucleotides	77
36	IL10+CpG stimulation induced proliferation is dependent on GOT2	79
37	<i>GOT2</i> expression is directly regulated by STAT3 and NF-κB	80
38	Proliferation of B cell lymphoma cell lines relies on different pathway activations . .	82
39	Proliferation of B cell lymphoma cell lines is glutamine dependent	83

40	Proliferation of lymphoma cells is amino transaminase dependent	83
41	Pathway dependent usage of GOT2 derived metabolites in lymphoma cells	84
42	High expression of <i>GOT2</i> in BL and ABC DLBCL patients	85
43	High <i>GOT2</i> expression is associated with decreased survival rates DLBCL patients .	86
44	Scheme of STAT3 and NF- κ B binding to target gene promoters.	89
45	Supposed metabolism in STAT3/NF- κ B and Myc mediated proliferation	93

1 Introduction

Normal and transformed germinal center (GC) B cells are embedded within a complex network of surrounding cells. The corresponding autocrine and paracrine signals are defining B cell fate as proliferation, growth, maturation or cell death. The pathways activated by these signals, when switched from acute or temporary to chronic or aberrant activation, are an important part in the transformation process from GC B cells to lymphoma cells (Rui *et al.*, 2011). Thereby cells must undergo gene expression changes to overcome cell cycle arrest and reprogram metabolism to induce sustained proliferation. These changes are so far best studied in the case of overexpression of the proto-oncogene *c-Myc* (*MYC*). However, less is known about gene expression changes mediated by other signaling pathways and the connections between proliferation and metabolism are not well characterized in B cells. Studying the effects and underlying mechanisms of signaling pathways and transcription factors on gene expression, proliferation and metabolism can therefore improve our understanding of B cell activation and lymphomagenesis and help to reveal new therapeutic targets in lymphoma with deregulated signaling. The following chapters will introduce the GC in context of B cell activation and lymphomagenesis and will focus on the signaling pathways involved in both processes. Gene expression changes that are needed to induce proliferation in B cells in general will be given on the example of *Myc* activation and new aspects of gene regulation by *Myc* will be presented.

1.1 Germinal centers: sites of mature B cell activation and transformation

B cells are immune cells of the adaptive defense that mature inside the bone marrow (LeBien & Tedder, 2008). After selection for a functional but non-selfreactive B cell receptor (BCR) they are released to the blood stream and migrate into the peripheral lymphoid organs like lymph nodes, tonsils, spleen and Peyer's patches. The function of mature B cells is to recognize foreign antigens by binding to different receptors, like the BCR or toll-like receptors (TLR). After activation by these antigens, B cell proliferation and interaction with other immune cells induces formation of a typical structure inside the peripheral lymphoid organs called germinal center (GC) (Klein & Dalla-Favera, 2008; Natkunam, 2007).

1.1.1 Germinal centers and mature B cell activation

There are two different antigens that can activate B cells: T cell independent (TI) and T cell dependent (TD) antigens (Maddaly *et al.*, 2010). TI antigens do not require direct contact with T cells or activation of the BCR (Fagarasan & Honjo, 2000). Instead pathogen recognition receptors TLRs directly recognize bacterial antigens. However, in some cases additional stimulation with cytokines released from T cells are required for full activation

(Bucala, 1992). In contrast, T cell dependent antigens are soluble proteins that are, after BCR binding, processed to peptides and presented by the major histocompatibility complex at the surface of the B cell (Parker, 1993). These peptides are then recognized by the T cell receptor of the T cell and trigger the expression of further co-receptors. Beside BCR activation, further stimulation through these co-receptor interactions and additional cytokine stimulations are required to activate complex signaling pathways inside the cell to induce B cell proliferation and differentiation. Therefore, the activation of B cells is dependent on a complex interaction of different factors and their corresponding signaling events.

Activation of B cells by these factors leads to formation of the GC, characterized by a typical structure: a dark and a light zone (MacLennan, 1994). The dark zone consists of proliferating B cells known as centroblasts, whereas the light zone is build up by smaller, non-dividing B cells called centrocytes, interacting with follicular dendritic cells (FDC), T cells and macrophages. Beside proliferation in centroblasts, the antigen affinity of the BCR is altered by somatic hypermutation of the immunoglobulin (Ig) locus. B cells then leave into the light zone, where B cells with high affinity BCR are positively selected by survival signals from FDC and T cells, while other B cells undergo apoptosis. Positively selected B cells enter a second round of hypermutation in the light zone or leave the GC as differentiated plasma or memory B cells.

1.1.2 Germinal centers and B cell transformation

The GC is an important structure in B cell activation and differentiation. However, analysis of Ig rearrangements and gene expression profiles revealed that GC cells are also precursors of the majority of mature B cell lymphomas (Küppers, 2005; Klein & Dalla-Favera, 2008). Typically, these B cell lymphomas are divided into Hodgkin lymphoma (HL) and aggressive Non-Hodgkin Lymphoma (NHL). In the following only lymphoma subtypes important for this study are presented.

Pathological alterations of glands and spleen in children were first described by Thomas Hodgkin in 1832 (Hodgkin, 1832). 30 Years later this disease was called Hodgkin disease and today it is known that this disorder is a B cell derived lymphoma (Küppers *et al.*, 2012). In general, HL are associated with a good overall survival (65-90% of patients are disease free in five years) and the current goal of HL treatment is the reduction of toxicity while maintaining treatment efficiency (Küppers *et al.*, 2012).

In contrast, aggressive NHL are more common than HL (9.3 per 100.000 people) and characterized by a more aggressive growth and worse clinical outcome (Ferlay *et al.*, 2013). With about 30% of all NHL Diffuse Large B Cell Lymphoma (DLBCL) are the most common subtype of NHL (Anderson *et al.*, 1998). However, chromosomal and gene expression analysis revealed that DLBCLs are not one kind of disease but clinically and morphological heterogenic (Morin *et al.*, 2013). Beside clinical and histochemical classifications, currently molecular classifications of DLBCL are in clinical implementation. One subgroup of DLBCL, characterized by a gene expression profile resembling *in vitro* activated B cells, was

called activated B cell like DLBCL (ABC DLBCL) (Alizadeh *et al.*, 2000). The other shows an expression profile comparable to GC B cells and was therefore called germinal center B cell like DLBCL (GCB DLBCL). Interestingly, patients with GCB classified lymphoma had a significant better overall survival than ABC patients. In general, therapy of DLBCLs dramatically increased by combining conditional CHOP treatment (cyclophosphamide, doxorubicin, vincristine, and prednisone) with the anti-CD20 monoclonal antibody rituximab (R-CHOP) (Sehn, 2010). Nevertheless, about 40 % of DLBCL still evade proper treatment. Investigating the molecular mechanisms characterizing different subtypes can therefore help to find new therapy targets and improve therapy of R-CHOP resistant lymphoma.

A third well studied aggressive NHL but different from DLBCL is called Burkitt Lymphoma (BL), which can be divided into an endemic and a sporadic subtype (Molyneux *et al.*, 2012). The endemic BL is a common tumor in central Africa and associated with Epstein barr virus and malaria infections. The sporadic subtype is not associated with any infection and mostly found in western Europe and the United States. A hallmark of Burkitt lymphoma is a special t(8;14) translocation, which affects the regulation of the proto-oncogene c-Myc (section 1.2.4). In contrast to DLBCLs that are mostly found in adult people, BLs only account for 1-2 % of adulthood lymphomas, while 30-40 % of childhood NHL are classified as BL (Mbulaiteye *et al.*, 2009). While the prognosis of BL in young patients was substantially improved since 1995, the 5 year-survival rate of patients over 60 year is still 50% or less (Castillo *et al.*, 2013).

All three described lymphoma entities frequently harbor gene mutations, that are possibly mediated by physiologic B cell activation and BCR rearrangement itself (Dunn-Walters *et al.*, 2001). Depending on the oncogenes or tumor suppressors that are deregulated by these mechanisms the different B cell lymphoma subtypes can develop (Küppers, 2005). Importantly, a single mutation does not seem to be sufficient to induce cell transformation alone, but a combination of mutations affecting different oncogenes and tumor suppressors is often found during DLBCL progression (Morin *et al.*, 2013). However, beside these classical mutations, it became evident that the microenvironment of the GC itself might be involved in lymphoma development and progression as well (Burger *et al.*, 2009), (Lenz *et al.*, 2008).

1.2 Signaling pathways involved in normal and aberrant B cell activation

Signaling cascades connect extracellular signals with intracellular events like gene regulation, proliferation and metabolism. Under physiological conditions these pathways are strongly regulated. However, in cancer cells specific mutations can led to aberrant activation of these pathways leading to an uncoupling of proliferation from physiological regulation (Hanahan & Weinberg, 2011). Previous experiments performed in the working group have shown that stimulation of a B cell line with GC derived factors can be used to mimic these aberrant

activated signaling pathways in lymphoma (Schrader *et al.*, 2012a). Here, activation of the NF- κ B, JAK/STAT, PI3K and MAPK signaling by stimuli treatment resulted in specific global gene expression changes. Sorting NHL-patients according to their similarity in the expression of TOP100 affected genes to the stimulated B cell discriminated individual DL-BCL subtypes. These experiments show, that *in vitro* stimulations of cell lines are a suitable tool to analyze pathway dependency in lymphoma.

In the next chapters the most important signaling cascades in lymphoma, which are important for the study, are described and how these pathways can be activated by either extracellular stimuli or corresponding pathway mutations in lymphoma. An overview about these pathways, stimuli and mutations is given in Figure 1.

1.2.1 Canonical and non-canonical NF- κ B signaling

NF- κ B signaling plays an important role in normal B cell activation and transformation. Main activators of the canonical (p65/p50) pathway are B cell receptor and toll-like receptor signaling while CD40 (cluster of differentiation 40) signaling is additionally activating non-canonical (p52/RelB) signaling in B cells (Figure 1A)(Vallabhapurapu & Karin, 2009). The BCR complex consists of a membrane bound immunoglobulin (Ig) and the two co-receptors Ig α (CD79a) and Ig β (CD79b) (Kurosaki, 2011). Crosslinking of the BCR by antigen binding results in tyrosine phosphorylation of the cytosolic regions of Ig α / β and recruitment of different tyrosine kinases. This process triggers the formation of the signalosome, a complex built up from various kinases, docking proteins and further signaling enzymes. A complex consisting of MALT1 (mucosa-associated lymphoid tissue lymphoma translocation protein), CARD11(caspase recruitment domain family, member 11) and TAK1 (transforming growth factor beta-activated kinase 1) is then activated, which in turn activates the inhibitor of nuclear factor kappa-B kinase (IKK). This leads to the phosphorylation and proteasomal degradation of the inhibitor of nuclear factor kappa-B (I κ B α), releasing the transcription factor NF- κ B (dimer of p50 and p65/RelA in case of canonical signaling), which further translocates into the nucleus. There NF- κ B is binding to a variety of target genes, including inflammation, survival, angiogenesis or proliferation associated genes, dependent on further posttranslational modifications or interactions with other transcription factors (Hayden & Ghosh, 2012).

Beside BCR activation, this signaling cascade can be activated by TLRs. Human B cells were shown to express TLR1, 6, 7, 9 and 10 depending on the maturation and differentiation status of the cells (Chiron *et al.*, 2008). Inside the GC high expression levels of *TLR9* were found (Månsson *et al.*, 2006). TLR9 is located in the endosome of the B cell, where it is activated by unmethylated double-stranded deoxyribonucleotides with repeating CpG motifs (further referred to as CpG). After ligand binding, the signaling adaptor MyD88 (myeloid differentiation primary response gene 88) is recruited (Peng, 2005). MyD88 activates IRAK1 (interleukin-1 receptor-associated kinase 1) and IRAK4, which then phosphorylate IKK, thereby activating canonical NF- κ B signaling. Due to the co-activation of other pathways

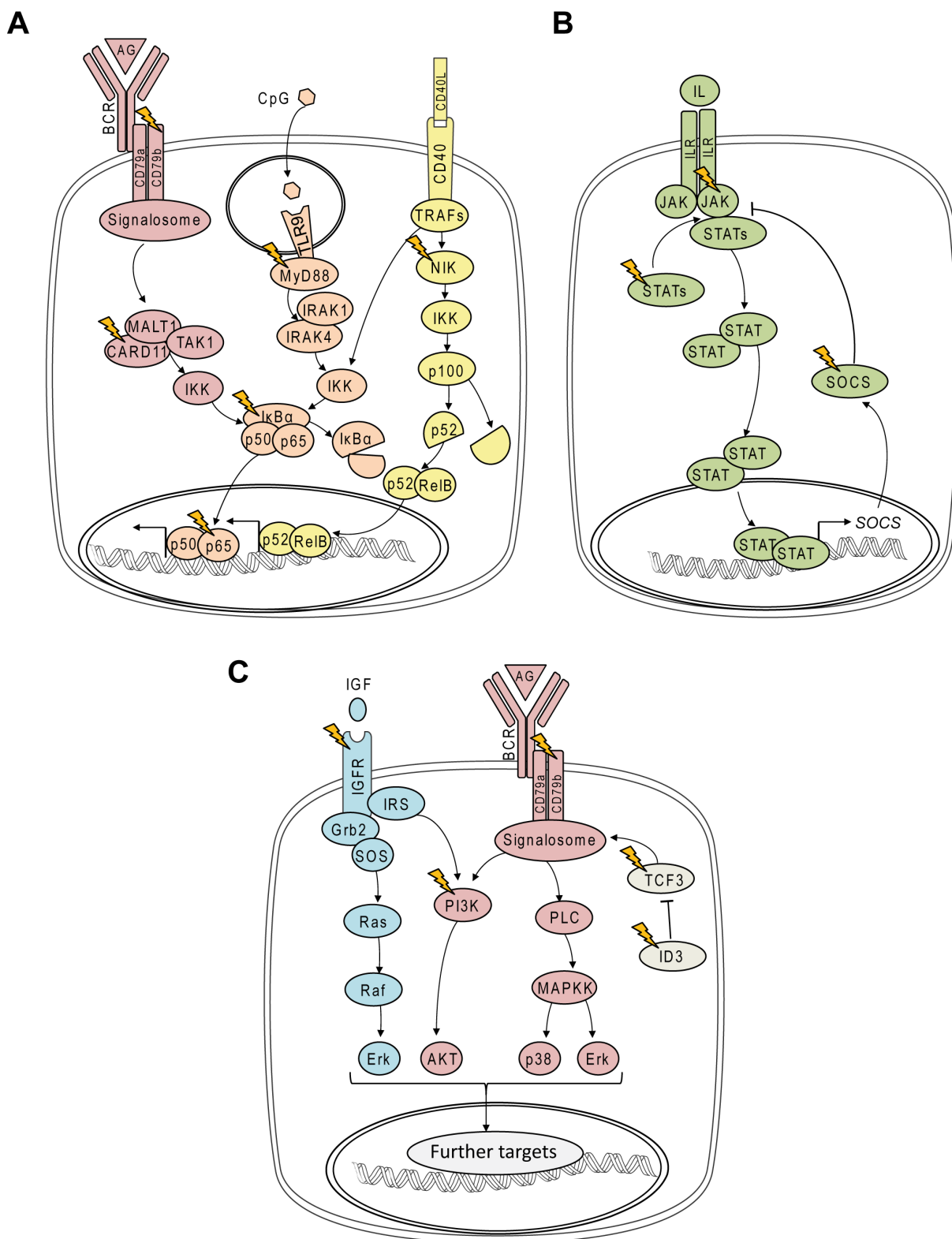


Figure 1: Scheme of main signaling nodes activated by a set of microenvironmental factors observed in activated B cells. (A) Under physiological conditions canonical NF-κB signaling can be activated via BCR, TLR or CD40 signaling, while non-canonical NF-κB signaling is activated by CD40L. Mutations in main components of these signaling pathways (indicated by lightnings) chronically activate these pathways in different mature B cell lymphoma (B) JAK/STAT signaling can be activated via interleukin binding or mutations affecting JAK/STAT itself or negative feedback loops. (C) PI3K and MAPK are activated by a variety of signaling pathways. The figure shows an example of PI3K and MAPK activated by BCR and IGF-1 signaling, that are chronically active in different B cell lymphoma.

by TLR signaling, the target genes of BCR activated NF- κ B signaling can differ from TLR activated signaling.

Another activator of canonical NF- κ B signaling is CD40 signaling. However, also non-canonical NF- κ B signaling is activated by CD40 signaling in B cells (Elgueta *et al.*, 2009). CD40 is a transmembrane glycoprotein receptor expressed at the surface of B cells that is activated by interaction with the CD40 ligand (CD40L/CD154) located on T cells. After receptor-ligand interaction intracellular mediators called TNF-receptor associated factors (TRAFs) are recruited and activated. While one TRAF is able to activate the canonical NF- κ B pathway via phosphorylation of IKK by TAK1, others activate the non-canonical NF- κ B pathway (p52/RelB). Thereby IKK α is phosphorylated by the NF- κ B inducing kinase (NIK). IKK α in turn phosphorylates p100, which is then partially degraded by the proteasome to its active form p52. This protein dimerizes with RelB (v-Rel avian reticuloendotheliosis viral oncogene homolog B), translocates into the nucleus and activates the gene expression of several cytokines, chemokines and typical B cell activation markers.

Deregulated NF- κ B signaling was shown to play an important role in lymphoma pathogenesis. For example, in DLBCL ABC patients a strong activation of canonical NF- κ B pathway was observed (Davis *et al.*, 2001). This activation was dependent on a chronic active BCR signaling mediated by either *CARD11* or *CD79B* mutation, amplification of *MALT1* or mutations activating *MYD88* connecting TLR signaling with DLBCL development (Davis *et al.*, 2010), (Sanchez-izquierdo *et al.*, 2003; Ngo *et al.*, 2011). Further, genomic amplification of *RELA* (p65) and *NIK* as well as mutations in the negative regulator I κ B α were found in HL and proliferation of HL cell lines was shown to be dependent on this NF- κ B activation (Joos *et al.*, 2002; Emmerich *et al.*, 2003; Bargou *et al.*, 1997). Therefore, NF- κ B signaling is not only involved in normal B cell activation, but, when aberrantly activated, a major player in lymphomagenesis.

1.2.2 JAK/STAT signaling

Main activators of the janus kinase/ signal transducer and activator of transcription (JAK/STAT) pathway are autocrine or paracrine secreted interleukins (IL) (Rawlings *et al.*, 2004) (Figure 1B). Beside IL4 and IL6, IL10 and IL21 were shown to be involved in differentiation processes in the GC (Yoon *et al.*, 2009). Thereby abundance of IL10 seems to be crucial for GC formation as it is regulating B cell survival as well as proliferation (Levy & Brouet, 1994; Rousset *et al.*, 1992). The major pathway activated by IL10 is the JAK1/STAT3 pathway (Sabat *et al.*, 2010). IL10 binds to the IL10 receptor (IL10R), leading to the dimerization of the two receptor units IL10R1 and IL10R2. While JAK1 is bound to IL10R1, the tyrosine kinase 2 (TYK2) is bound to IL10R2. Dimerization of the subunits leads to close proximity of JAK1 and TYK2 and concurrent trans-phosphorylation. Thereby, the kinases are activated and in turn are now able to phosphorylate STATs, mostly STAT3 in case of IL10 signaling. This phosphorylation triggers dimerization and activation of STAT3 itself, which translocates into the nucleus and induces target gene expression. Beside proliferation,

survival and inflammation associated genes, STAT3 regulates the transcription of suppressors of cytokine signaling (SOCS)(Carpenter & Lo, 2014; Yoshimura, 2009). SOCS3 itself deactivates STAT3 signaling by direct binding to the IL10R and inhibiting further STAT3 phosphorylation building a negative feedback loop. Beside STAT3 other STATs like STAT1, STAT5 or STAT6 can be activated by the different interleukins.

In addition to NF- κ B signaling, deregulated JAK/STAT signaling is often found in lymphoma. Importantly, STAT3 mutations can be found in DLBCL and STAT3 and IL10 levels themselves are associated with a worth clinical outcome in DLBCL (Wu *et al.*, 2011), (Lech-Maranda *et al.*, 2006). But also in HL JAK/STAT activation was described. For example, mutations in *JAK2* and in *SOCS1* were found (Weniger *et al.*, 2006),(Joos *et al.*, 2000). In line with the found mutations, proliferation of HL cell lines was shown to be dependent on STAT5 as well as STAT3 signaling (Scheeren *et al.*, 2008; Holtick *et al.*, 2005).

1.2.3 PI3K/MAPK signaling

Phosphoinositide-3-kinase (PI3K) and mitogen activating protein kinase (MAPK) are important components of B cell activation. They are activated by variety of external stimuli and regulate cell cycle as well as metabolism by activating further downstream targets (Figure 1D).

After B cell activation, these pathways are activated by the signalosome (section 1.2.1) (Kurosaki, 2011). In brief, PI3K generates the signaling molecule phosphatidylinositol-3,4,5-trisphosphate and thereby activates the downstream kinase AKT by triggering tyrosine and serine phosphorylation. Phosphorylated AKT in turn regulates proliferation, growth and survival via phosphorylation of a variety of proteins. In parallel, activation of phospholipase C (PLC) leads to the generation of diacylglycerol and Ca^{2+} release, which activate protein kinase C (PKC) and cooperatively induce MAPK signaling, including extracellular-signal regulated kinase (Erk) and p38 phosphorylation.

Beside BCR activation different growth factors, including the insulin-like growth factors (IGFs), play an important role in PI3K and MAPK activation and within the last two decades an emerging role for IGF1 signaling in B cell development and differentiation was shown (Adams *et al.*, 2000; Smith, 2010). In general, IGF1 binds to the IGF1 receptor (IGF1R), thereby inducing auto-phosphorylation of intracellular domains of the IGF1R (O'Connor *et al.*, 2008). This phosphorylation recruits the insulin receptor substrate (IRS), growth factor receptor-bound protein 2 (Grb2) and son of sevenless (SOS). IRS activation leads to increased metabolism and survival via activation of the PI3K/AKT pathway, while Grb2 and SOS activate Erk signaling to induce proliferation.

PI3K and MAPK signaling are important for physiological BCR activation. However, PI3K signaling was also found in Burkitt cell lines, which was dependent on transcription factor 3 (TCF3) and ID3 (inhibitor of DNA binding 3) activity (Schmitz *et al.*, 2012). Importantly, these factors are frequently mutated in BL patients indicating an important role for

PI3K signaling in BL development and progression (Richter *et al.*, 2012; Love *et al.*, 2012). Another indication for PI3K and MAPK signaling is given from HL, where overexpression of the IGF-1R is associated with a favored outcome, but the underlying mechanism is still unclear (Liang *et al.*, 2014).

1.2.4 The proto-oncogene c-Myc

c-Myc (Myc) is a major regulator of proliferation, metabolism and differentiation in different tissues and cell types and one of the most important oncogenes (Meyer & Penn, 2008). However, no *MYC* expression was found in centroblast in the dark zone of the germinal center although these cells are highly proliferative (Klein *et al.*, 2003). Nevertheless, Myc activity was shown to be important for the formation and maintenance of the GC (Dominguez-sola *et al.*, 2012; Calado *et al.*, 2012). Both studies showed that Myc is expressed in the early stages of B cell activation and then repressed by the transcriptional regulator BCL-6 (B cell lymphoma 6 protein). In the light zone interaction with follicular and T cells leads to downregulation of BCL-6 and therefore reinduction of Myc in centrocytes. Furthermore, Myc was shown to be essential for BCR and CD40L/IL-4 mediated B cell proliferation (Murn *et al.*, 2009; de Alboran *et al.*, 2001). Beside downregulation of BCL-6, these stimuli can directly increase Myc levels by transcriptional and posttranscriptional regulation by NF- κ B, STAT3 or Erk/PI3K activation (Basso *et al.*, 2012; La Rosa *et al.*, 1994; Ling & Arlinghaus, 2005; Sears, 2000).

Importantly, deregulated *MYC* expression resulting from gene translocations and mutations or chronic active signaling events is associated with the development of aggressive lymphomas (Slack & Gascoyne, 2011). Effects of *MYC* overexpression are best studied in BL. On the molecular level BL are characterized by a high *MYC* expression and activity (Hummel *et al.*, 2006). In about 70-80% of BL a t(8;14)(q24;q32) translocation can be found, which results in translocation of the *MYC* gene into the *IGH* region and therefore deregulation of its expression in B cells (Zech *et al.*, 1976). Notably, also in DLBCL high expression levels or activity of *MYC* were found but correlated with worse clinical outcome than BL (Schrader *et al.*, 2012b; Horn *et al.*, 2013).

1.2.5 Myc as a global gene amplifier

Myc is a basic helix-loop-helix leucine zipper that binds together with its dimerization partner Max to so called E-box motifs (Grandori *et al.*, 2000). These motifs can be found in the majority of genes at approximately every 1000 base pairs (bp). In 2012 two groups showed that under physiological conditions Myc is bound to canonical E-boxes of all actively transcribed genes (Lin *et al.*, 2012; Nie *et al.*, 2012). Moreover, under overexpressing conditions Myc also binds to non-canonical E-box motifs, which can be found mostly in enhancers. This binding increasing the expression of already activated genes and but not the number of target genes in total. By this mechanism Myc is thought to increase the expression of for example cell cycle and metabolism genes over a certain threshold, thereby inducing prolifer-

eration. As an additional effect, *MYC* overexpression leads to a global increase of all active genes in the cell which is accompanied by an increase of total RNA in the cell (Lin *et al.*, 2012), (Nie *et al.*, 2012). Lovén *et al.* (2012) showed, that this global amplification of RNA influences gene expression analysis in general and recommended gene normalization on total cell numbers by using external spike-in controls.

1.2.6 Cooperation of signaling pathways

The previous sections described different signaling pathways activations by the microenvironment that are involved in B cell activation. Importantly, these factors do not act independently but rather cooperative or even synergistic in changing B cell fate (Galibert *et al.*, 1996; Rousset *et al.*, 1992; Nikitin *et al.*, 2014). This is further supported by the fact that TD and TI B cell activation depends on additional coactivating signals from surrounding cells (sec. 1.1.1). But also in B cell lymphoma evidence about cooperation of signaling pathways exist. For example, it was shown, that *MYC* overexpression alone is not sufficient to induce BL like tumors in mice, but that coactivation of the PI3K pathway is needed (Sander *et al.*, 2012). Another working group showed, that this PI3K activation in *MYC* overexpressing mice activates NF- κ B and STAT3 signaling, that are both involved in lymphoma proliferation and survival (Han *et al.*, 2010). Further evidence for an interaction of NF- κ B and STAT is given by the fact, that both, DLBCL and HL, frequently harbor mutations affecting both signaling pathways. First evidence about a cooperational role for STAT3 and NF- κ B signaling in DLBCL ABC exist (Lam *et al.*, 2008). Therefore, the interaction of different signaling pathways is important for B cell activation as well as lymphoma pathogenesis.

To date there are hints, that one pathway can influence the activity of the another by regulating the gene expression of main signaling components. For example, it was shown that NF- κ B can upregulate *IL6* gene expression, which activates STAT3 in a feedback loop (Lam *et al.*, 2008). In the same study, it was supposed that STAT3 and NF- κ B can interact to induce gene expression in B cells as it was shown in solid tumors before (Grivennikov & Karin, 2010). Moreover, BCR activation can induce gene expression of *TLR9* on naive B cells making them reactive towards CpG stimulation (Bernasconi *et al.*, 2003). However, it is not known if and how other signaling pathways interact and which of these interactions is most potent in changing gene expression to mediate proliferation and metabolism in B cells.

1.3 Regulation of cell cycle and metabolism

Regardless of normal B cell activation or transformation, specific gene expression changes occur to induce proliferation in cells (Whitfield *et al.*, 2006). Important stages are overcoming the restriction point of the cell cycle and the evasion of further cell cycle check points by increasing and activating positive cell cycle regulators, while negative regulators must be shut down (Malumbres & Barbacid, 2001). However, in the last years an important role for metabolic adaptations for sustained proliferation became evident (Vander Heiden *et al.*, 2011). So far less is known about how the previously described signaling pathways, or their combinations, regulate cell cycle or metabolism in B cells. On the other hand, Myc was shown to be a major regulator of all these steps in other cell entities (Bouchard *et al.*, 1998; Dang, 2012). Using the example of Myc, important cell cycle and metabolic adaptations that are needed to induce cell proliferation will be described in the following chapters.

1.3.1 Cell cycle regulation

The cell cycle is composed of different cell cycle phases (Norbury & Nurse, 1992). The most important ones are the synthesis (S) phase, where DNA replication takes place, and the mitosis (M) phase, where cells start to divide. Between these so called gap (G) phases are defined. In the G1 phase, cells start to prepare for the DNA synthesis, whereas in the G2 phase, between the S and M phase, cells are checked for DNA damage and prepare for the progress of division. Naive B cells are stuck in the G0 of the cell cycle. Within this quiescent stage of the cell cycle they achieve growth signals that activate cell cycle regulators to enter the G1 phase. These regulators are a group of serine/threonine kinases called cyclin dependent kinases (CDK) that form active heterodimers with so called cyclin proteins (Johnson & Walker, 1999). The entry into a new cell cycle is controlled by the binding of cyclin D's (gene names *CCND1* to *CCND3*) to CDK4 and/or CDK6. In activated B cells, the gene expression of cyclin D can be induced by activating B cell signaling including transient *MYC* expression (Richards *et al.*, 2008). However, in lymphoma cells *MYC* overexpression alone is sufficient to increase cyclin D and CDK4 to overcome this threshold (Pajic *et al.*, 2000). CDK4 and CDK6 phosphorylate the retinoblastoma (Rb) protein, which sequesters the transcription factor E2F. After phosphorylation Rb dissociates from E2F, which becomes activated and induces expression of G1 and S phase regulatory genes. Within them cyclin E (*CCNDE*) and A (*CCNDA*) are increased, which bind to CDK2 and CDK1 and promote S phase progression by phosphorylation of genes involved in DNA replication. Like cyclin D, the expression of cyclin E and cyclin A can be further increased by Myc thereby promoting this step (Hanson *et al.*, 1994). Additionally, Myc decreases the expression of the negative regulators of CDK activity (p16/*CDKN2A*, p21/*CDKN1A* and p27/*CDKN1B*), which inhibit CDK activity by direct interactions. By analog sequential gene expression regulation of the different cyclins, CDKs and their negative regulators, also the transition into the next

cell cycle stages is regulated. After division, cells can become quiescent again (G0) or in case of *MYC* overexpression enter a new round of cell cycle.

1.3.2 Metabolic regulation

Activated and transformed lymphocytes are thought to undergo similar metabolic reprogramming to support proliferation since both highly increase glucose and glutamine metabolism (Altman & Dang, 2012; Macintyre & Rathmell, 2013). Thereby glucose is metabolized to lactate even if oxygen is present, a process which was first described by Otto Warburg (Warburg, 1956; Greiner *et al.*, 1994). While regulation and fate of glucose metabolism was extensively described, the role of glutamine in lymphocyte proliferation is not well described (Vander Heiden *et al.*, 2001; Jacobs *et al.*, 2008).

Glutamine is a major carbon as well as nitrogen source, being involved in the tricarboxylic acid cycle (TCA), amino acid and nucleotide synthesis but also redox balance (Newsholme, 2001). Thereby glutamine is metabolized via a process called glutaminolysis. The first step of glutaminolysis is the conversion of glutamine to glutamate catalyzed by the glutaminase (GLS). Glutamate is then metabolized to α -ketoglutarate (aKG) via deaminases (GLUD) or aminotransaminases (Glutamic Oxaloacetic Transaminase/ GOT or Glutamic Pyruvate Transaminase/ GPT). Please note, that through this study official gene names instead of the protein names are used to facilitate comparison with gene expression data. To enable differentiation of proteins and genes, gene names are written in italic letters.

Via multiple steps, aKG is oxidized inside the TCA to generate the reduction equivalents (NADH and FADH₂). These molecules can be used for anabolic biosynthesis processes, redox balance or as proton donors in the respiratory chain to produce adenosine triphosphate (ATP) in order to meet energy demands. Additionally, aspartate transaminases generate the amino acid aspartate from glutamate which is important for further biosynthesis processes like nucleotide synthesis. Importantly, lymphocytes do not proliferate in the absence of glutamine indicating that at least one of this glutamine dependent processes is essential for their proliferation (Newsholme *et al.*, 1985; Crawford & Cohen, 1985).

The best described regulator of lymphocyte and cancer metabolism is Myc (Wise *et al.*, 2008; Wang *et al.*, 2011). Myc was described to increase the expression of *GLS* (Gao *et al.*, 2009). A glucose independent role for glutamine in TCA function was further described in Myc overexpressing cells, but also amino acid and nucleotide synthesis can be regulated by Myc (Le *et al.*, 2012; Liu *et al.*, 2012). However, whether these metabolic changes are restricted to aberrant *MYC* expression still needs to be investigated in more detail. First experiments in T-cells show that CD28 activation increases *GLS* expression independent from Myc by a pathway that involves activation of the Erk MAP kinase (Carr *et al.*, 2010). Thereby, Erk directly increases *GLS* expression by a mechanism distinct to Myc activation. These data imply that glutamine metabolism can be increased by other signaling pathways and that the mechanism can be different from Myc activity. However, the direct link between glutamine metabolism and proliferation in B cells is not well characterized.

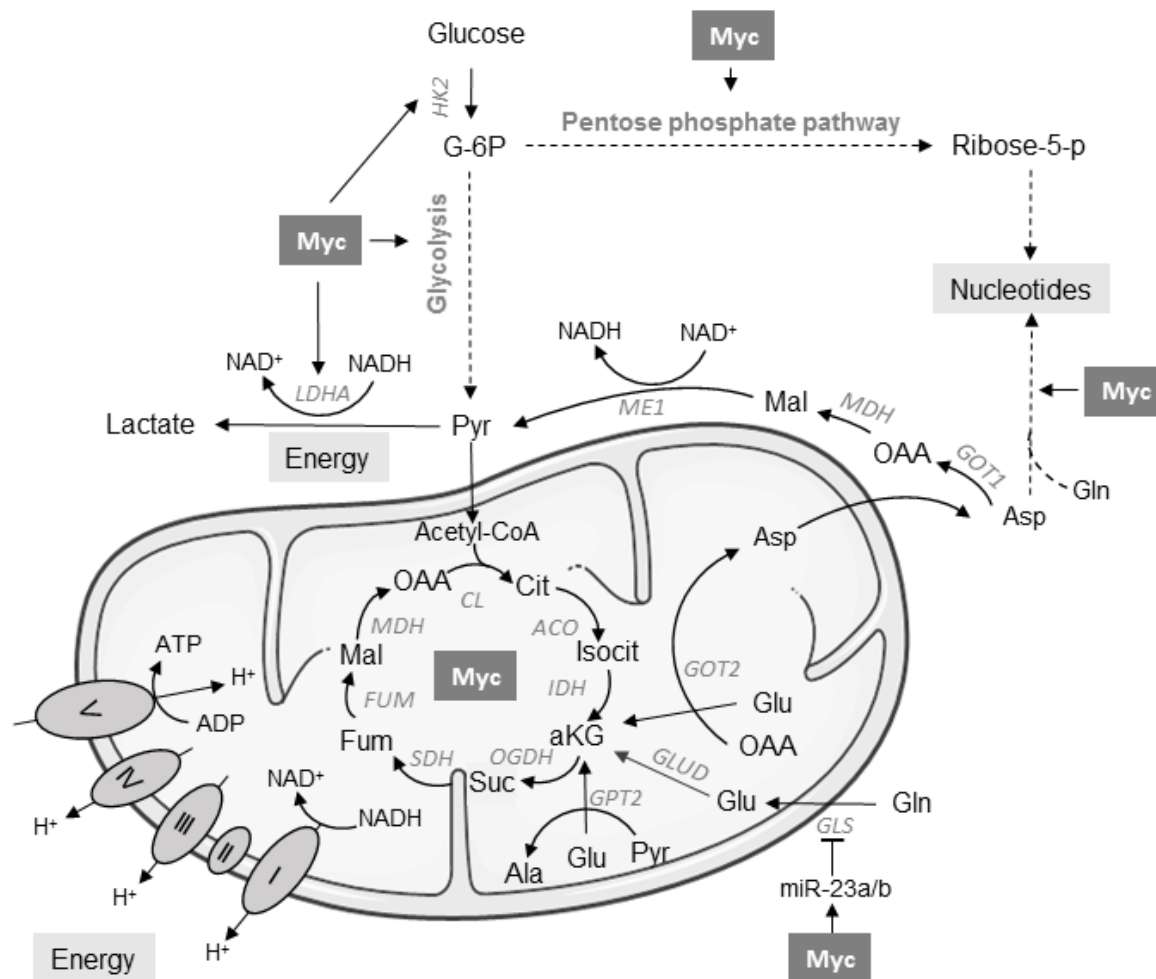


Figure 2: Schematic presentation of selected metabolic pathways affected by high MYC expression. Metabolic changes support proliferation by providing energy (ATP), reducing equivalents (NADH) and biosynthesis building blocks (as for example nucleotides). Glucose and glutamine (Gln) are main sources for these processes and the gene expression of key metabolic enzymes (*HK2*, *GLS*) for their metabolism is regulated by Myc. Glucose can be metabolized via the pentose phosphate pathway to synthesize ribose molecules for nucleotide synthesis or degraded via glycolysis to pyruvate, which can be anaerobically converted to lactate or used to fuel the TCA via acetyl-CoA. The TCA can also be fueled by Gln via aminotransferases (GOT and GPT) or deaminases (GLUD). Reduction equivalents from the TCA are then used in the respiration complex to build up a membrane potential which is necessary to generate ATP. Beside energy production amino acids like aspartate are generated from Gln which are important precursors for nucleotide synthesis. Gene names of important enzymes are shown in grey and italic letters. Gln = glutamine, Glu = glutamate, Ala = alanine, Asp = aspartate, aKG = α -ketoglutarate, Suc = succinate, Fum = fumarate, Mal = malate, OAA = oxaloacetate, Cit = citrate, Isocit = Isocitrate, Pyr = pyruvate.

1.4 Aim of the study

Mutual interacting signaling pathways activated by factors of the cellular environment define B cell homeostasis and are thought to be involved in transformation processes. While the effects of the proto-oncogene *c-Myc* on these processes are increasingly understood less is known about how aberrant B cell signaling pathway activations and their interactions, like NF- κ B or JAK/STAT signaling, regulate metabolic adaptations for B cell proliferation. From a previous study of Schrader *et al.* (2012a) evidence was provided that stimulation of a B cell line with factors of the cellular environment allows to stratify lymphoma samples and partially to predict pathways involved. However, pathway cross talks were not taken into account in this approach, the used cell line was transformed by *Myc* and the effects of global gene expression changes on key biological functions as cell proliferation or metabolism were not defined. This study intends to get further insight into the interaction of signaling pathways and their potential to induce proliferation and associated metabolic reprogramming in resting B cells. Thereby, answering the following questions is aimed:

- (i) What is the impact of combination of factors of the B cell environment on global gene expression and the metabolome?
- (ii) Are pathway interaction networks able to reprogram the metabolism of resting B cells to support B cell proliferation?
- (iii) What is common or different in gene expression, proliferation and metabolism of stimulated and *Myc* transformed cells?
- (iv) Are these pathway dependent interactions/mechanisms also important for lymphoma?

To answer these questions, the P493-6 B cell line with a conditional *MYC* expression is used to enable the modeling of combinations of stimuli and *Myc* activation on the same genetic background. Analysis of global gene expression and metabolic changes in relation to proliferation of B cells are performed and the following analyses are conducted:

- (i) Qualitative and quantitative assessment of the effects of selected single and combined microenvironmental factors on global gene expression and metabolome in relation to cell proliferation and in comparison to *MYC* overexpressing cells.
- (ii) Functional assessment of pathway interactions and underlying mechanisms in the context of gene expression, proliferation and related metabolic reprogramming.
- (iii) Evaluation of identified regulatory circuits in different lymphoma cells and patients derived data.

This study design will enable to characterize molecular pathways and new regulatory circuits for a better understanding of B cell homeostasis but also lymphoma biology and hopefully improve some aspects of diagnosis, prediction and perhaps treatment of lymphoma patients.

2 Material and Methods

2.1 Material, recipes and equipment

2.1.1 Biological material

Cell lines according to Table 1 were used in this study.

Table 1: Cell lines

Cell line	Source	Distributor	Reference
P493-6	<i>Homo sapiens</i> Myc transformed lymphoblastoid cell line	Bornkamm, Munich	(Polack <i>et al.</i> , 1996)
CA-46	<i>Homo sapiens</i> Burkitt Lymphoma	DSMZ, Brunswick	(Magrath <i>et al.</i> , 1980)
OCI-Ly3	<i>Homo sapiens</i> Diffuse Large B Cell Lymphoma (ABC)	DSMZ, Brunswick	(Tweeddale <i>et al.</i> , 1987)
L-428	<i>Homo sapiens</i> Hodgkin Lymphoma	DSMZ, Brunswick	(Schaadt <i>et al.</i> , 1980)
Schneider (S)-2	<i>Drosophila melanogaster</i> late embryo cells	DSMZ, Brunswick	(Schneider, 1972)

2.1.2 Chemicals and consumable supplies

Chemicals and consumables used in the present study are listed in Table 2 and Table 3, respectively.

Table 2: Chemicals

Chemical	Manufacturer
4-Iodophenylboronic acid (4-IPBA)	Sigma-Aldrich, Munich GER
5-Bromo-2-deoxyuridin (BrdU)	Sigma-Aldrich, Munich GER
Acrylamid/Bisacrylamid 40%	BioRad, Munich GER
Agarose	Sigma-Aldrich, Munich GER
Ammonium persulphate	Sigma-Aldrich, Munich GER
Bovine serum albumin (BSA)	Serva, Heidelberg GER
Bradford solution	RotiQuant-Roth, Karlsruhe GER
Bromphenol blue	Sigma-Aldrich, Munich GER
Cell-Tak Cell and Tissue Adhesive	Corning Incorporated, Corning USA
Deoxyribonucleoside triphosphates	PrimeTech LTD, Minsk BY
cOmplete protease inhibitor cocktail	Roche, Mannheim GER
Dimethyl sulfoxide (DMSO)	Sigma-Aldrich, Munich GER

Chemical	Manufacturer
di-Sodium tetraborate decahydrate	Merck, Darmstadt GER
Ethanol (100%)	J.T. Baker, Deventer NL
Ethidiumbromid	Sigma-Aldrich, Munich GER
Ethylenediaminetetraacetic acid (EDTA)	Riedel-de Haen, Seelze GER
FACS Flow	Becton Dickinson, Heidelberg GER
Formaldehyde	Sigma-Aldrich, Munich GER
Full Range Rainbow Molecular	GE Healthcare, Munich GER
Glycerol	Roth, Karlsruhe GER
Glycine	Roth, Karlsruhe GER
HEPES	Sigma-Aldrich, Munich GER
Hot FIREpol DNA polymerase (5 U/ μ l)	PrimeTech LTD, Minsk BY
Hydrochloric acid (37%)	Merck, Darmstadt GER
Hydrogen peroxide	Sigma-Aldrich, Munich GER
Isopropanol	Sigma-Aldrich, Munich GER
Luminol	Sigma-Aldrich, Munich GER
Methanol 100%	J.T. Baker, Deventer NL
Milk powder	Roth, Karlsruhe GER
Nonidet P-40	Sigma-Aldrich, Munich GER
Phenylmethylsulfonyl fluoride (PMSF)	Sigma-Aldrich, Munich GER
Phosphatase inhibitor PhosSTOP	Roche, Mannheim GER
Propidium iodide	Sigma-Aldrich, Munich GER
RPMI-1640	Lonza, Basel CH
RPMI-1640 w/o glucose w/o glutamine	PAN-Biotech, Aidenbach GER
Sodium chloride	Merck, Darmstadt GER
Sodium deoxycholate	Merck, Darmstadt GER
Sodium dodecyl sulfate (SDS)	Merck, Darmstadt GER
Sodium hydrogen carbonate	Merck, Darmstadt GER
Sodium hydroxide	Merck, Darmstadt GER
Tetramethylethylenediamine (TEMED)	Sigma-Aldrich, Munich GER
Thioglycerol	Sigma-Aldrich, Munich GER
Trisbase	Sigma-Aldrich, Munich GER
Triton X-100	Sigma-Aldrich, Munich GER
Trypanblue 0.4% in PBS	Life Technologies, Eggenstein GER
Tween-20	Merck, Darmstadt GER
Water HPLC grade	Merck, Darmstadt GER

Table 3: Consumables

Consumables	Manufacturer
96 well plate, round/flat bottom	Sarstedt, Nümbrecht GER
384-Well clear optical reaction plate	Applied Biosystems, Foster City USA
Optical adhesive covers	Applied Biosystems, Foster City USA
Amicon ultra-4 centrifugal filter units	Millipore, Schwalbach/Ts. GER
Cell culture flasks	Sarstedt, Nümbrecht GER
Cryo box	Nunc, Wiesbaden GER
Cryotubes	Nunc, Wiesbaden GER
Diethylaminoethyl-cellulose	Whatman, International Ltd UK
Electroporation cuvettes	BioRad, Munich GER
FACS tubes	Becton Dickinson, Franklin Lakes, USA
Falcon tubes	Sarstedt, Nümbrecht GER
Filter tips	Starlab, Ahrensburg GER
Micro touch examination gloves	Ansell, Munich GER
Pasteur pipettes	Sarstedt, Nümbrecht GER
Pipette tips w/o filters	Sarstedt, Nümbrecht GER
Reaction tubes	Sarstedt, Nümbrecht GER
Serological pipettes	Sarstedt, Nümbrecht GER
Tissue culture plates	Sarstedt, Nümbrecht GER
XFe96 fluxPak	Seahorse Bioscience, Copenhagen, DNK

2.1.3 Buffers, solutions and media

Buffer solutions, recipes and cell culture media used in this study are listed in Table 4 till Table 6.

Table 4: Ready to use solutions/buffers

Solution	Manufacturer
4x loading buffer	Roti-Load Roth, Karlsruhe GER
HEPES Buffer	Millipore, Schwalbach/Ts. GER
PBS pH 7.4 (cell culture grade)	Lonza, Verviers BEL
Ponceau S	Sigma-Aldrich, Munich GER
Reblot plus mild antibody stripping solution (10x)	Millipore, Schwalbach/Ts. GER
Roti-Quant Bradford assay	Roth, Karlsruhe GER

Table 5: Buffer recipes

Buffer	Recipe
RIPA buffer 150 mM NaCl	50 mM TrisHCl pH 7.4 0.1 % (w/v) SDS 1 % (v/v) NP-40 0.25 % Sodium-deoxycholat
Running buffer (1x):	25 mM Tris-base 192 mM Glycin 34.67 mM SDS
Transfer buffer (1x)	25 mM Tris-base 192 mM Glycin 15 % (v/v) MeOH
Separation gel mix	250 mM Tris-base, pH 8.8 25 % (v/v) Acrylamid/Bis solution (40 %) 0.0004 % (w/v) APS 0.00125 % (v/v) TEMED
Stacking gel mix	250 mM Tris Base pH 6.8 12.5 % (v/v) Acrylamid/bis solution (40 %) 0.0004 % (w/v) APS 0.00125 % (v/v) TEMED
TBS (1x)	20 mM Tris-base 137 mM Sodium chloride Adjusted to pH 7.6
TBS-T	1x TBS 0.1 % (v/v) Tween-20
Chemiluminescence solution 1	100 mM Tris/HCl pH 8.8 2.5 mM Luminol 4 mM 4-IPBA
Chemiluminescence solution 2	100 mM Tris/HCl pH 8.8 5.3 mM H ₂ O ₂
PCR buffer (10x)	750 mM Tris-HCl pH 8.8 200 mM Ammonium sulfate 0.1 % (v/v) Tween-20 in depc water

Buffer	Recipe
SybrGreenMix	1x PCR buffer 33 mM MgCl ² 1:80 000 SyberGreen 0.2 mM dNTP each 20 U/ml Hot FIREpol DNA polymerase 0.25 % (v/v) Triton X-100 0.5 mM Trehalose in depc water
PIPES buffer	10 mM PIPES 0.1 mM NaCl 2 mM MgCl ₂ 0.1 % (v/v) Triton
ChIP lysis buffer	50 mM Tris-HCl pH 8.0 2 mM EDTA 1 % (v/v) Igepal 10 % (v/v) Glycerol
ChIP sonification buffer	50 mM Tris-HCl pH 8.0 1 % (w/v) SDS 10 mM EDTA
ChIP RIPA	50 mM HEPES-KOH pH 7.6 500 mM LiCl 1 mM EDTA 1 % (v/v) Igepal 0.7 % (w/v) Na-Deoxycholate
TE buffer	1 M Tris-HCl pH 8.0 0.5 M EDTA pH 8.0

Table 6: Media

Medium	Recipe/ Manufacturer
<i>Drosophila</i> medium	Schneiders <i>drosophila</i> medium (Gibco) 10 % (v/v) FBS (Gibco) 200 U/ml penicillin + 200 µg/ml streptomycin
Freezing medium (<i>drosophila</i>)	45 % (v/v) FBS (Gibco) 45 % (v/v) conditioned <i>drosophila</i> medium 10 % (v/v) DMSO
Cell culture medium I	RPMI-1640 with glutamine (Lonza) 10 % (v/v) FBS (Gibco) 200 U/ml penicillin + 200 µg/ml streptomycin
Cell culture medium II	RPMI-1640 w/o glucose w/o glutamine (PAN) 10 % (v/v) FBS (Gibco) 200 U/ml penicillin + 200 µg/ml streptomycin 2 mM L-glutamine 2 g/l (11 mM) glucose
Gln labelling Medium	RPMI-1640 w/o glucose w/o glutamine 10 % (v/v) FBS (Gibco) 200 U/ml penicillin + 200 µg/ml streptomycin 2 mM ¹³ C5-glutamine 2 g/l (11 mM) glucose
Freezing medium (human)	90 % (v/v) FBS (Gibco) 10 % (v/v) DMSO
XF Base Medium	Seahorse Bioscience, Massachusetts USA

2.1.4 Equipment

Equipment was used as shown in Table 7.

Table 7: Equipment

Instrument	Manufacturer
7900HT Fast Real-Time PCR System	ThermoFisherScientific, Massachusetts USA
Accu-jet	Brand, Hamburg GER
Bioanalyser 2100	Agilent technologies, Santa Clara, USA
Biofuge Pico	Heraeus Instruments, Hanau GER
Biofuge Primo R	Heraeus Instruments, Hanau GER
CAT RM 5 horizontal roller	CAT M Zipperer, Staufen GER
Centrifuge 5451D	Eppendorf, Hamburg GER
Consort E734 Power Supply	Schütt Labortechnik, Göttingen GER
FACSscan flow cytometer	Becton Dickinson, Heidelberg GER
Hera freeze -80°C freezer	Heraeus Instruments, Hanau GER
IKA KS 260 shaker	IKA, Staufen GER
IKAMAG RCT magnetic stirrer	IKA, Staufen GER
Incubator Cytoperm	Heraeus Instruments, Hanau GER
Incudrive incubator	Schütt Labortechnik, Göttingen GER
LAS-4000 Image Reader	Fujifilm, Düsseldorf GER
Microcoolcentrifuge 1-15k	Sigma, Munich GER
Microflow Laminar Downflow Workstation	Bioquell, UK
Multifuge 3 L-R	Heraeus Instruments, Hanau GER
ND-1000 Spektralphotometer	NanoDrop, Wilmington USA
Neubauer Counting Chamber Improved	Lo Labor Optik, Friedrichsdorf GER
Power Pac 300 Power Supply	Bio-Rad, Munich GER
Sunrise™ Microplate Reader	Tecan, Crailsheim GER
Thermocycler 60	Biomed, Theres GER
Thermocycler Mastercycler	Eppendorf, Hamburg GER
Thermocycler T3000	Biometra, Göttingen GER
Thermomixer Compact	Eppendorf, Hamburg GER
Vortex Genie 2	Schütt Labortechnik, Göttingen GER
Water bath	Köttermann Labortechnik, Hänigsen GER
XFe96 analyser	Seahorse Bioscience, Copenhagen, DNK

2.1.5 Cell culture supplements, inhibitors and siRNA

Cells were stimulated with soluble stimulation factors shown in Table 8. Table 9 shows metabolites and their working concentrations used for glutamine rescue experiments. Inhibitors used in cell culture experiments are shown in Table 10, inhibitors used in respiratory analysis in Table 11 and siRNA for transient transfection in Table 12.

Table 8: Stimulants

Stimulant	Source	Working concentration	
		Full	Reduced
goat anti human IgM F(ab)2	Jackson ImmunoResearch, Hamburg GER	1.3 µg/ml	26 ng/ml
ODN2006 (CpG)	InvivoGen, Toulouse FR	0.5 µM	0.1 µM
recombinant human IGF-1	Peptotech, Hamburg GER	100 ng/ml	20 ng/ml
recombinant human IL10	Peptotech, Hamburg GER	25 ng/ml	5 ng/ml
sCD40L	Autogen bioclear, Wiltshire UK	100 ng/ml	20 ng/ml

Table 9: Metabolites

Metabolite	Source	Working concentration
¹³ C5-Glutamine	Campo Scientific, Berlin GER	2 mM
Adenine	Sigma-Aldrich, Munich GER	100 µM
Aspartate	Sigma-Aldrich, Munich GER	10 mM
Diethyl malate	Sigma-Aldrich, Munich GER	1 mM
Dimethyl 2-oxoglutarate	Sigma-Aldrich, Munich GER	1 mM
Glucose	Sigma-Aldrich, Munich GER	11 mM
Glutamine	Biochrom/ Merck, Berlin GER	2 mM
Oxaloacetic acid	Sigma-Aldrich, Munich GER	1 mM
Pyruvate	Sigma-Aldrich, Munich GER	1 mM
Thymine	Sigma-Aldrich, Munich GER	100 µM

Table 10: Inhibitors used in cell culture

Inhibitor	Source	Working concentration
10058-F4	Sigma-Aldrich, Munich GER	60 μ M
Aminooxyacetic acid (AOA)	Sigma-Aldrich, Munich GER	500 μ M
CB-839	Selleckchem, Munich GER	1 μ M
IKK2 inhibitor VIII (ACHP)	Calbiochem/Merck, Darmstadt GER	7 μ M
JAK inhibitor I (Pyridone 6)	Calbiochem/Merck, Darmstadt GER	1 μ M
MLN120b	MedChemExpress, Princeton USA	5 μ M
PD0332991	Selleckchem, Munich GER	0.5 μ M
Ruxolitinib	Selleckchem, Munich GER	1 μ M

Table 11: Inhibitors used for respiratory analysis

Inhibitor	Source	Working concentration
Oligomycin	Sigma-Aldrich, Munich GER	1.5 μ M
Carbonylcyanide-4-(trifluoromethoxy)-phenylhydrazone (FCCP)	Sigma-Aldrich, Munich GER	0.5 μ M
Antimycin	Sigma-Aldrich, Munich GER	2 μ M
Rotenon	Sigma-Aldrich, Munich GER	1 μ M

Table 12: siRNA

siRNA	Source
Silencer Select Negative Control No. 1	ThermoFisherScientific, Massachusetts USA
SMARTpool: ON-TARGETplus <i>STAT3</i>	Dharmacon, Lafayette, USA
SMARTpool: ON-TARGETplus <i>RELA</i>	Dharmacon, Lafayette, USA
SMARTpool: ON-TARGETplus <i>GOT1</i>	Dharmacon, Lafayette, USA
SMARTpool: ON-TARGETplus <i>GOT2</i>	Dharmacon, Lafayette, USA
SMARTpool: ON-TARGETplus <i>MYC</i>	Dharmacon, Lafayette, USA

2.1.6 Antibodies

Antibodies used for chromatin immunoprecipitation (ChIP, Table 13), Flow Cytometry (Table 14) and Immunoblot analysis (Table 15) are listed below.

Table 13: ChIP antibodies

Antibody	Order nr.	Source	Working concentration
α -IgG	sc-2027	Santa Cruz, Heidelberg GER	5 μ g per IP
α -STAT3	sc-482	Santa Cruz, Heidelberg GER	5 μ g per IP
α -p65	sc-372	Santa Cruz, Heidelberg GER	5 μ g per IP

Table 14: Flow cytometry antibodies

Antibody	Order nr.	Source	Working concentration
NF- κ B p65	#8242	Cell Signalling Technology, Frankfurt a. M. GER	1:400
Alexa 488 mouse α -pSTAT3 (pY705)	#557814	BD Biosciences, Oxford UK	1:5
FITC donkey α -rabbit IgG	#406403	Biologend, San Diego US	1:50
Alexa 488 mouse α -BrdU	B35139	Life technologies, Carlsbad US	1:15

Table 15: Immunoblot antibodies

Antibody	Order nr.	Source	Working concentration
rabbit α -p-STAT3 (Tyr705)	#9131	Cell Signalling Technology, Frankfurt a. M. GER	1:1 000
rabbit α -STAT3	#9132	Cell Signalling Technology, Frankfurt a. M. GER	1:1 000
rabbit α -p-p38	#4511	Cell Signalling Technology, Frankfurt a. M. GER	1:1 000
rabbit α -p-p42/p44	#4377S	Cell Signalling Technology, Frankfurt a. M. GER	1:1 000
rabbit α -p-Akt (Ser473)	#4060	Cell Signalling Technology, Frankfurt a. M. GER	1:1 000
rabbit α -I κ B α	#4812	Cell Signalling Technology, Frankfurt a. M. GER	1:1 000
rabbit α -p-p65 (Ser536)	#3033	Cell Signalling Technology, Frankfurt a. M. GER	1:1 000
rabbit α -p65	#4764	Cell Signalling Technology, Frankfurt a. M. GER	1:1 000
mouse α -tubulin	#05-829	Millipore, Schwalbach GER	1:5 000
rabbit α -c-Myc	ab32072	Abcam, Cambridge UK	1:10 000
mouse α -GAPDH	ab8245	Abcam, Cambridge UK	1:20 000
rabbit α -GOT2	14886	Proteintech, Manchester, UK	1:1 000
rabbit α -GOT1	14800	Proteintech, Manchester, UK	1:1 000
goat α -rabbit IgG-HRP	sc-2004	Santa Cruz, Heidelberg GER	1:2 000
goat α -mouse IgG-HRP	sc-2005	Santa Cruz, Heidelberg GER	1:2 000

2.1.7 Oligonucleotides

Oligonucleotides used for quantitative real time PCR (qRT PCR) and ChIP analysis are shown in Table 16 and Table 17, respectively.

Table 16: Oligonucleotides used for qRT PCR

Gene	Forward primer (5'-3')	Reverse Primer (5'-3')
<i>ACT42A</i>	CTAAGCAGTAGTCGGGCTGG	GTCTGCAATGGGTGTGTTTCG
<i>CDK4</i>	AGGCGACTGGAGGCTTTTG	GTGGCACAGACGTCCATCAG
<i>CDK6</i>	GCTGGTAACTCCTTCCCCAG	GTCCAGAATCATTGCACCTGA
<i>CCND3</i>	CTGACCATCGAAAACTGTGCA	AGGTCCCACCTTGAGCTTCCCT
<i>SOCS3</i>	ATGGTCACCCACAGCAAGTTTC	GTTAAAGCGGGGCATCGTACT
<i>NFKBIA</i>	TAGAAAACCTTCAGATGCTGCC	TCGTCCTCTGTGAACTCCGTG
<i>GOT2</i>	GATGCTGGCATGCAGCTACAA	TCCACAGCGCCTGTGAAGTC

Table 17: Oligonucleotides used for ChIP analysis

Gene	Forward primer (5'-3')	Reverse Primer (5'-3')
<i>PRAME</i>	TCTCCATATCTGCCTTGCAGAGT	GCACGTGGGTCAGATTGCT
<i>CDK4</i>	TCAAGCGGTCACGTGTGATA	GACAGGAGGTGCTTCGACT
<i>SOCS3</i>	TCTCTGCTGCGAGTAGTGAC	CTGGAACTGCGCGGC
<i>NFKBIA</i>	TTCTGGTCTGACTGGCTTGG	CCCTATAAACGCTGGCTGGG
<i>GOT2</i>	TCGCTGTGACGTGGCTC	TGAAGGTAAGGACAGGGACTTC

2.1.8 Ready to use reaction systems

Commercial ready to use reaction systems are shown in Table 18.

Table 18: Reaction Systems

Description	Manufacturer
NucleoSpin RNA Isolation Kit	Machery-Nagel, Düren GER
SuperscriptII RT Kit	Invitrogen, Karlsruhe GER
Nucleofector Kit V	Lonza, Basel CH
Nucleofector Kit L	Lonza, Basel CH
ERCC RNA Spike-in Mix 1	ThermoFisher Scientific, Massachusetts, USA

2.1.9 Software

If not stated elsewhere the following software products were used: the present thesis was written with LaTeX and BibTeX. Literature-management and bibliography were generated using Mendeley Desktop Version 1.15.3. Graphs were created using GraphPad PRISM 6 or 'R' version 3.3.0. Figures were assembled using Adobe Illustrator CS2 and Microsoft Office PowerPoint 2010. Real time analysis was performed using SDS 2.4 and RQ Manager 1.2.1 (Applied Biosystems). Schemes were drawn with the help of items taken from servier medical art (www.servier.com).

2.2 Cell biology

2.2.1 Cell culture techniques

***Drosophila* cell cultivation and spike-in preparation**

Schneider-2 (S2) cells were cultured in *drosophila* medium at room temperature and normal air pressure. Cells were seeded in tissue flasks at $2 \cdot 10^6$ cells/ml and maintained below $20 \cdot 10^6$ cells/ml by splitting 1:2 to 1:5 twice a week.

For spike-in preparation, S2 cells were counted using a hemocytometer and trypan blue exclusion. Cells were sedimented (centrifugation $300 \times g$, 7 min at RT) and resuspended at a density of $1 \cdot 10^6$ cells/ml in *drosophila* freezing medium and aliquoted in vials of 1 ml. Isopropanol filled cryo boxes were used to gradually cool down cells to -80°C and cryotubes were stored at -150°C .

Human B cell cultivation

All human cell lines used in this study were cultured in RPMI-1640 supplemented with 10% FBS, penicillin/streptomycin and stable glutamine (cell culture medium I) at 37°C , 5% CO_2 . Living cells were counted by using a hemocytometer and trypan blue exclusion. The human B cell lines P493-6, OCI-Ly3 and L-428 cells were maintained in a density between $0.5 \cdot 10^6$ - $1.5 \cdot 10^6$ cells/ml by splitting two to three times a week. Human BL derived CA-46 was cultured in a lower density between $0.3 \cdot 10^6$ - $1.0 \cdot 10^6$ cells/ml. P493-6 cells were cultured without the addition of tetracycline or estradiol to generate Myc overexpressing cells (Myc^{high}) or treated with 1 ng/ml doxycycline for at least 16h to decrease MYC expression (Myc^{low}). One day prior all experiments, all cell lines were seeded in fresh cell culture medium II including freshly added glutamine (P493-6 = $1 \cdot 10^6$ cells/ml, OCI-Ly3/ L-428 = $5 \cdot 10^5$ cells/ml, CA-46 = $3 \cdot 10^5$ cells/ml). For generation of Myc^{low} cells 1 ng/ml doxycycline was added to P493-6 cells at this step.

For cryopreservation, cells were centrifuged ($250 \times g$, 5 min at RT) and resuspended in human freezing medium. Per aliquot $5 \cdot 10^6$ cells were frozen using cryoboxes as described above. For revitalization, cells were thawed in 37°C water bath, transferred to 5 ml of warm medium and sedimented as described above. Cells were seeded in fresh media at mentioned cell densities.

Activation of P493-6 cells with soluble factors

To stimulate P493-6 cells for transcriptomic and metabolic analysis, cells were counted, centrifuged and seeded in fresh cell culture medium II at a density of $1 \cdot 10^6$ cells/ml. As depicted cells were treated with either anti human IgM F(ab)2 fragment (α -IgM), sCD40L (CD40), rh IGF-1 (IGF), rh IL-10 (IL10), ODN2006 (CpG) or combinations of those (for concentrations see Table 8). For all single stimulations a full dosage of stimuli were used (depicted as 1), while a reduced dosage was included in combinatorial experiments (depicted as 0.2). Combinations of stimuli used for linear regression experiments are shown in Table 19.

To analyze pathway activation (immunoblot) cells were stimulated for 1 h at 37°C 5% CO_2 . For gene expression, metabolome and cell cycle analysis cells were stimulated for 24 h at 37°C 5% CO_2 . Precise harvest procedure is described in corresponding method sections.

Inhibitor treatment

Cells were seeded in fresh cell culture medium II (P493-6 = $1 \cdot 10^6$ cells/ml, other cell lines $0.5 \cdot 10^6$ cells/ml) and treated with inhibitors listed in Table 10. In case of stimulated P493-6 Myc^{low} cells, cells were treated with stimuli 3 h after inhibitor treatment. As described before, cells were harvested after 24 h for transcriptomic or metabolome analysis. Samples for western analysis were taken 2 h after inhibitor treatment in OCILy-3, L-428 and CA-46, and 1 h after stimulation in P493-6 Myc^{low} cells. Details for harvesting of cells are described in corresponding method sections.

Transfection of siRNA

For knockdown experiments, siRNA pools against specific targets (see Table 12) were used. siRNAs were transfected into cells by electroporation using Amaxa Nucleofector system according to manual instructions (analog to protocol for Ramos cells). Cell line specific modifications are shown in Table 20. P493-6 cell line was transfected in Myc^{high} state and doxycycline was added 3 h after transfection to generate Myc^{low} cells. All following experiments, including western blot analysis to analyze knockdown efficiency, were performed 24 h after knockdown.

Table 20: Cell line specific transfection parameters

Shown are values for a single transfection.

Cell line	Number of cells	siRNA	Kit	program
P493-6	$4 \cdot 10^6$	4 μg	V	C-009
OCI-Ly3	$2 \cdot 10^6$	2 μg	V	A-020
L-428	$2 \cdot 10^6$	2 μg	L	X-001
CA-46	$2 \cdot 10^6$	2 μg	V	R-013

Table 19: Matrix of stimuli combinations used for linear regression experiments. P493-6 Myc^{low} (0) and Myc^{high} (1) cells were each stimulated with combinations of α -IgM, CD40L, CpG, IGF-1 or IL10. 1 = full concentration, 0.2 = reduced concentration, 0 = no stimulus added. Horizontal lines separate batches.

Sample	CD40L	BCR	IGF	CpG	IL10	Myc	Sample	CD40L	BCR	IGF	CpG	IL10	Myc
1	1	0	0	0	0	1	51	1	0	0	0	0	1
2	0	1	0	0	0	0	52	0	1	0	0	0	0
3	0	0	0	0	0	0	53	0	0	0	0	0	0
4	0	0	0	0	0	1	54	0	0	0	0	0	1
5	0	1	1	1	1	1	55	0	0	0	0.2	1	1
6	1	1	1	1	1	1	56	0.2	0.2	0.2	1	1	1
7	1	1	0	1	0	1	57	0.2	1	1	0	0	1
8	1	0	0	1	1	0	58	1	1	0	1	1	0
9	0.2	1	1	0	1	0	59	1	1	1	1	1	0
10	0	0	0	1	1	0	60	0.2	0	1	0.2	1	0
11	0	1	0	0	0	1	61	0	1	0	0	0	1
12	0	0	1	0	0	0	62	0	0	1	0	0	0
13	0	0	0	0	0	0	63	0	0	0	0	0	0
14	0	0	0	0	0	1	64	0	0	0	0	0	1
15	0	1	0.2	0.2	0	1	65	0.2	1	1	0	1	1
16	1	0.2	0.2	0	0	1	66	1	0.2	0	0	1	1
17	1	1	1	1	0.2	1	67	1	1	0	1	1	1
18	0.2	0.2	0.2	0.2	0.2	0	68	0	0.2	0	0.2	1	0
19	1	0.2	0	0	1	0	69	1	1	1	1	0.2	0
20	0.2	1	0.2	0	0.2	0	70	1	1	0	1	0	0
21	0	0	1	0	0	1	71	0	0	1	0	0	1
22	0	0	0	1	0	0	72	0	0	0	1	0	0
23	0	0	0	0	0	0	73	0	0	0	0	0	0
24	0	0	0	0	0	1	74	0	0	0	0	0	1
25	0.2	0.2	0.2	0	0	1	75	0	0.2	0	0.2	1	1
26	0.2	1	0	0	1	1	76	0.2	0.2	0.2	0.2	0.2	1
27	1	0	0	1	1	1	77	0.2	1	0.2	0	0.2	1
28	0.2	1	0.2	1	0	0	78	0	1	1	1	1	0
29	0	0	0	0.2	1	0	79	0.2	0.2	0	1	1	0
30	0.2	1	0.2	0.2	0.2	0	80	0.2	0.2	0.2	1	1	0
31	0	0	0	1	0	1	81	0	0	0	1	0	1
32	0	0	0	0	1	0	82	0	0	0	0	1	0
33	0	0	0	0	0	0	83	0	0	0	0	0	0
34	0	0	0	0	0	1	84	0	0	0	0	0	1
35	0.2	1	0.2	0.2	0.2	1	85	0.2	1	1	0.2	0	1
36	1	1	0.2	0.2	0	1	86	0.2	0.2	1	0	0.2	1
37	0.2	0	1	0.2	0	1	87	1	0	1	1	0.2	1
38	1	1	0.2	0.2	0	0	88	0	1	0.2	0.2	0	0
39	0.2	1	1	0.2	0	0	89	0.2	0.2	1	0	0.2	0
40	1	0	1	1	0.2	0	90	1	0	1	0.2	0	0
41	0	0	0	0	1	1	91	0	0	0	0	1	1
42	1	0	0	0	0	0	92	1	0	0	0	0	0
43	0	0	0	0	0	0	93	0	0	0	0	0	0
44	0	0	0	0	0	1	94	0	0	0	0	0	1
45	0	0	0	1	1	1	95	1	0	1	0.2	0	1
46	0.2	0.2	0	1	1	1	96	0.2	1	0.2	1	0	1
47	0.2	0	0.2	1	0	1	97	0.2	0	1	0.2	1	1
48	0.2	0.2	0.2	0	0	0	98	0.2	1	1	0	0	0
49	0.2	1	0	0	1	0	99	0.2	0	1	0.2	0	0
50	0.2	0	0.2	1	0	0	100	1	0.2	0.2	0	0	0

Cell duplication assays

To analyze the proliferation capacity of cell lines under different conditions, cell doubling was analyzed 48 h after treatment. For this cells were seeded into 100 μ l of culture medium II using a 96 round bottom well plate. In case of metabolic depletion experiments, culture medium II without the addition of either glutamine or glucose was used. Rescue experiments of glutamine deprivation were performed by adding metabolites listed in Table 9 directly to the media. After addition of metabolites, pH of cell culture media was adjusted to pH 7 by adding 1 M NaOH or 1 M HCl. To account for different cell doubling times, cells were seeded at different densities (P493-6/ OCILy-3 = $5 \cdot 10^5$ cells/ml, L-428 = $3 \cdot 10^5$ cells/ml, CA-46 = $2 \cdot 10^5$ cells/ml). Cells were treated as depicted and incubated at 37 °C 5% CO₂ for 48 h. In case of stimulated P493-6 Myc^{low}, cell stimulation was repeated 24 h after first treatment. After 48 h the total number of viable cells was calculated using hemocytometer and trypan blue exclusion.

2.2.2 Respiratory analysis

To simultaneously measure oxygen consumption rates (OCR) and extracellular acidification rates (ECAR) in stimulated P493-6 Myc^{low} cells the Seahorse XFe96 system was used.

Coating of cell culture plates

To measure suspension cells in a XF analyzer, attachment of the cells to the culture plate was needed. Therefore, a Seahorse 96 cell culture microplate was coated with Cell-Tak according to manufactures protocol. In brief, 18.8 μ l Cell Tak were dissolved in sterile 2.5 ml 0.1 M sodium bicarbonate (pH 8.0) and 9 μ l of 1 M NaOH was added to start adsorption to the plastic surface. 25 μ l of this solution was added to each well of a 96 cell culture plate, incubated for 20 min and washed two times with sterile H₂O.

Measurement of respiratory parameters

P493-6 Myc^{low} cells were stimulated for 24 h in medium II (supplemented with 11 mM glucose and/or 2 mM glutamine), counted and 100 000 cells per well were seeded in XF Base medium (supplemented with 11 mM glucose and/or 2 mM glutamine) according to manufactures protocol for suspension cells. Cells were incubated for 30 min at 37 °C without the addition of CO₂ to allow cells to attach to the surface. In the meantime inhibitors of mitochondrial respiration complexes were prepared and loaded to hydrated assay cartridge. Port loading and concentrations are described in Table 21. The assay cartridge was calibrated, cell plate loaded into XFe analyzer and cycles were performed as listed in Table 23. From these data respiratory parameters were calculated according to manufactures protocol (Figure 3)

Table 21: Injection order for measuring respiratory parameters

Port	Substance	Concentration
A	Oligomycine	1.5 μ M
B	FCCP	0.5 μ M
C	Rotenone	2 μ M
D	Antimycin A	1 μ M

Table 22: Injection order for measuring glutamine dependency

Port	Substance	Concentration
A	Gln	2 mM
B	AOA	500 μ M
C	CB-839	1 μ M
D	Antimycin A	1 μ M

Table 23: Mix and measuring cycle times for XF assay

Command	Time(min)	Port	Repeats
Calibrate			
Equilibrate			
Mix	2		
Wait	2		3
Measure	4		
Inject		A	
Mix	2		
Wait	2		3
Measure	4		
Inject		B	
Mix	2		
Wait	2		3
Measure	4		
Inject		C	
Mix	2		
Wait	2		3
Measure	4		
Inject		D	
Mix	2		
Wait	2		3
Measure	4		

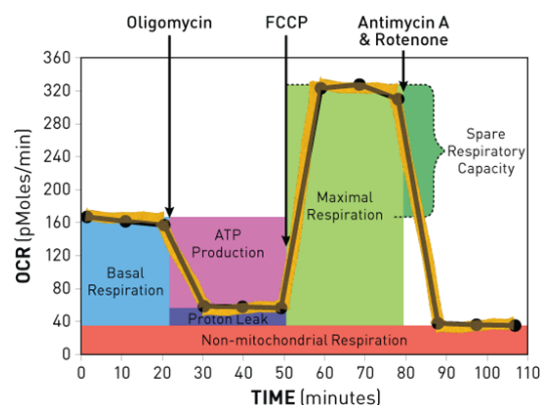


Figure 3: Calculation of resp. parameters
 Picture was taken from manufactures protocol (www.seahorsebio.com).

Measurement of glutamine dependency

Myc^{low} cells were stimulated for 24 h in medium II without glutamine. Cells were counted and 100 000 cells per well were seeded in XF Base without glutamine. Cells were allowed to attached, ports were loaded with inhibitors described in Table 22 and assay was run as described before (Table 23).

2.2.3 Flow cytometry

BrdU proliferation assay

To analyze cell cycle distribution and number of cells in synthesis-phase (S), $5 \cdot 10^5$ P493-6 Myc^{low} cells were labeled with 20 μ M 5-bromo-2'-deoxyuridine (BrdU) for 1h at 37°C 5% CO₂. Cells were centrifuged (400 x g, 3 min, 4°C), resuspended in 300 μ l PBS and three times 300 μ l ice cold 100% EtOH was added stepwise. Cells were fixed at 4°C for at least 3h. Afterwards, cells were centrifuged (400 x g, 3 min, RT) and pellet was permeabilized by incubating in 500 μ l 2 N HCl/0.5% Triton-X100. After centrifugation cells were neutralized by adding 500 μ l 0.1 M sodium tetraborat (pH 8.5) and washed once with 500 μ l 1% BSA in TBS. Cells were resuspended in 50 μ l 1:15 Alexa488 anti-BrdU mouse antibody (diluted in 1% BSA in TBS-T) and stained over night at 4°C. Next day, cells were washed with 1% BSA in TBS-T, resuspended in 1% BSA in TBS and 1 μ g/ml propidium iodide (PI) was added. Fluorescence of cells was analysed in BD FACScan System with gating scheme shown in Figure 4. Cell doublets were excluded by propidium iodide area versus width exclusion.

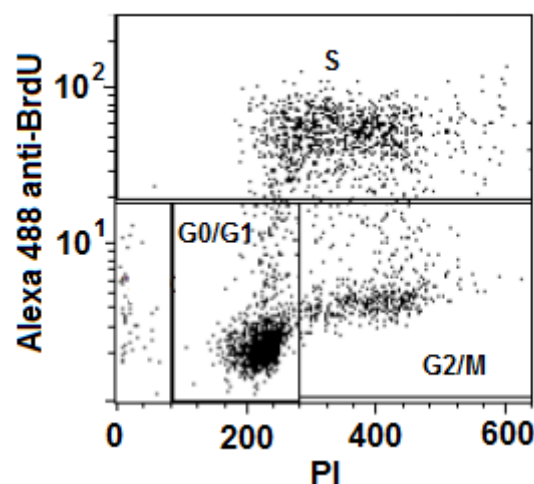


Figure 4: BrdU gating scheme. G0 = resting phase, G1 = Gap 1 phase, S = synthesis phase, G2 = Gap 2 phase, M= mitosis

To analyze cell cycle phase length a BrdU pulse change experiment was performed. P493-6 Myc^{low} cells were stimulated with IL10, CpG or IL10+CpG for 12h to allow cells to enter S-phase. $5 \cdot 10^5$ cells per sample were then pulsed with 20 μ M BrdU for 20 min. Cells were washed once in PBS and seeded in fresh media. After indicated time points cells were harvested and fixed with EtOH as described before. Samples were stained as described before and cell cycle distribution of S-phase gated cells was analyzed by using propidium iodide.

STAT3/NF- κ B translocation assay

To analyze STAT3 and NF- κ B pathway activation, nuclear staining of p-STAT3 and total p65 was performed as previously described (Blaecke *et al.*, 2002). P493-6 Myc^{low} cells were

stimulated with IL10, CpG or both and $5 \cdot 10^5$ cells were collected (400 x g, 3 min, 4 °C) after indicated time points. Pellet was washed one with ice cold PBS and lysed in 500 μ l PIPES (Table 5) for 30 min on ice. Nuclei were isolated by centrifugation (2000 x g, 3 min, 4 °C) and washed two times with cold washing buffer (PBS + 0.1 % BSA + 2 mM MgCl₂) to remove cytosolic proteins. For p-STAT3 staining, nuclei were incubated in 25 μ l 1:5 diluted Alexa488 anti-pSTAT3 (Y705) in washing buffer for 30 min at 4 °C. For NF- κ B staining, nuclei were incubated first in 25 μ l of 1:400 α -NF- κ B in washing buffer (30 min, 4 °C), washed once, followed by a second incubation in 25 μ l of 1:50 FITC anti-rabbit antibody in washing buffer (30 min, 4 °C). After staining nuclei were washed once in washing buffer and propidium iodide was added. Gating for single nuclei was performed using area versus width of the propidium iodide channel.

2.3 Protein biochemistry

2.3.1 Preparation of lysates

Protein lysates were prepared separately for pathway activation analysis or knockdown efficiency control after siRNA knockdown.

Lysates for pathway analysis

After stimulation $1 \cdot 10^6$ cells were sedimented (300 x g, 5 min, 4 °C), washed once in cold PBS and dry pellets were stored at -20 °C. For lysis, cells were thawed on ice and resuspended in cold RIPA buffer (Table 5) supplemented with protease inhibitor cocktail and phosphatase inhibitor (Roche). Cells were lysed on ice for 30 min and debris was removed by centrifugation (13x000 g, 15 min, 4 °C). Supernatant was transferred into a new tube and protein concentration was measured by Bradford assay (Roth) according to manufactures protocol. Protein concentrations of all samples were diluted to 1 μ g/ml with RIPA buffer and 4x loading buffer. Proteins were denaturated for 10 min at 95 °C and directly loaded on a SDS-PAGE or stored at -20 °C.

Lysates after siRNA knockdown

To check knockdown efficiency, 250 000 cells were harvested 24 h after siRNA transfection. Cells were sedimented (300 x g, 5 min, 4 °C) and washed once with PBS. Pellet was directly resuspended in 25 μ l 1x loading buffer diluted with RIPA. Cells were cooked for 10 min at 95 °C and DNA was sheared by sonification (Bioruptor, 6 times 10 sec on/off, high power) to facilitate lysate loading. Lysates were directly loaded on SDS-Page or stored at -20 °C.

2.3.2 SDS-PAGE

For separation of proteins according to molecular weight a sodium dodecyl sulfate (SDS) polyacrylamide gel electrophoresis (PAGE) was used (Laemmli, 1970). Modified gel buffers listed in Table 5 were used to prepare 10 % separation and 5 % stacking gels. Gels were loaded

with 15 µg protein lysate per sample and electrophoresis was performed in 1x Laemmli buffer at constant 40 mA for approximately 1h.

2.3.3 Immunoblotting

Separated proteins were transferred from SDS gel onto a hydrophobic membrane using wet tank sandwich method (Towbin *et al.*, 1979; Renart *et al.*, 1979). Instead of nitrocellulose a PVDF membrane was used, which was activated in 100% MeOH (10 sec), rehydrated in H₂O (2 min) and equilibrated in transfer buffer (5 min, Table 5) prior to use. Membrane and gel were stacked into a wet tank chamber and transfer was performed at 4 °C at 100 V for 1 h. Effective transfer of proteins was visualized by ponceau S staining and unspecific binding sites were blocked using 5% BSA or milk powder for 1 h at RT. After blocking, antibody solutions listed in Table 15 were added over night at 4 °C. Next day, blots were washed three times 10 min with 1x TBS-T and a secondary antibody against the species of the first was added for 1 h at RT. After three additional washing steps, bound antibodies were visualized using a self-prepared luminol/peroxide solution according to Haan & Behrmann (2007) Table 5 and LAS-4000 Image Reader. For reblotting, membrane was stripped for 15 min with 1x ReBlot buffer mild, blocked in 5% BSA or milk powder for 30min at RT and another antibody was added over night as described before.

2.4 Molecular Biology

2.4.1 Spike-in for transcriptomic data

To account for global gene expression shifts in transcriptomic data, a new spike-in method was developed. For this a whole cell spike-in was directly added to a constant number of sample cells during the harvest of treated cells: Sample cells were counted and (if not otherwise depicted) 1·10⁶ cells were transferred into a reaction tube. Previously frozen *drosophila* S2 cells (see section 2.2.1) were thawed in a 37 °C water bath and quickly suspended. 100 µl *drosophila* cell suspension (= 100 000 cells) were added to each prepared human sample. Cells were centrifuged (300 xg, 5 min, 4 °C), washed with cold PBS and stored as dry pellet at -80 °C till RNA isolation.

2.4.2 RNA Isolation

Total RNA of cells was isolated using NucleoSpin RNA kit according to manufactures protocol and RNA was eluted in 50 µl RNase free H₂O. For comparison of whole cell spike-in and commercial gold standard 2 µl of 1:100 diluted ERCC Mix 1 was directly added to the elution volume. RNA concentration was measured by NanoDrop and quality of RNA for sequencing was analyzed using Bioanalyser 2100.

2.4.3 Reverse Transcription

Messenger RNA was transcribed into cDNA using SuperScript II Reverse Transcriptase Kit. In brief, 2 μ l of random hexamer primers (IBA Biotechnology) were added to 1 μ g of total RNA and filled up with H₂O to a total volume of 10 μ l. Sample was denaturated at 70 °C for 10 min and 8 μ l of master reaction mix (Table 24) were added. Reverse transcription was performed in a thermocycler according to Table 25.

Table 24: cDNA master mix

Amount	Substance
4 μ l	5x First strand buffer
2 μ l	0.1 M DTT
1 μ l	Super Script II RT
1 μ l	dNTP mix (each 10 mM)

Table 25: cDNA cycler program

Temperature	Cycle length
25 °C	10 min
42 °C	60 min
65 °C	10 min
4 °C	pause

2.4.4 qRT-PCR (quantitative Reverse-Transcriptase-Polymerase Chain Reaction)

Gene expression was analyzed by SYBR green-based real-time PCR using 7900HT Fast Real-Time PCR System in 384 well plates (Zipper *et al.*, 2004). Per sample 10 μ l reaction solution was used, containing 10 ng DNA and 5.6 μ l self-made SYBR green mix (Table 5) and 3 pmol/ μ l of primer pair. Primer sequences used in this study are listed in Table 16. Amplification cycles were performed as shown in Table 26 and melting curves of amplified products were used as quality control.

Table 26: qRT PCR cycle program

Temperature	Cycle length	Number of cycles
95 °C	15 min	
95 °C	15 sec	
60 °C	1 min	40
95 °C	15 sec	
60 °C	15 sec	
95 °C	15 sec	

The number of cycles used to overcome a certain fluorescent signaling threshold (threshold cycle CT) directly correlates with the amount of DNA used in this assay.

To account for technical differences between samples a first normalization relative to an internal or external (spike-in) housekeeper gene is made:

$$\Delta CT = CT_{geneofinterest} - CT_{housekeeper}$$

To calculate relative changes between a treatment sample and an untreated control a second quotient of ΔCT is formed:

$$\Delta\Delta CT = \Delta CT_{treatment} - \Delta CT_{control}$$

As the number of cycles exponentially correlates with amount of DNA in the sample, relative n-fold changes can be calculated as:

$$Rq = 2^{-\Delta\Delta CT}$$

All ΔCt values in this study were normalized to *Act42A* expression of the *drosophila* spike-in using SDS Rq Manager. Relative fold changes were calculated as $2^{-\Delta\Delta CT}$ relative to the depicted sample.

2.4.5 RNA Sequencing

RNA sequencing was performed in the Transcriptome and Genome Analysis Laboratory (TAL) in Göttingen. Libraries were prepared from 1 μ g total RNA (containing the spike-in cells and the ERCC spike-in Mix 1) using the TrueSeq RNA Sample Preparation Kit v2 (Illumina). Libraries were sequenced in single end mode for 100 cycles on an Illumina HiSeq 2000 with a mean sequencing depth of approximately 40 mio reads/sample.

Normalization and differential gene expression

Read mapping, normalization and calculation of differential gene expression was performed in R in cooperation with the bioinformatic group from the institute of functional genomics (University of Regensburg). Analysis of the spike-in experiment and stimulation experiment was performed by Franziska Taruttis. Analysis of the RNASeq data of IL10+CpG stimulated P493-6 cells was performed by Paula Perez-Rubio and Julia Engelmann. In brief, RNASeq read counts were assigned to Ensembl gene identifiers using 'featureCounts' version 1.4.5. For all datasets, human genes with more than 100 counts for each sample were selected for normalization and differential gene expression analyses of the respective dataset. Global normalization based on endogenous (human) genes was performed using library size factors calculated by 'DESeq2', followed by differential gene expression analysis to estimate log2 fold changes between all sample groups (Love *et al.*, 2014). To estimate log2 fold changes based on the *drosophila* spike-in cells or ERCC kit, library size factors were calculated on the counts of the *drosophila* genes or synthetic gene counts by 'DESeq2', and applied to the human gene counts of each sample.

Gene set enrichment and heatmap calculation

Gene set enrichments were calculated using the top 2000 genes from DESeq2 analysis (sorted after p-value, $\log_2FC > 1$) and online DAVID bioinformatics annotation tool (Huang *et al.*, 2009). Heatmaps of differential gene expression were calculated using the 'heatmap.2' function in the 'gplots' package in R.

2.4.6 Chromatin Immunoprecipitation

Sample lysis and sonification

To analyze binding of STAT3 and p65 to target genes, chromatin immunoprecipitation according to Nowak *et al.* was performed (Nowak *et al.*, 2005). In brief, P493-6 Myc^{low} cells were stimulated with IL10, CpG or IL10+CpG for 1h at 37°C and washed once with PBS. Crosslinking of proteins and chromatin was performed with 2 mM DSG in PBS for 45 min at RT, followed by a second crosslinking with 1 % formaldehyde for 15 min RT. The reaction was stopped by adding 0.1 M glycine for 10 min RT and cells were washed twice with cold PBS (12.000 x g, 1 min, 4°C). Cells were lysed for 15 min on ice in ChIP lyses buffer (Table 5). Isolated nuclei were sedimented (12.000 x g, 1 min, 4°C) and resuspended in ChIP sonification buffer (Table 5). Chromatin was sheared in Bioruptor NextGen using four cycles of 10 min (10 sec on/off duty time) at high power. SDS was quenched by adding 1 % Triton X-100 and debris was removed by centrifugation (13 000 x g, 10 min, 4°C). A small sample was taken for agarose gel analysis and remaining chromatin was quickly frozen in liquid nitrogen and stored at -150°C.

Sonification test

To check for proper chromatin shearing, DNA was precipitated from chromatin by adding two times 100 % EtOH over night at -20°C. DNA was pelleted (15 000 x g, 30 min, 4°C), washed in 70 % EtOH and dried at RT. RNA was digested by adding 3.3 µg/ml RNase for 1 h at 37°C. 15 µl 20 % Chelex solution was added, DNA resuspended and heated at 95°C for 10 min. After cooling, 0.5 µl 20 µg/ml proteinase K was added and protein was digested by heating to 55°C for 30 min. Samples were centrifuged (13 000 x g, 1 min) and 20 µl supernatant was transferred into a new reaction tube. Orange G staining solution was added and samples were run at a 1.5 % agarose gel for 45 min with 100 V. For further proceeding DNA fragments had to be at a size of about 500 bp. Smaller fragmentation could not be achieved due to two-step crosslinking method.

Immune precipitation

For one IP 50 µl of protein A coupled magnetic beads (dynabeads) were washed three times in 0.5 % BSA in PBS. Afterwards, 5 µg of α -IgG, α -STAT3 or α -p65 according to Table 13 were added overnight at 4°C. After three additional washing steps, sheared chromatin of $2 \cdot 10^6$ cells were added to the beads and incubated overnight at 4°C. Next day, beads were washed four times with ChIP RIPA buffer (Table 5) and once in TE buffer. 10 % Chelex were added to the washed beads, resuspended and heated for 10 min 95°C. Protein was digested by

adding 2 μ l of 20 μ g/ml Proteinase K (30min, 65°C) and afterwards inactivated by heating to 95°C for 10 min again. Samples were centrifuged at 12 000 g for 1 min at 4 °C, supernatant transferred into a new tube and DNA was stored at -20 °C.

Preparation of input sample

For each stimulation a portion of the sonificated chromatin was used for generating an input control. 100 % EtOH was added twice the volume of chromatin overnight at -20 °C. Chromatin was centrifuged (12 000 x g, 4 °C, 20 min), washed twice with 70 % EtOH and dried at RT. Afterwards DNA was extracted using Chelex method described above.

Real-time PCR

For quantification of precipitated DNA sequences, qRT-PCR described in section 2.4.4 was used. Isolated DNA was diluted 1:10 and directly used in the described assay. Primers for sequence detection are listed in Table 17. All data were normalized to an inactive (closed chromatin) region called *PRAME* and fold changes were calculated relative to unstimulated Myc^{low} cells.

2.5 Metabolomics

Extraction, measurement and analysis were performed in cooperation with the NMR/mass spectrometry group of the functional genomics department in Regensburg. NMR analysis and mass spectrometry of unlabeled metabolites were performed by Philipp Schwarzfischer, analysis of ¹³C-glutamine labeling by Paul Heinrich.

2.5.1 Sample preparation

¹³C-Glutamine labeling

To analyze fate of glutamine in metabolism, stable isotopic labeling was performed. P493-6 Myc^{high} and Myc^{low} cells were washed once in warm PBS and seeded in cell culture medium II supplemented with 2 mM ubiquitously labeled ¹³C-glutamine. Myc^{low} cells were stimulated with IL10, CpG and IL10+CpG as described before and cells were incubated at 37 °C 5 % CO₂. To confirm steady state of isotopic labeling distribution, time course was performed between 18 h and 30 h after stimulation. No significance difference in isotopic distribution in organic acids was observed, indicating a steady state during this time frame. Therefore, all labeling were performed for 24 h.

Harvest of cells and supernatants

After 24 h cells were counted and 5·10⁶ cells were centrifuged (300 x g, 5 min, 4°C). Supernatants were transferred into a new tube, while cell pellets were washed two times in cold PBS and resuspended in ice cold 80 % MeOH. In the meantime, 10 kD ultra centrifugal filters were activated by adding 3 ml of H₂O and centrifuged for 30 min at 4 000 g. Supernatants were loaded onto filters and centrifuged for 30 min, 4 000 g at 4 °C. Filtrate was transferred into a new tube and both, supernatant and pellet, were stored at -80 °C.

Metabolite extraction form cell pellets

Metabolites were extracted using methanol method as described previously (Dettmer *et al.*, 2011). In brief, cell pellets were vortexed in 80% MeOH and centrifuged (10 000 x g, 6 min, 4 °C). This step was repeated two more times and all supernatants were combined, dried for 2 h in a vacuum evaporator and stored at -80 °C.

2.5.2 NMR spectrometry

Ultrafiltrate of supernatants was mixed with phosphate buffer and 4, and 3-trimethylsilyl-2,2,3,3-tetradeuteropropionate (TSP) dissolved in deuterium oxide as internal standard. NMR measurement was performed on a 600 MHz Avance III spectrometer (BrukerBioSpin, Rheinstetten, Germany) and 1D ¹H and 2D ¹H-¹³C heteronuclear single-quantum correlation (HSQC) spectra were acquired as published before (Gronwald *et al.*, 2008). Absolute concentrations from 1D and 2D NMR data were calculated employing individual peak calibration factors using the NMR quantification tool MetaboQuant (Klein *et al.*, 2013).

2.5.3 Mass spectrometry

Measurement of amino acid, tryptophan derivates, organic acids and MTA metabolites was performed as previously described (van der Goot *et al.*, 2012; Zhu *et al.*, 2011; Stevens *et al.*, 2010). For each metabolite an internal isotope labeled standard was used.

2.6 Statistical and bioinformatic analyses

Linear regression and survival analysis were performed in cooperation with the bioinformatic group of the institute of functional genomics (University of Regensburg). Linear regression of stimulation combinations was performed by Thorsten Rehberg. Kaplan-Meyer curves of GOT2 and comparisons were calculated by Paula Perez-Rubio. Comparative statistics of qRT and cell number data was performed by me.

Linear regression analysis

Linear regression analysis on RNASeq and metabolome data were performed in R with the 'glmnet' package using Lasso regression (Friedman *et al.*, 2010). The Lasso parameter lambda was selected such that it minimizes the cross-validation error. Linear regression analysis on cell cycle regulator gene expression values from RT-PCR measurements and percentage of S-phase were performed within the statistical framework R using the 'lm' function of the 'stats' package. Coefficients of the main effects and the interaction term of IL10 and CpG were estimated and tested for deviation from zero with the t-test using the 'summary.lm' function.

GOT2 survival curves

R-CHOP treated DLBCL patient from Lenz et al. were classified according to their *GOT2* gene expression (Lenz *et al.*, 2008). Only patients with ABC and GCB classification were included. Patients with a *GOT2* expression higher than the median expression of the group were defined as GOT2high whereas patients with an expression level lower than the median were classified as GOT2low. For both groups Kaplan-Mayer curves were calculated and survival curves of groups were compared using the 'survdif' and 'coxph' function in R.

Comparative statistics

Data are shown as mean \pm SD. Statistical analysis of cell numbers and qRT data was performed using Graphpad Prism 6. For all samples, standard normal distributions were assumed and equal variances distributions were tested using Brown-Forsythe test. For multiple comparisons of more than two groups One-way or Two-way ANOVA was used as depicted in figure legends using Bonferroni's post-hoc test for pair-wise group comparisons. P-values of less than 0.05 were regarded as significant.

3 Results

The aim of the study was to identify if and how factors of the GC and more importantly their combinations affect global gene expression in B cells with low levels of the proto-oncogene *c-Myc*. Furthermore the investigation of these stimuli induced gene expression changes on metabolism and proliferation in comparison to *MYC* overexpressing cells was aimed.

Therefore, a B cell model with conditional *MYC* expression was stimulated with different GC derived stimuli and random combination of those. Transcriptome, metabolome and proliferation data of these stimulations were analyzed by linear regression analysis to reveal effects of single stimuli and their combinations on these parameters. To enable the comparison of Myc and stimuli induced gene expression, a normalization on total cell numbers per sample by adding an external spike-in was performed.

From these data, the combination of IL10 and CpG was selected and further analyzed in detail. Proliferation and metabolism of Myc depleted cells after IL10+CpG stimulation was compared to *MYC* overexpressing cells. The involvement of Myc, JAK/STAT and NF- κ B signalling on IL10+CpG stimulation induced gene expression and proliferation was analyzed in more detail. Therefore inhibition of selected pathways by specific small molecule inhibitors and siRNA mediated knockdown of important pathway components were performed. Influence of these pathways on gene expression were analyzed by qRT PCR and chromatin immunoprecipitation.

Finally, similarities and differences of Myc and IL10+CpG stimulation on glutamine metabolism were investigated. Thereby, metabolome as well as glutamine tracing analysis was performed. Dependency of proliferation on different glutamine derived metabolites was revealed by inhibitor treatment, knockdown of metabolic enzymes and metabolic rescue experiments.

The last part, focuses on the validation of the found metabolic dependencies in lymphoma cell lines with aberrant signaling pathway activation and previously published patient data.

3.1 A resting B cell model by Myc withdrawal in P493-6 cells

To compare effects of different signaling pathway and Myc activation in B cells a suitable model cell line is needed. This cell line should show no other variables than the pathway activation and *MYC* expression. For example, stimulated primary B cells cannot easily be compared with a Myc transformed cancer cell line as the latter will have additional genetic alterations. Same genetic differences are also expected when comparing different cancer cell lines. As Myc was described to amplify all genes with open chromatin, the genetic and epigenetic background of a sample greatly influences the targets that are activated by Myc and this might also be true for other signaling pathways (Lin *et al.*, 2012; Nie *et al.*, 2012). To ensure that only pathway dependent changes are observed, a model cell line was needed in which all perturbations were performed on the same genetic background.

3.1.1 Simulating resting B cells by Myc withdrawal in P493-6

The human P493-6 B cell line fulfilled the criteria mentioned above. This B cell line carries a tetracycline repressible *MYC* expression plasmid (Polack *et al.*, 1996). As published before, treating these cells with doxycycline rapidly decreased Myc protein within four to eight hours (Figure 5A) (Polack *et al.*, 1996). While untreated P493-6 cells were highly proliferative, addition of doxycycline greatly decreased the number of cells in S-phase 24 h after treatment accompanied by an arrest of the cells in the G0/G1 cell cycle phase (Figure 5B). Additional to the cell cycle effects, a loss of cell size can be observed within this time frame (Figure 5C). Therefore, the already published data for P493-6 cells (Schuhmacher *et al.*, 1999), (Pajic *et al.*, 2000) could be reproduced and this cell line was chosen as a model for resting (Myc^{low}) and transformed (Myc^{high}) B cells on the same genetic background for most experiments in this study.

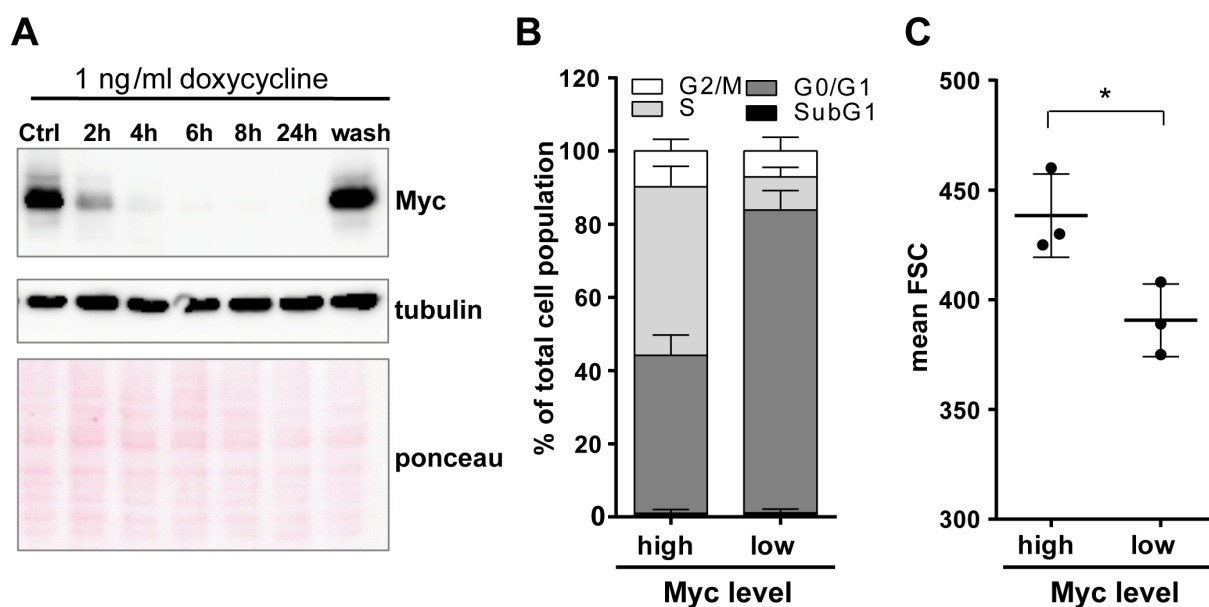


Figure 5: Validation of conditional *MYC* expression, proliferation and growth in P493-6 cells. Previously published experiments were repeated to evaluate P493-6 cells as a suitable model system for further studies (Pajic *et al.*, 2000; Schuhmacher *et al.*, 1999). (A) Immunoblot analysis of Myc protein levels in untreated and doxycycline treated P493-6 cells over time. Removal of doxycycline by multiple washing steps (wash) restored high Myc level. Tubulin and ponceau staining indicate equal loading of samples. (B) Cell cycle analysis of P493-6 Myc^{high} and Myc^{low} cells 24 h after doxycycline treatment. Cell cycle phases were separated by BrdU and PI staining using flow cytometry. Means and SD of three independent replicates are shown. (C) Cell size of Myc^{high} and Myc^{low} cells 24 h after doxycycline treatment. Shown are mean forward scatter (FSC) and SD from samples in B.

3.1.2 Factors of the B cell microenvironment activate P493-6 Myc^{low} cells

Previous experiments in our lab have shown that stimulation of a B cell line with single microenvironmental factors can predict aberrantly activated signaling pathways in lymphoma and can be used to stratify lymphoma patients (Schrader *et al.*, 2012a). However, the used BL-2 cell line already overexpressed Myc and therefore was unable to model activated B cells or lymphoma cells without Myc aberrations. In addition, P493-6 cells with conditional *MYC*

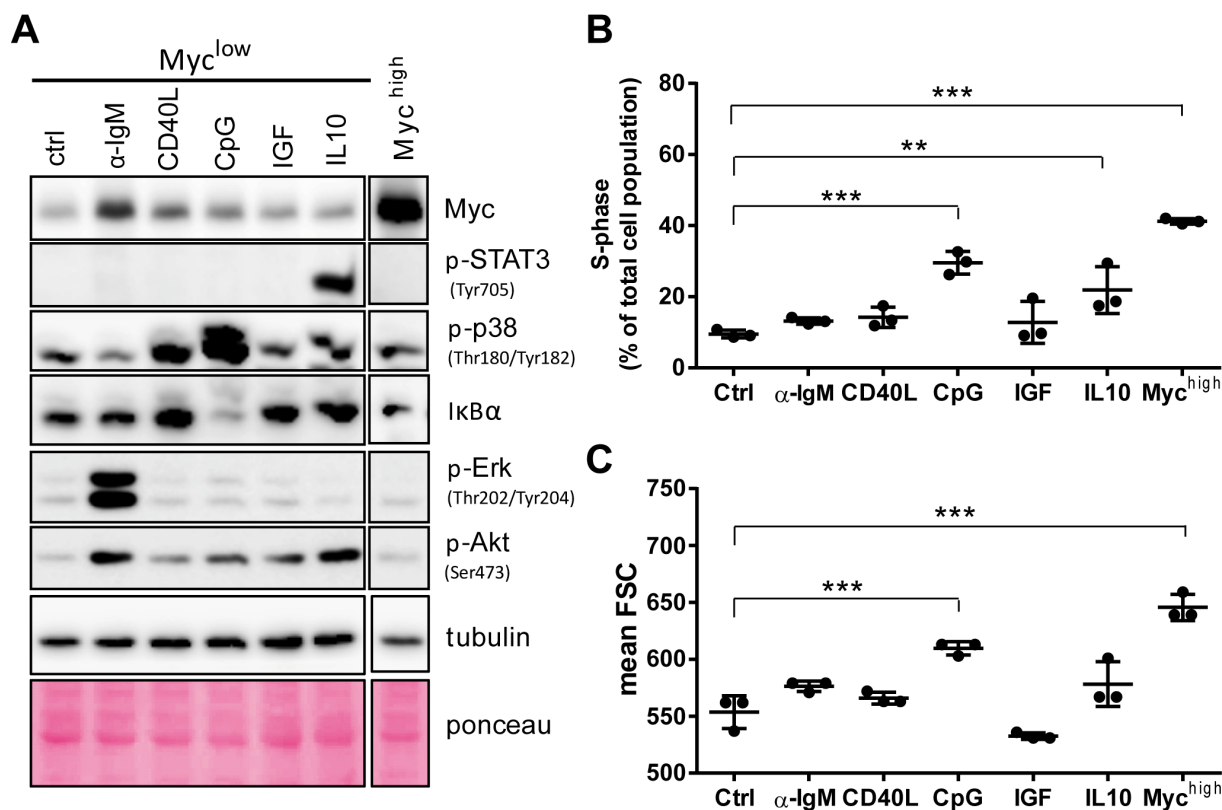


Figure 6: P493-6 Myc^{low} cells respond to stimulation with single B cell activating factors. Myc^{low} cells were stimulated with full concentrations of α-IgM, recombinant CD40L, CpG, recombinant IGF-1 and recombinant IL10 as described in section 2.2.3. (A) Immunoblot analysis of stimulated Myc^{low} and unstimulated Myc^{high} cells. Activation of STAT3, p38, Erk and Akt pathways was detected by phosphorylation specific antibodies 1 h after stimulation. NF-κB activation was accessed by degradation of IκBα. Tubulin and ponceau staining indicate equal loading of protein per sample. (B) Number of cells in S-phase 24 h after stimulation measured by BrdU incorporation and flow cytometry. (C) Cell sizes of stimulated cells shown as mean FSCs from samples described in (B). All experiments were performed in three independent replicates. Mean ± SD and one-way ANOVA results (Bonferroni's posttest) are shown in B and C (** p < 0.01, *** p < 0.001).

expression were frequently used as a model for resting and Myc transformed B cells before (Polack *et al.*, 1996; Pajic *et al.*, 2000). To analyze the effect of microenvironmental factors in Myc depleted cells, P493-6 Myc^{low} cells were used in this study. Cells treated with α-IgM for B cell receptor (BCR) activation, recombinant CD40 ligand (CD40L), the toll like receptor (TLR9) ligand CpG, insulin like growth factor 1 (IGF-1) and interleukin 10 (IL10) and pathway activation was monitored by immunoblot. Activation of different pathways by the stimuli was observed in Myc^{low} cells by visualizing corresponding protein phosphorylation (Figure 6A). Crosslinking of the BCR by α-IgM resulted in a strong activation of the Erk MAPK and PI3K/Akt pathway. Stimulation with CD40L and IGF-1 showed moderate activating effects on the p38 MAPK and Akt. Furthermore, activation of the NF-κB pathway after CpG stimulation was observed by degradation of IκBα, whereas IL10 treatment strongly activated STAT3 signaling, specifically. To analyze the functional impact of these pathway activations on resting P493-6 Myc^{low} cells, cell cycle distribution and cell growth was analyzed 24 h after stimulation by BrdU staining and flow cytometry. Interestingly,

stimulation with either CpG or IL10 significantly increased the number of cells in S-phase while the other factors only mildly affected S-phase entry (Figure 6B). This increase was accompanied by a significant increase in cell size in CpG treated cells as revealed by an increased forward scatter. Only a tendency towards greater cell size was observed after the other stimulations (Figure 6C). These experiments show that P493-6 Myc^{low} cells are reactive towards B cell activating factors and that some of the stimuli can activate these resting cells in terms of inducing cell cycle entry and cell growth. It was therefore concluded that stimulated P493-6 cells are a useful model for to study different pathways activation by stimuli in B cells.

3.2 Development of a cell spike-in to reveal global gene expression changes

Myc was described to dramatically increase total RNA levels in the cell accompanied by an increase in cell size (Lin *et al.*, 2012; Nie *et al.*, 2012). Comparing *MYC* overexpressing with other cells on transcriptomic levels is therefore challenging as total RNA levels can greatly differ between these groups. These differences were shown to hamper gene expression analysis in a way that can only be solved by normalizing gene expression to a constant number of cells (Lovén *et al.*, 2012). As shown in Figure 6 not only Myc but also stimulation can affect the cell size, suggesting that also total RNA levels are affected by the different stimulations. Therefore, normalization on total cell numbers was performed in all stimulation experiments. This normalization can be done by using a stable external normalization control called spike-in like synthetic nucleotides developed by the External RNA Controls Consortium (ERCC)(consortium, 2005). However, commercial available spike-in kits are expensive, limiting their use in daily lab routine for example in qRT experiments. Therefore, a new spike-in method was developed, which is affordable, easy to use and should be applicable for normalization of RNASeq as well as quantitative reverse transcriptase PCR (qRT PCR) data throughout the whole study.

3.2.1 *Drosophila melanogaster* is a suitable spike-in organism

Sun *et al.* (2012) first described whole cell spike-ins in the context of dynamic gene expression analysis. They added a fixed number of 4-thiouridin-labeled whole cells of a different yeast strain to the sample yeast cells and hybridized this mixture to a custom microarray. While this method reliably controls for all technical variations and global gene expression changes in microarray analysis of yeast strains, it is not applicable for RNASeq of human samples. Therefore, an improvement of this methods was aimed in this study in which the addition of whole spike-in cells of a foreign organism to a constant number of human cells controls for technical and biological variations. To reliable normalize human gene expression to genes of a foreign organism both genomes must be as different as possible to minimize the number of genes that would be fitted to both organisms in RNASeq analysis. In contrast, cells

should have equal lysis properties to reliably control for technical variances during cell lysis, excluding bacteria or fungi cells as suitable spike-in cells. For animal cells that fulfill these criteria, cell lines should be available and the genome must be completely annotated, like for example mouse or *drosophila melanogaster*. While human and mouse genomes show a broad overlap of conserved gene sequences, *drosophila* genes should be evolutionally distant enough to distinguish most of the genes.

In cooperation with the biostatistical group from Regensburg an *in situ* experiment was performed to evaluate the overlap of between human and *drosophila* genes. Hence RNASeq libraries from *drosophila* S2 cell line (accession numbers SRR569914 and SRR424185) and human P493-6 cell line (accession numbers SRR567561 and SRR567562) from the SRA database were compared. Using bioinformatical tools, reads from one organism were aligned to the genome of the organism itself or a concatenated genome consisting of all *drosophila* and human genes. Mapping human or *drosophila* gene counts to the concatenated genome showed that the *drosophila* spike-in did not significantly alter the number of genes that are uniquely identified as human genes and vice versa.

In summary, *drosophila* cells might be a suitable spike-in organism, as equal lysis properties are expected and gene sequences are distant enough from human to be reliably distinguished in RNASeq analysis.

3.2.2 *Drosophila* spike-in reliably detects global gene expression changes

Next, an *in vitro* experiment was designed to proof the capacity of *drosophila* spike-in cells to reveal global gene expression changes. Different total amounts of RNA per cell were simulated by using increasing amounts of human P493-6 B cells as follows. Fixed numbers of P493-6 cells ($0.5 \cdot 10^6$ cells, $1 \cdot 10^6$ cells and $2 \cdot 10^6$ cells) were spiked each with an equal amount of *drosophila* cells. For this, aliquots of $1 \cdot 10^6$ frozen *drosophila* cells (from one freezing stock) were thawed and $100 \mu\text{l}$ (= 100 000 cells) were directly added to each sample (see scheme in Figure 7A). Cells were equally harvested, lysed and total RNA was extracted in equal volumes. After extraction an equal amount of commercial ERCC nucleotide spike-in was added as gold standard. This experimental setup resulted in an increased total RNA content between the different conditions (Figure 7B) and also enabled precise fold changes predictions between the groups (Figure 7C). The experiment was designed to predict a fold change of two between groups B and A as well as C and B (\log_2 fold change = 1), while between sample C and A a fold change of four (\log_2 fold change = 2) was predicted.

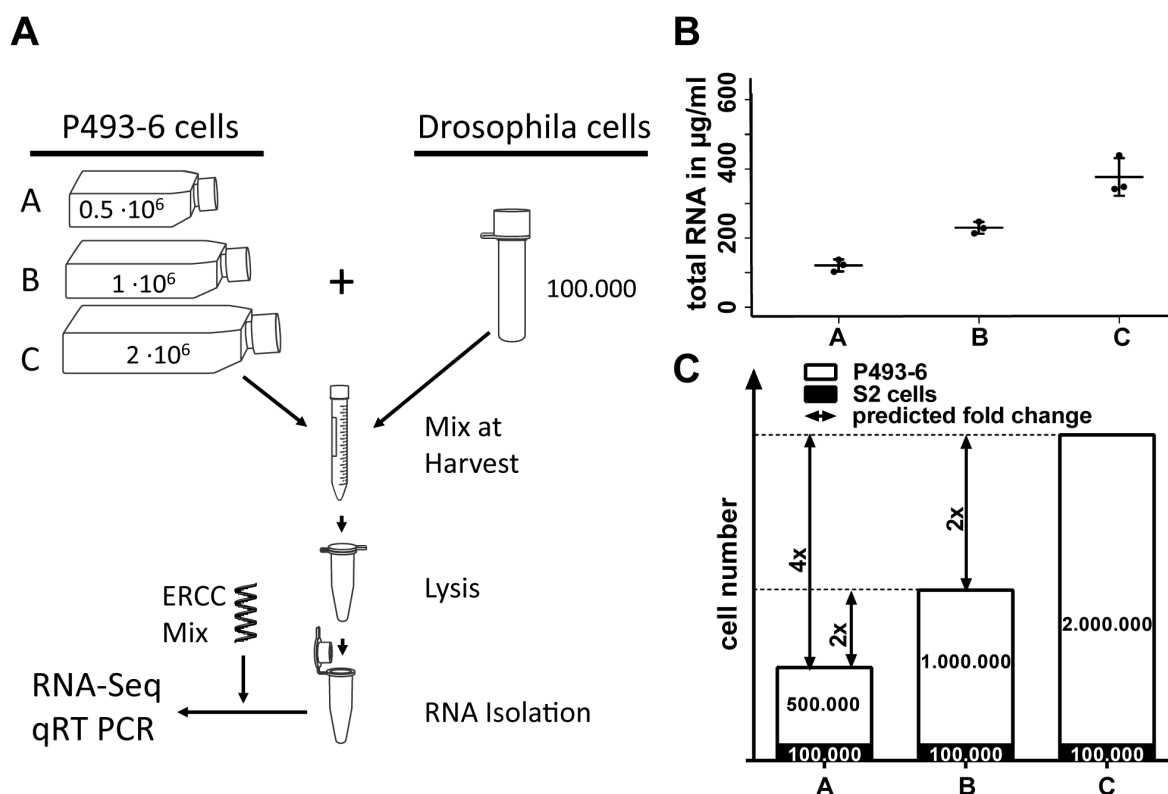


Figure 7: Experimental design of *drosophila* spike-in experiment.

(A) Scheme of dilution experiment. 100 000 *drosophila* cells were directly added to sample tubes containing $0.5 \cdot 10^6$, $1 \cdot 10^6$ and $2 \cdot 10^6$ cells. Cells were centrifuged together, washed and lysed. RNA was isolated in equal amounts of water and ERCC spike-in mix was added to total RNA solution. Samples were then sequenced or analyzed by qRT PCR. (B) Total RNA concentration of samples described in A after elution. (C) Scheme of sample composition and predicted fold changes of the experiment in A.

Isolated RNA of all samples were sequenced and gene expression was normalized on cell number by factors calculated from *drosophila* gene count or ERCC spike-in. As reference, gene expression was normalized without spike-in assuming a constant RNA amount between all samples. Both cell count based normalization models correctly revealed fold changes of total RNA leading to a distance of \log_2 fold change to the expected fold change about zero (Figure 8A). However, *drosophila* spike-in even outperformed ERCC spike-in with a median directly at zero. In contrast, calibration assuming a constant RNA amount failed to predict any fold changes leading to a difference between one and two. In addition to prediction of global fold changes, normalization on *drosophila* spike-in revealed true fold changes on single gene expression levels as shown for the gene *ABL* (Figure 8B). These fold changes were not only observed in RNASeq data, but could be confirmed in qRT PCR on the same samples as well (Figure 8C). For this a primerset against the *drosophila* actin gene (*ACT42A*) was designed, which showed high enough expression levels to be precisely detected in the added 100 000 *drosophila* cells. Calculation of ΔCt between the human *ABL* and *drosophila* *ACT42A* revealed two fold changes between the groups B and A and C and B (\log_2 fold change = 1). A fold change about four (\log_2 fold change = 2) was observed between C and A. Importantly, calculating ΔCt relative to the human housekeeper *GAPDH* did not result in any difference between the groups.

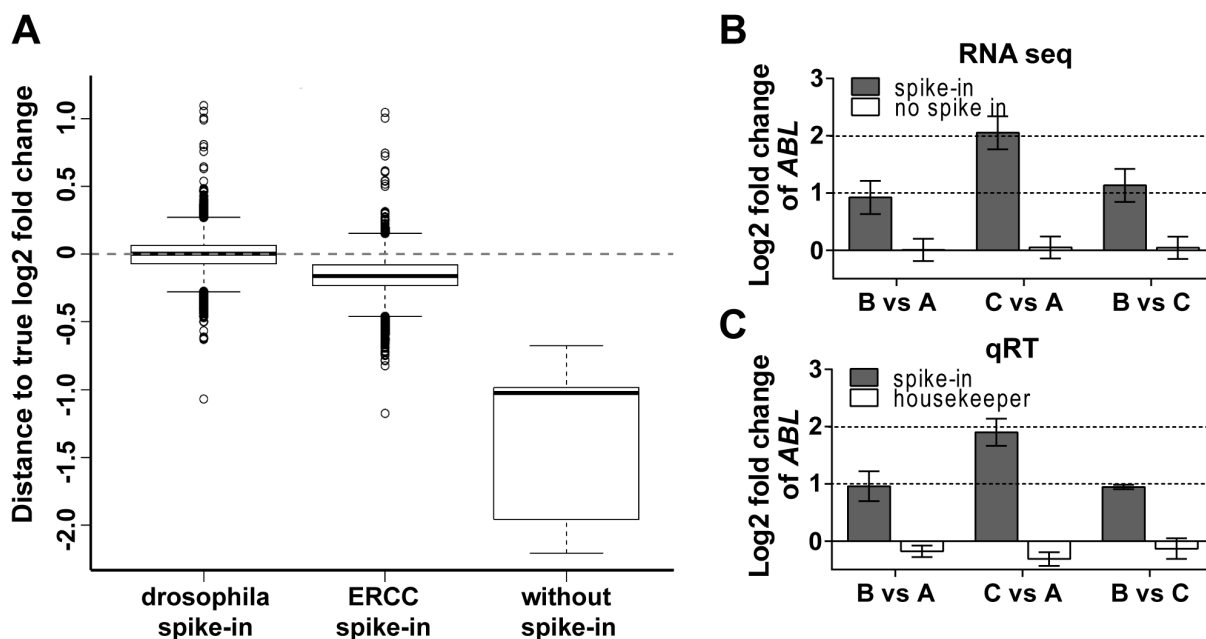


Figure 8: Gene expression normalization on *drosophila* spike-in reveals true fold changes in dilution experiment.

(A) Distance of RNASeq log₂ fold changes relative to predicted log₂ fold changes of samples described in Figure 7. Fold changes between samples were normalized either to *drosophila* cell spike-in, ERCC mix or constant RNA amount (without spike-in). Correct fold changes scatter around zero (dashed line). (B) RNASeq log₂ fold change of *ABL* expression of samples in A calculated with or without *drosophila* spike-in normalization. Means \pm SD are shown. (C) qRT analysis of *ABL* gene expression from same RNA samples as used for A and B. Fold changes were calculated relative to *drosophila ACT42* (spike-in) or human *GAPDH* (housekeeper). Shown are mean expression values \pm SD of three replicates. Dashed lines represent predicated fold changes.

Therefore it was concluded that normalization on *drosophila* spike-in cells is able to expose global gene expression amplification in RNASeq as well as qRT PCR data.

3.2.3 Proof of principle: Spike-in cells reveal Myc induced global amplification

Next, the already published differences in total RNA levels between P493-6 Myc^{high} and Myc^{low} cells were used to proof the capacity of *drosophila* cells to reveal global gene expression amplification. Thus, a constant number of Myc^{high} and Myc^{low} cells were spiked with *drosophila* cells, harvested and RNA was isolated. Measurement of total RNA proofed that Myc^{high} cells contained two times more total RNA per cell as Myc^{low} cells consistent with the previously published data (Figure 9A). Gene expression of both samples was then analyzed by RNASeq and qRT PCR. The published amplification of gene expression was not detected in RNASeq data when both samples were normalized on equal RNA amounts (Figure 9B). However, when genes were normalized on *drosophila* gene expression a global shift of human gene expression about two to four times was observed in Myc^{high} compared to Myc^{low} cells(log₂ fold change between one and two). As shown in the dilution experiment described before, this amplification could be confirmed on single gene expression level by qRT PCR (Figure 9C). While normalization to the human *GAPDH* housekeeper predicted equal up and down regulation in the selected gene set (*IL10R*, *SOCS1*, *ID3*, *CDKN1A*, *PARP*,

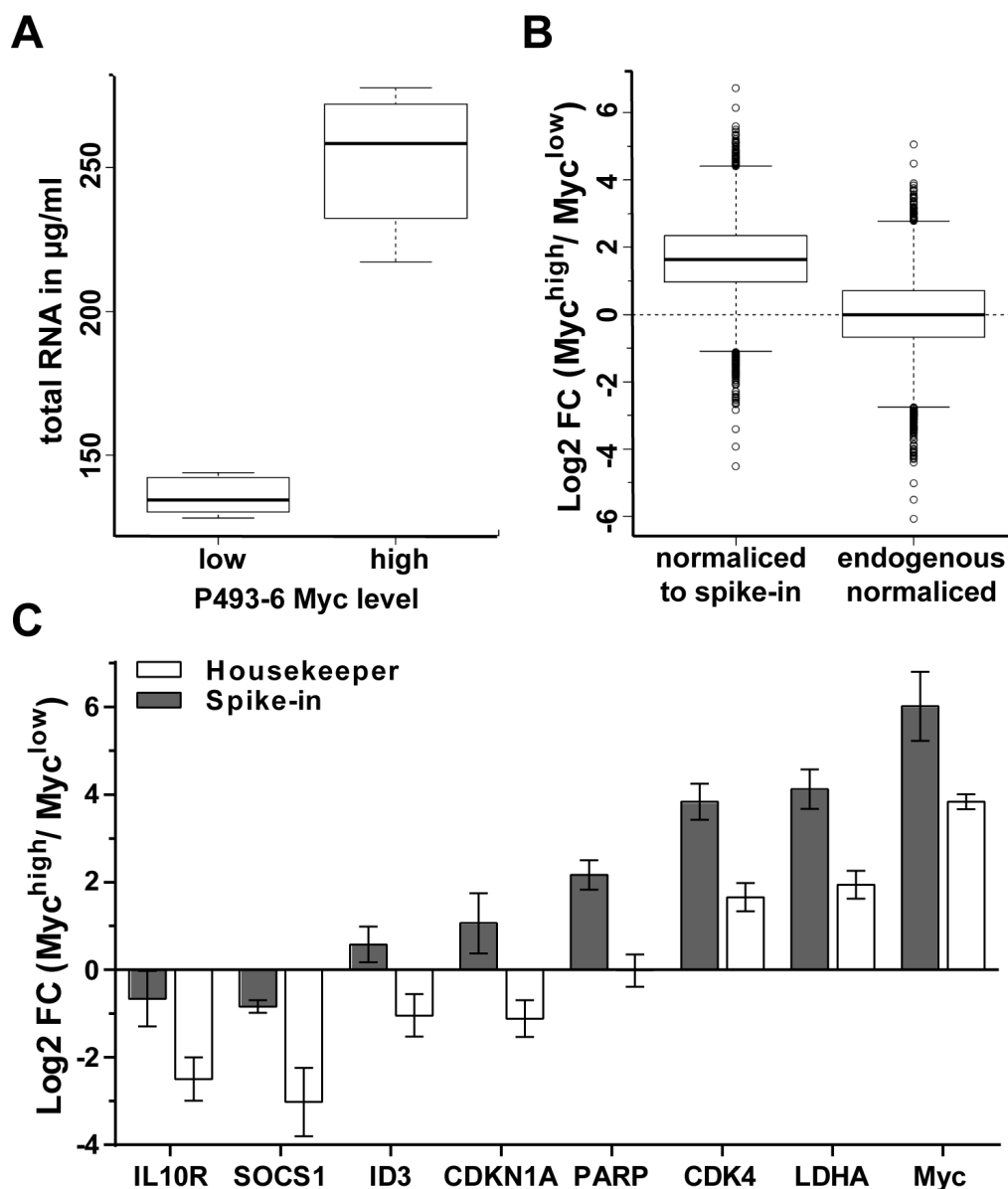


Figure 9: Normalization on *drosophila* spike-in reveals global gene up-regulation in Myc^{high} cells.

(A) Total RNA concentrations of one million Myc^{low} and Myc^{high} cells ($n=10$). (B) Log_2 fold changes of RNASeq data between Myc^{high} and Myc^{low} cells. Data was normalized either on *drosophila* gene counts (spike-in) or left without spike-in calibration (endogenous) ($n=10$). (C) qRT analysis of a panel of differential regulated genes. Gene expression changes between Myc^{high} and Myc^{low} cells were either normalized to human *GAPDH* (housekeeper) or *drosophila ACT42A* (spike-in). Mean expressions \pm SD of three independent replicates are shown.

(*CDK4*, *LDHA*, *MYC*), normalization to *drosophila* genes shifted expression of these genes upwards. Thereby, only expression of *IL10R* and *SOCS1* were repressed by Myc upregulation, while other genes were variably up regulated. Therefore, the global RNA amplification due to Myc and its impact on gene expression normalization could be also confirmed in qRT PCR data. As *drosophila* cells are a reliable tool to detect global gene expression amplification in B cells, this spike-in method was used in all following gene expression analyses to enable the comparison of gene expression of Myc depleted, Myc overexpressing and stimulated cells.

3.3 Analysis of combinatorial stimulation effects in Myc^{low} cells

Physiological activation of B cells is not mediated by a single factor, but by a mixture of different stimuli and pathway activations (Galibert *et al.*, 1996; Rousset *et al.*, 1992). To achieve highest variability in signaling pathway activation, Myc^{low} and Myc^{high} cells were each stimulated with 40 different combinations of α -IgM, CD40L, IGF-1, CpG and IL10, each in two different concentrations (see Table 19, p. 28). Due to the high number of samples experiments were performed in 10 batches each consisting of an unstimulated Myc^{low} and Myc^{high} sample, one single simulation and three combinatorial stimulations per Myc status leading to 100 samples in total. Thereby, stimulations were distributed randomly to minimize batch effects. From all stimulations, samples were taken for RNASeq, intracellular metabolome analysis and BrdU staining 24 h after stimulation. In cooperation with the Biostatistical Institute of the University of Regensburg, effects of one single stimulus or the combination of two stimuli on gene expression, metabolism and proliferation of Myc^{low} cells were calculated by linear regression. Notably, higher combinations of stimuli (for example combination of three stimuli) were not considered as they would have led to overfitting of the data. Stimulations of Myc^{high} were needed to increase the statistical power and minimize cross validation errors. *MYC* expression levels were considered as independent factors and effects of stimuli on Myc^{low} cells were predicted by setting the Myc coefficient and $\text{Myc}/\text{stimuli}$ interaction terms to zero in the linear regression model. Therefore, only effects of the stimuli on Myc^{low} cells on global gene expression, metabolism and proliferation are presented below.

3.3.1 Stimuli combinations induce cooperative changes in global gene expression and metabolome in Myc^{low} cells

Linear regression analysis of the spike-in normalized RNASeq data of the stimulated P493-6 cells revealed that all stimuli used in this study increased the expression of the majority of genes, while nearly no genes were downregulated (Figure 10A). Values of gene expression up-regulation greatly differed between single stimuli. While IGF-1 and CD40L mildly increased global gene expression, α -IgM, CpG and IL10 stimulated cells showed an even increased expression of the same genes. Investigating stimuli combinations, strong positive synergistic effects on global gene expression could be observed after CD40L+IGF-1 and IL10+CpG stimulation. In these cases the combinations of stimuli resulted in a stronger increase in gene expression than the simple addition of the single stimulation effects. As IGF-1 and CD40L showed only minor effects on gene expression in single stimulations, their combination just increased gene expression to a level comparable to α -IgM or CpG alone. In contrast, IL10 and CpG already showed strong positive effects on gene expression leading in combination to the highest changes in expression levels of all calculated stimuli combinations. In contrast to these two combinations, the majority of stimuli combinations showed additive or synergistic negative effects on gene expression. In the last case, a lesser increase in gene expression than

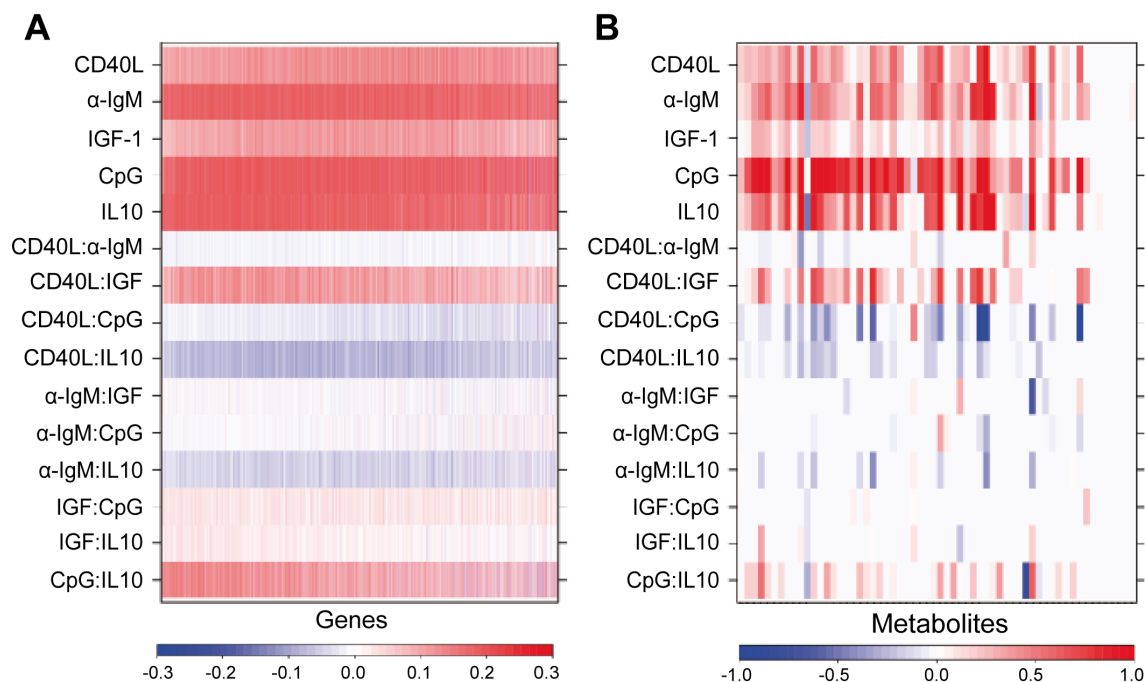


Figure 10: Linear regression analysis reveals cooperative effects of stimuli on global gene expression and metabolite abundance.

(A) Heatmap of regression coefficients of single stimuli and the interaction terms of two stimuli on gene expression in *Myc*^{low} cells. *Myc*^{low} and *Myc*^{high} cells were stimulated with α-IgM, CD40L, IGF-1, CpG and IL10 according to Table 19 (p. 28), RNASeq was performed and data was normalized on *drosophila* cell spike-in. Coefficients and interaction terms of stimuli and *Myc* were calculated by linear regression analysis and coefficients of *Myc* and *Myc* interaction terms were set to zero. Red color indicates increased gene expression for single stimulations. For combinations of stimuli the following color code is used: blue = synergistic negative effects, white = additive effects, red = synergistic positive effects. (B) Heatmap of regression coefficients of intracellular metabolite abundance (pmol/1·10⁶ cells) measured by mass spectrometry of samples in A. Analysis was performed analog to A. Same color code is used. Scaled regression coefficients of A and B are provided as digital data (Supplemental Table 1+2, Appendix, p. 119).

the theoretical addition of the single stimuli was observed. This negative interactions on gene expression are a hint for negative influences between the different signaling pathways or a saturation of a common used pathway.

Interestingly, a comparable pattern of effects could be observed in changes of intracellular metabolite abundance measured by mass spectrometry (Figure 10B). Strongest changes were mediated by CpG stimulation alone, followed by IL10 and α-IgM. Again, CpG and IL10 combination showed largest changes in intracellular metabolite abundance based on a positive synergistic effect.

In summary, a quantitative but not qualitative difference induced by the different stimuli was observed on global gene expression. This quantitative response was further modified by costimulation with a second stimulus, mostly resulting in additive or less than additive effects. Importantly, IL10 and CpG combination showed clear synergistic effects on gene expression as well as metabolite abundance leading to the strongest overall changes in gene expression and metabolites observed in this study.

3.3.2 Stimulation induced cell cycle entry correlates with metabolic changes

Due to the qualitative equal patterns of global gene expression and metabolism changes and the increase in S-phase shown for single stimuli (Figure 6), a strong correlation of both factors to cell proliferation was considered. To test if metabolic changes correlated with cell cycle changes in Myc^{low} cells, supernatant metabolite turnover and intracellular metabolite abundance were plotted against the number of cells in S-phase 24 h after stimulation. Combination of stimuli resulted in a variety of S-phase values and as expected, most of the measured metabolites correlated with these (data provided at the). Most of all, glutamine and glucose uptake and lactate secretion fitted the number of cells that entered S-phase (Figure 11).

Thereby, an increase of replication and metabolism comparable to unstimulated Myc^{high} cells was achieved by a defined set of stimuli combinations. This positive correlation was also reflected in the abundance of TCA intermediates represented by intracellular citrate levels (Figure 12A). In contrast, a negative correlation between intracellular aspartate levels and cell cycle entry was observed (Figure 12B). Interestingly, while nearly all measured metabolites correlated with the number of cells in S-phase, alanine levels were only increased in Myc^{high} cells but not in any of the stimulations in Myc^{low} cells (Figure 12C). This difference indicates specific metabolic reprogramming in Myc^{high} cells.

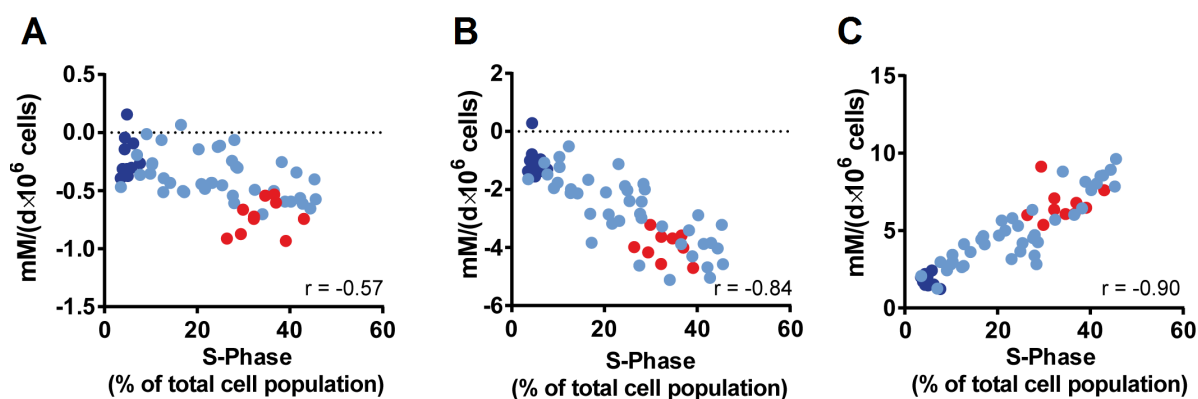


Figure 11: Extracellular turnover of metabolites correlates with cellular replication.

Correlation of daily metabolite turnover from cell culture media and corresponding number of cells in S-phase of unstimulated Myc^{low} , Myc^{high} and stimulated Myc^{low} cells 24 h after stimulation. Shown are consumption of glucose (A), glutamine (B) and secretion of lactate (C) from ten replicates of Myc^{low} (dark blue), nine replicates of Myc^{high} (red) and 40 different stimulations of Myc^{low} cells (light blue) according to Table 19 (p. 28). Pearson correlation coefficients (r-values) are shown in the lower right. Further S-phase and metabolite measurements are provided as digital data (Supplemental Table 3, Appendix, p. 119).

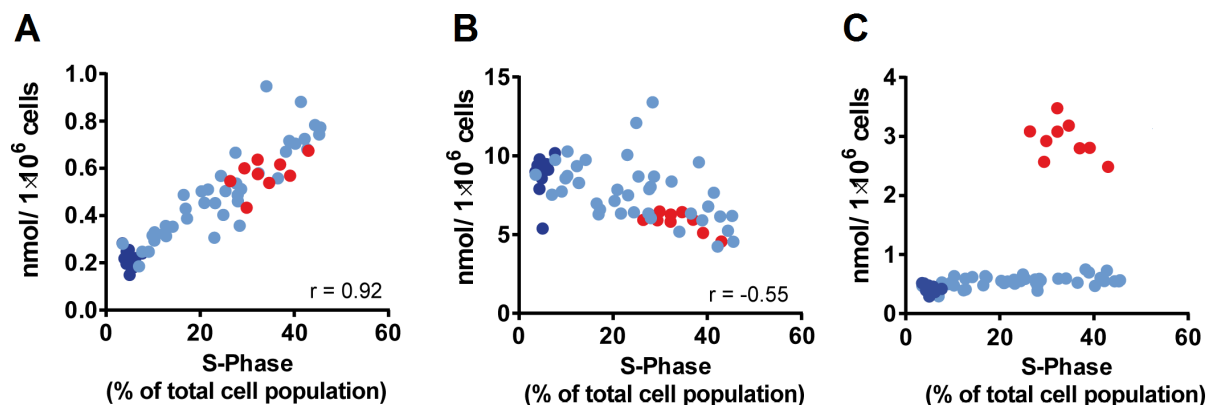


Figure 12: Intracellular metabolites differentially correlate to cellular replication rates.

Correlation of intracellular metabolites and corresponding number of cells in S-phase of unstimulated Myc^{low} , Myc^{high} and stimulated Myc^{low} cells 24 h after stimulation. Shown are intracellular levels of citrate (A), aspartate (B) and alanine (C) from ten replicates of Myc^{low} (dark blue), nine replicates Myc^{high} (red) and 40 different stimulations of Myc^{low} cells (light blue) according to Table 19 (p.28). Pearson correlation coefficients (r-values) are shown in the lower right. Further S-phase and metabolite measurements are provided as digital data (Supplemental Table 3, Appendix, p.119).

3.3.3 S-phase entry of Myc^{low} cells is mainly driven by combined IL10 and CpG stimulation

As described above, IL10+CpG stimulation synergistically increases metabolite abundance and global gene expression in Myc^{low} cells (Figure 10). To reveal the effect of stimuli combination on proliferation in Myc^{low} cells linear regression analysis of BrdU incorporation, representing the number of cells in S-phase, was performed. Thereby, the regression analysis was able to predict BrdU incorporation after single stimulation comparable to the values observed above (Figure 6B). Additionally, linear regression analysis predicted a strong increase in BrdU incorporation for IL10+CpG and CpG+a-IgM stimulation (Figure 13). In contrast, a less than additive S-phase entry was predicted for most of the other stimulation combinations and total incorporation was not further increased than only CpG stimulation alone.

As described in the introduction a synergistic effect of CpG+BCR was analyzed in B cells before (Bernasconi *et al.*, 2003). In contrast, no synergy of IL10 and CpG on gene expression, metabolism or proliferation was described so far. Therefore, stimulations of Myc^{low} cells with IL10+CpG were chosen for further detailed analysis in this thesis work.

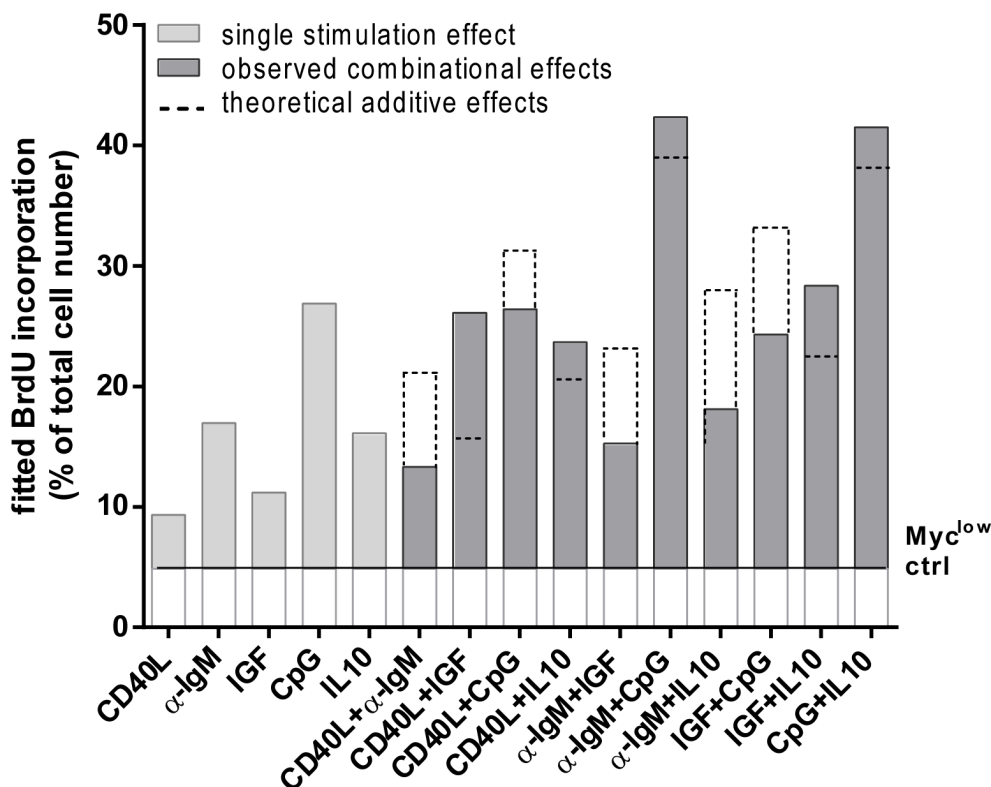


Figure 13: IL10+CpG stimulation synergistically induce S-phase entry in Myc^{low} cells.

Linear regression analysis of BrdU incorporation 24 h after stimulation of P493-6 according to Table 19 (p. 28). Regression coefficients for single stimuli and combinations were calculated as described before. Intersect of regression is shown as Myc^{low} ctrl line. Single stimuli are shown by their coefficients, combinations by the addition of the coefficients of the two single stimuli plus their interaction term. Expected additive effects of two stimuli are shown as dashed line. Observed effects under the line represent negative synergistic effects, above positive synergism. Absolute linear regression coefficients are shown in Table 30 (Appendix, p. 117)

3.4 Comparison of IL10+CpG and Myc induced gene expression

So far predictions of the stimuli on gene expression were performed by linear regression analysis and thus limited for functional analysis. To get further insight in the synergistic effect of IL10+CpG stimulation and to compare its gene expression to Myc induced gene expression changes, RNASeq of untreated Myc^{low} , IL10, CpG and IL10+CpG stimulated Myc^{low} and Myc^{high} cells was performed in triplicates and fold changes relative to Myc^{low} cells were compared. Figure 14 shows \log_2 fold changes (\log_2FC) of the top 200 differentially regulated genes in IL10+CpG stimulated Myc^{low} cells.

As predicted by the linear regression analysis (Figure 10A), single IL10, CpG and IL10+CpG stimulation increased the expression of the same set of genes. Furthermore, a stronger up-regulation of these genes was observed in IL10+CpG stimulated cells, which was mostly qualitative and qualitative comparable to Myc overexpression. However, a small set of genes was only increased after IL10+CpG stimulation, while some genes were even stronger up-regulated in Myc^{high} cells.

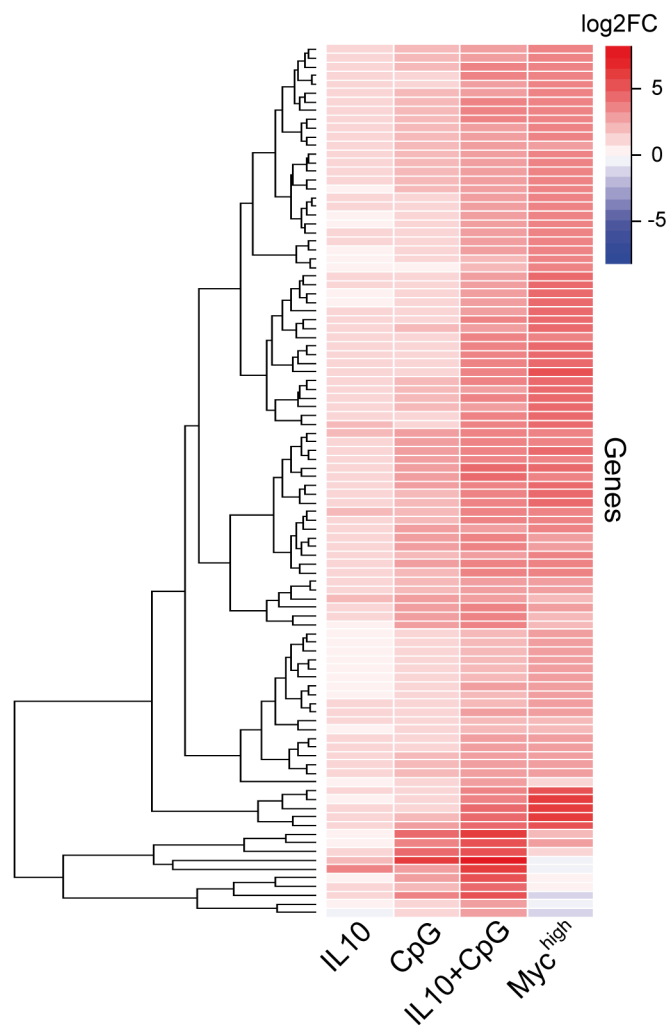


Figure 14: Comparison of IL10, CpG, IL10+CpG stimulation and Myc induced gene expression.

Heatmap of gene expression changes of three replicates of IL10 and CpG single and double stimulated Myc^{low} and Myc^{high} cells 24 h after stimulation. Gene expression was normalized on *drosophila* spike-in and differential expressed genes relative to unstimulated Myc^{low} cells were calculated for each sample. The top 200 differential regulated genes of IL10+CpG stimulated cells are shown. Heatmap color code of log2 fold changes is shown in the upper right. Original Log2FC data are provided digitally (Supplemental Table 4 , Appendix, p. 119)

To define which genes were differently expressed between IL10+CpG stimulated Myc^{low} and Myc^{high} cells, a more detailed comparison of IL10+CpG and Myc induced genes was performed. For this the top 2000 upregulated genes in IL10+CpG stimulated Myc^{low} and Myc^{high} cells were calculated ($\log_2\text{FC} > 1$, ranked by p-value). Overlap of these gene sets is shown in Figure 15A. Out of the top 2000 genes of each stimulation there is an overlap of 1376 that are upregulated in each scenario. Gene set enrichment analysis of this overlap showed, that both, IL10+CpG stimulation and *MYC* overexpression, highly induced the expression of cell cycle and various metabolism associated genes (Figure 15B and Table 29, Appendix p. 115) in line with the predicted DNA replication and metabolism changes shown above (Figure 11).

About 600 genes were only found within the top 2000 of either IL10+CpG stimulated Myc^{low} or Myc^{high} cells (Figure 15A). Gene set enrichment analysis of these genes showed, that the genes induced by IL10+CpG stimulation mainly included JAK/STAT and TLR signaling associated genes (Figure 15C and Table 27, Appendix p. 114), reflecting the extracellular pathway activation by IL10+CpG stimulation that was missing in Myc overexpressing cells. On the other hand, Myc^{high} cells showed greater induction of ribosomal and metabolic genes including alanine metabolism (Figure 15D and Table 28, Appendix p. 114). However, it has to be mentioned that in both cases nearly 10 000 genes were differently to unstimulated Myc^{low} cells expressed. Therefore some of these genes upregulated under one condition might also be upregulated in the other condition, but to a much lesser extent. In summary, the by linear regression analysis predicted synergistic effect of IL10+CpG stimulation on gene expression was confirmed. Furthermore, gene expression changes affecting cell cycle and most metabolic genes were mostly qualitative and quantitative comparable to Myc induced gene expression. Nevertheless, some stimulation and Myc specific changes seem to exist which also may affect metabolism in Myc^{high} cells. Therefore, in a step by step approach similarities and differences in cell proliferation and metabolism of both Myc^{high} and IL10+CpG stimulated Myc^{low} cells were analyzed.

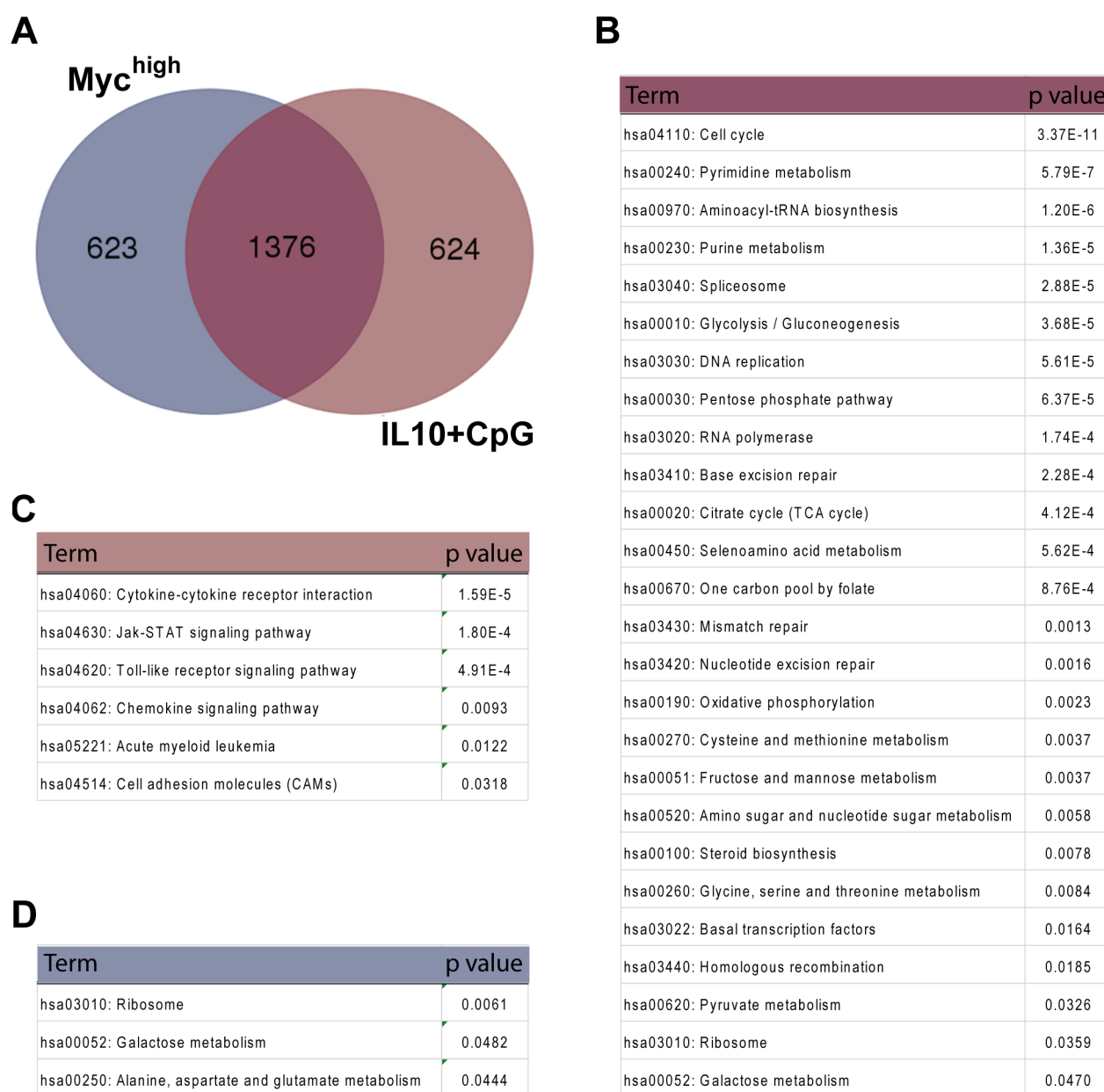


Figure 15: Comparison and functional annotation of IL10+CpG stimulation and Myc induced gene expression.

(A) Venn diagram of top 2000 differential expressed genes ($\log_2FC > 1$, p-value ranked) of IL10+CpG stimulated Myc^{low} and Myc^{high} cells compared to Myc^{low} cells. (B-D) KEGG pathway enrichment of genes grouped in A calculated by DAVID online annotation tool (Huang *et al.*, 2009). Gene set enrichment of the overlap in A is shown in Figure B. Pathways of only IL10+CpG stimulation induced genes are shown in C, only Myc induced genes in D. Pathways with adjusted p-values smaller than 0.05 were assumed to be significant enriched of the differential expressed genes. List of genes included in each gene set is shown in Table 29 to Table 28 in the Appendix (p. 115). \log_2FC of the genes are provided digitally as Supplemental Table 4 (Appendix, p. 119.)

3.5 Investigation of IL10R and TLR9 activation in B cell proliferation

The previous results suggest a synergy of IL10 and CpG stimulation on proliferation. This assumption was based on the linear regression analysis of cells entering S-phase after stimuli combination and an increase of cell cycle associated genes after combined IL10+CpG stimulation (Figure 13 and Figure 15). To get further inside into the synergy of IL10+CpG stimulation on proliferation, cell cycle phases and cell doubling after stimulation were analyzed in detail.

3.5.1 Combined IL10 and CpG stimulation induces cell doubling in *Myc*^{low} cells

To confirm the synergistic effect of IL10+CpG stimulation on S-phase entry, *Myc*^{low} cells were treated with single IL10 or CpG or the combination of both for 24 h and BrdU incorporation was compared to *Myc*^{high} cells. As predicted an additional increase in BrdU incorporation was observed after IL10+CpG stimulation which was comparable to *MYC* overexpression (Figure 16A). However, the number of cells undergoing active DNA synthesis does not necessarily reflect cell proliferation as cells also must be able to divide and constantly enter a new round of cell cycle to effectively double cell numbers over time. Therefore, cells were stimulated every 24 h and proliferation of cells was accessed by daily cell counting (Figure 16B). Interestingly, only IL10+CpG but not IL10 or CpG stimulated cells were able to exponentially increase the number of cells over three days. Furthermore, a comparable proliferation of IL10+CpG stimulated *Myc*^{low} to *Myc*^{high} cells was observed.

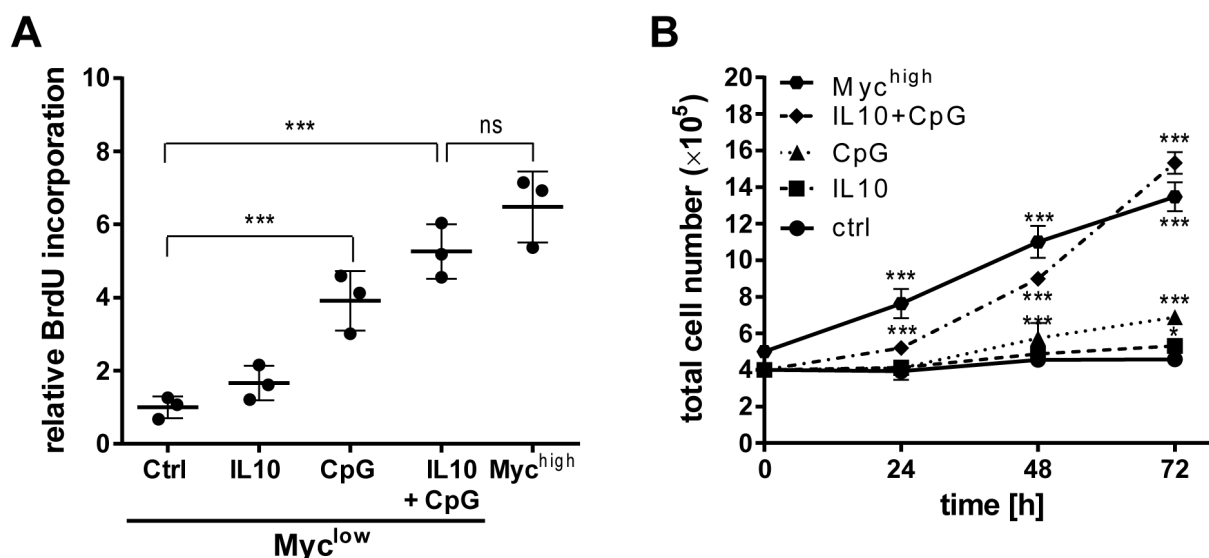


Figure 16: IL10+CpG stimulation induces proliferation in *Myc*^{low} cells comparable to *MYC* overexpression.

(A) BrdU incorporation of IL10, CpG and IL10+CpG stimulated *Myc*^{low} and *Myc*^{high} cells 24 h after stimuli treatment. Results of three independent experiments are shown. Error bars represent standard variations. One-way ANOVA results (Bonferroni's posttest) are shown. (B) Numbers of cells counted via hemocytometer over three days. *Myc*^{low} cells were stimulated with IL10, CpG or both every 24 h. Number of unstimulated *Myc*^{high} cells were analyzed in parallel. Means \pm SD of three independent experiments are shown. Two-way ANOVA was calculated (Bonferroni's posttest) (* $p < 0.05$, ** $p < 0.01$, *** $p < 0.001$).

3.5.2 IL10+CpG stimulation induces G1/S-phase entry in Myc^{low} cells

To analyze why only IL10+CpG but no single stimulated cells doubled cell number over time, further cell cycle analysis using BrdU pulse chase was performed. By quick pulsing with BrdU and sequential cell cycle analysis by flow cytometry, a small fraction of cells can be followed during its passage throughout the cell cycle (gating example shown in Figure 17A). This setting allows the detailed analysis of single cell cycle stages of a selected set of cells. In unstimulated Myc^{low} and IL10 treated cells only a small fraction of cells was labeled with BrdU (compare with Figure 16A). Therefore, the fate of these cells was difficult to follow over time. In contrast, CpG and IL10+CpG stimulated cells incorporated high amounts of BrdU (Figure 16A) and entered G2/M phase synchronously 8h after labeling (Figure 17B). However, after 24h unstimulated and single stimulated Myc^{low} cells were arrested in the G0/G1 phase again. Importantly, in IL10+CpG stimulated Myc^{low} cells a fraction of previously BrdU labeled cells entered S-phase again after 24h (Figure 17C). Therefore, a high number of cells enter a first round of cell cycle in IL10+CpG stimulated Myc^{low} cells and in contrast to single stimulated cells these cells are also able to undergo a second round of cell cycle. Thereby, IL10+CpG stimulation but not the single stimulations is able to induce exponential proliferation in Myc^{low} cells.

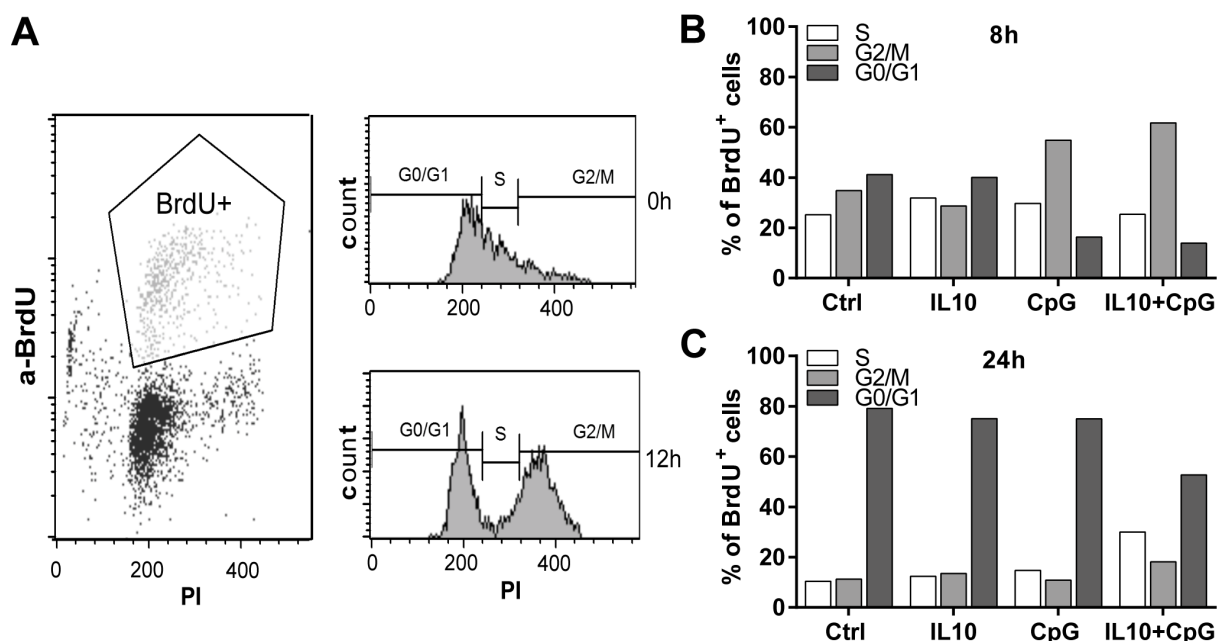


Figure 17: IL10+CpG stimulation increases S-phase entry compared to single stimulations in Myc^{low} cells.

(A) Gating scheme of BrdU pulse chase experiment. Myc^{low} cells were stimulated with IL10, CpG and IL10+CpG for 12h to induce S-phase entry and pulsed with BrdU for 20 min. Afterwards samples were harvested every two 2h and cell cycle distribution of BrdU labeled cells was analyzed by propidium iodide (PI) staining. (B) Cell cycle distribution of BrdU labeled cells 8h after labeling. (C) Cell cycle distribution of labeled cells 24h after labeling. Representative experiment out of two is shown. Further analysis time points are shown in Table 31 (Appendix, p. 117).

3.5.3 Synergistic upregulation of G1/S cell cycle regulators in IL10+CpG stimulated cells

To analyze which cell cycle regulators are differently regulated in single and double treated *Myc*^{low} cells, the expression of differentially expressed cell cycle genes from the previously shown RNASeq data (Figure 14) was compared. Gene clustering revealed that some genes were already upregulated by CpG alone and not further increased by IL10+CpG stimula-

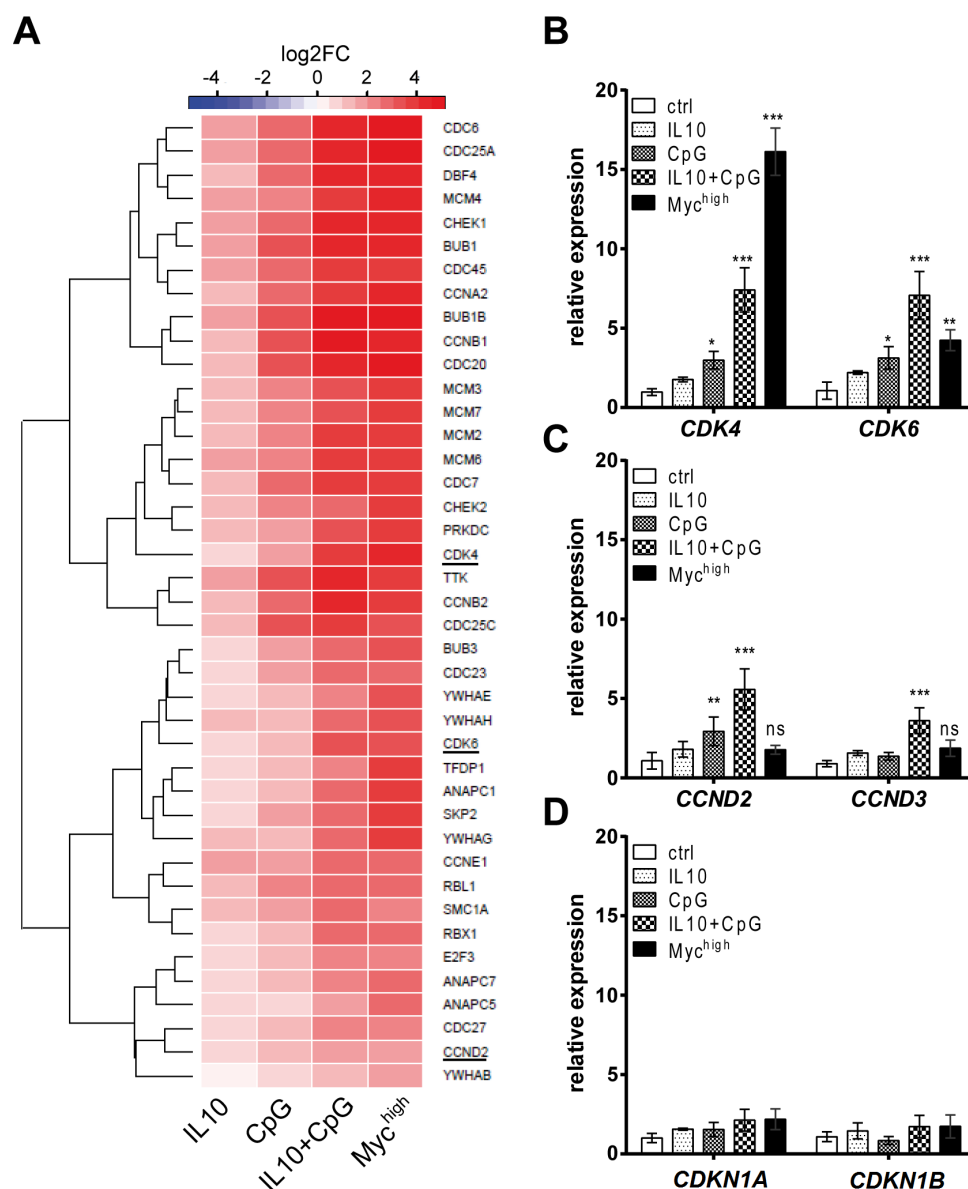


Figure 18: IL10+CpG stimulation synergistically increases G1/S regulator gene expression. (A) Heatmap of log₂ gene expression changes of IL10, CpG, IL10+CpG stimulated *Myc*^{low} and *Myc*^{high} cells relative to unstimulated *Myc*^{low}. Genes annotated as cell cycle regulators calculated in gene set enrichment from the overlap in Figure 15 are shown. Log₂FC values of the genes are provided digitally in Supplemental Table 4 (Appendix, p. 119). (B-D) Relative expression of a selected set of G1/S cell cycle regulators measured by qRT PCR 24h after stimulation of *Myc*^{low} cells. Expression of *CDK4*, *CDK6*, *CCND2*, *CCND3*, *CDKN1A*(*p21*) and *CDKN1B*(*p27*) was calculated relative to *drosophila ACT42A* and unstimulated *Myc*^{low} cells. Mean ± SD of three independent experiments are shown. Significant changes relative to unstimulated *Myc*^{low} cells were calculated by one-way ANOVA (Bonferroni's posttest) (* *p* < 0.05, ** *p* < 0.01, *** *p* < 0.001).

tion or *MYC* overexpression. These included the S-phase transition regulator cyclin A2 (*CCNA2*) and the mitotic regulators like cyclin B (*CCNB1/2*), BUB1 (*BUB1*, *BUB1B*) or *CDC20* (Figure 18A). Instead, G1/S regulators were stronger activated in IL10+CpG stimulated *Myc*^{low} and *Myc*^{high} cells than after single stimulations including *CDK4*, *CDK6* and *CCND2*, which was validated by qRT PCR (Figure 18B-D).

Using a qRT PCR expression based linear regression analysis, significant effects of the interaction of IL10 and CpG were calculated to analyze if the additional effect of both stimuli was only additive or synergistic (Table 32, Appendix p. 117). The interaction term for *CDK4/6* expression by IL10 and CpG stimulation was significant in this analysis, including main effects for IL10 and CpG besides the interaction term (*CDK4*, $p=0.003$; *CDK6*, $p=0.026$) suggesting a synergistic effect of the two stimuli. By the same means an additive increase in *CCND2* ($p=0.09$) and synergistic activation of *CCND3* ($p=0.015$) was observed. However, no significant change in *CDKN1A* (p21) or *CDKN1B* (p27) expression was revealed. Therefore, it is reasonable to suggest that IL10+CpG stimulation enables *Myc*^{low} cells to increase gene expression of positive cell cycle regulators, including *CDK4*, to overcome the G1 restriction point and to enter a new cell cycle.

To further validate the importance of G1/S cell cycle regulators in IL10+CpG stimulation mediated proliferation, an inhibitor against CDK4 and CDK6 complexes, called PD0332991, was used. *Myc*^{low} cells were simultaneously stimulated with IL10, CpG or IL10+CpG as well as the inhibitor and cell number was determined after 48 h. The CDK4/6 inhibitor completely blocked cell doubling of CpG, IL10+CpG stimulated *Myc*^{low} and *Myc*^{high} cells, while the slight increase in cell number after IL10 stimulation was not affected by this

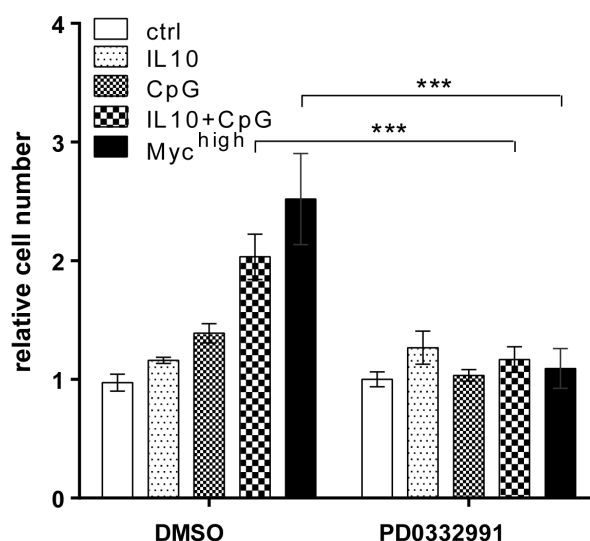


Figure 19: IL10+CpG stimulation and *Myc* mediated proliferation is dependent on CDK4/6 activity.

Relative cell number of stimulated *Myc*^{low} and *Myc*^{high} cells after CDK4/6 inhibition by 0.5 μ M PD0332991. Cells were treated with inhibitor or DMSO 3 h prior to IL10, CpG and IL10+CpG stimulation. Cell number was accessed 48 h after stimulation. Experiment was performed in triplicates and cell numbers \pm SD relative to unstimulated DMSO treated *Myc*^{low} cells are shown. Significant differences were calculated by one-way ANOVA (Bonferroni's posttest)(* $p < 0.05$, ** $p < 0.01$, *** $p < 0.001$).

inhibitor (Figure 19). It was concluded, that CDK4 and CDK6 complexes play an important role in IL10+CpG stimulation and Myc mediated proliferation.

3.5.4 Synergistic effect of IL10+CpG stimulation on proliferation is Myc independent

Myc is a well known regulator of cell cycle genes and *CDK4* is a direct target of Myc (Pajic *et al.*, 2000; Hermeking *et al.*, 2000). Therefore, the involvement of endogenous Myc induction in IL10+CpG stimulation mediated proliferation was accessed. Immunoblotting 2 h after IL10+CpG stimulation revealed a more than 2-fold increase of Myc protein levels compared to unstimulated *Myc*^{low} cells (Figure 20A). To estimate the effect of this Myc increase on proliferation and *CDK4* expression, a transient knockdown of *MYC* by siRNA was performed

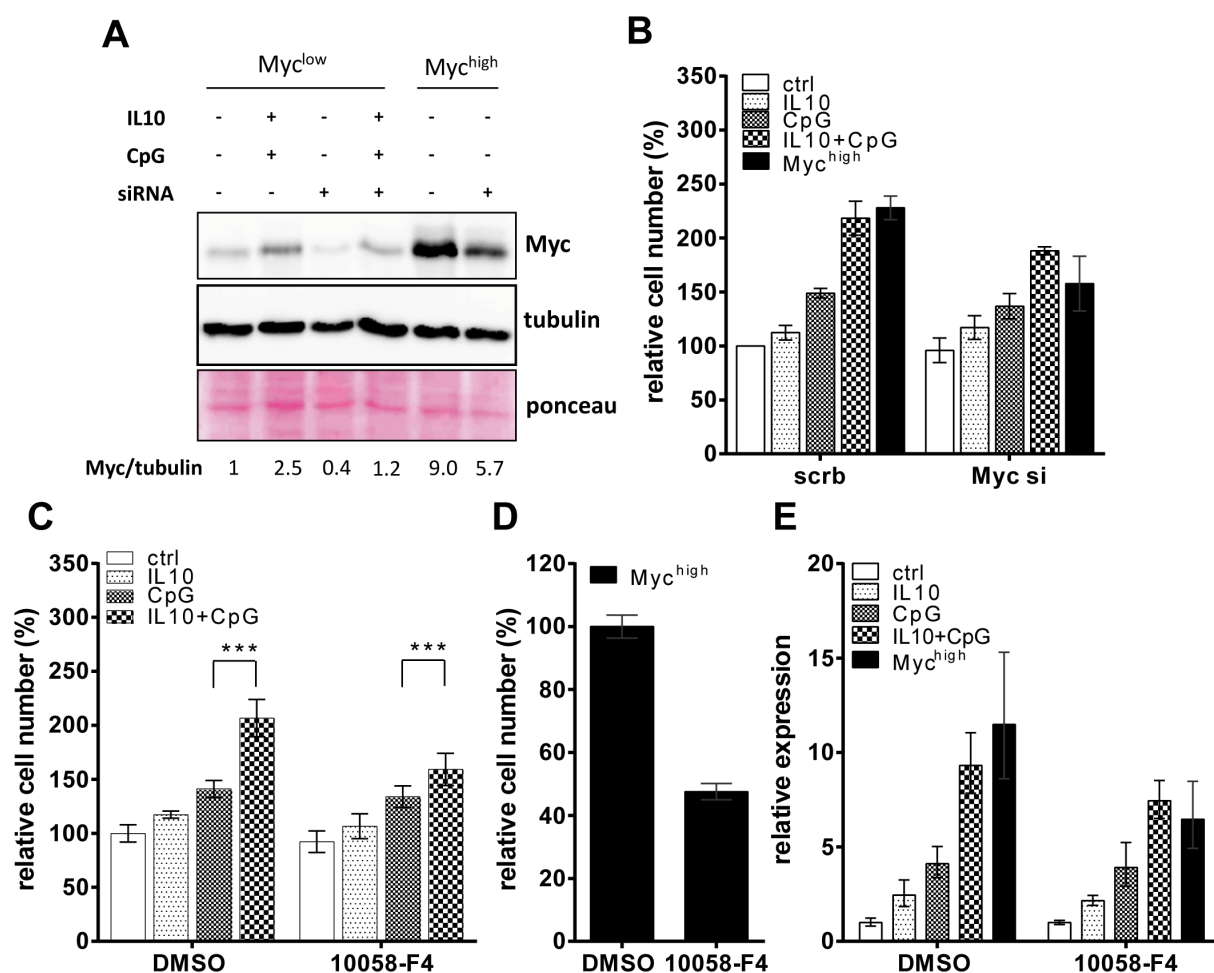


Figure 20: Endogenous Myc induction is dispensable for IL10+CpG stimulation induced proliferation.

(A) Immunoblot of *Myc*^{low} and *Myc*^{high} cells after *MYC* siRNA transfection. 24 h after transfection cells were stimulated with IL10+CpG for 2 h. Knockdown efficiency (Myc/tubulin) relative to non-target (scrub) control cells was calculated using Image J. (B) Relative cell numbers of IL10, CpG and IL10+CpG stimulated *Myc*^{low} and untreated *Myc*^{high} cells 72 h after *MYC* knockdown and 48 h after stimulation. Stimuli were added every 24 h. Mean \pm SD of three independent experiments is shown. (C+D) Relative cell numbers 48 h after Myc inhibition by 60 μ M 10058-F4 in stimulated *Myc*^{low} cells (C) and unstimulated *Myc*^{high} cells (D). Mean \pm SD of three experiments is shown. (E) qRT analysis of relative *CDK4* expression 24 h after 10058-F4 treatment of simultaneous stimulated *Myc*^{low} and unstimulated *Myc*^{high} cells. Gene expression was normalized on *drosophila ACT42A* and DMSO treated unstimulated *Myc*^{low} cells. One representative out of three experiments is shown. (* $p < 0.05$, ** $p < 0.01$, *** $p < 0.001$).

in Myc^{low} and Myc^{high} cells. This knockdown reduced *Myc* levels of IL10+CpG stimulated cells back to the bases of unstimulated Myc^{low} cells (Figure 20A). The reduced *MYC* expression only affected IL10+CpG stimulation induced cell proliferation about 10 to 20% after 48 h and more importantly did not block the synergistic effect of IL10+CpG stimulation (Figure 20B). However, a reduction of cell proliferation was observed in Myc^{high} cells at a knockdown about 40%. These results were confirmed by inhibition of *Myc*-Max dimerization by the small molecule inhibitor 10058-F4 (Follis *et al.*, 2008). Incubation with 10058-F4 of Myc^{low} cells 3 h prior to stimulation, reduced IL10+CpG stimulation mediated cell doubling, but was not able to block the additional effect of IL10+CpG stimulation on cell doubling compared to CpG stimulation alone (Figure 20C). In contrast, a complete block of *Myc* induced proliferation was observed after 10058-F4 treatment (Figure 20D). This proliferation block was accompanied by a decreased *CDK4* expression in Myc^{high} cells, while the IL10+CpG stimulation mediated *CDK4* expression increase was largely unaffected (Figure 20E). Considering both, *Myc* knockdown and inhibition experiments, it can be concluded that *Myc* is only partially involved in IL10+CpG stimulation induced proliferation. Therefore it is proposed that the synergistic effect of IL10 and CpG on *CDK4* expression and proliferation is mainly driven by other factors than *Myc*.

3.5.5 IL10+CpG stimulation induced proliferation is NF- κ B and STAT3 dependent

IL10 and CpG have been shown to activate STAT3 and NF- κ B in P493-6 Myc^{low} cells, respectively (Figure 6). Combined stimulation with both factors activated the same pathways in Myc^{low} cells (Figure 21). Within one hour CpG and IL10+CpG stimulation induced

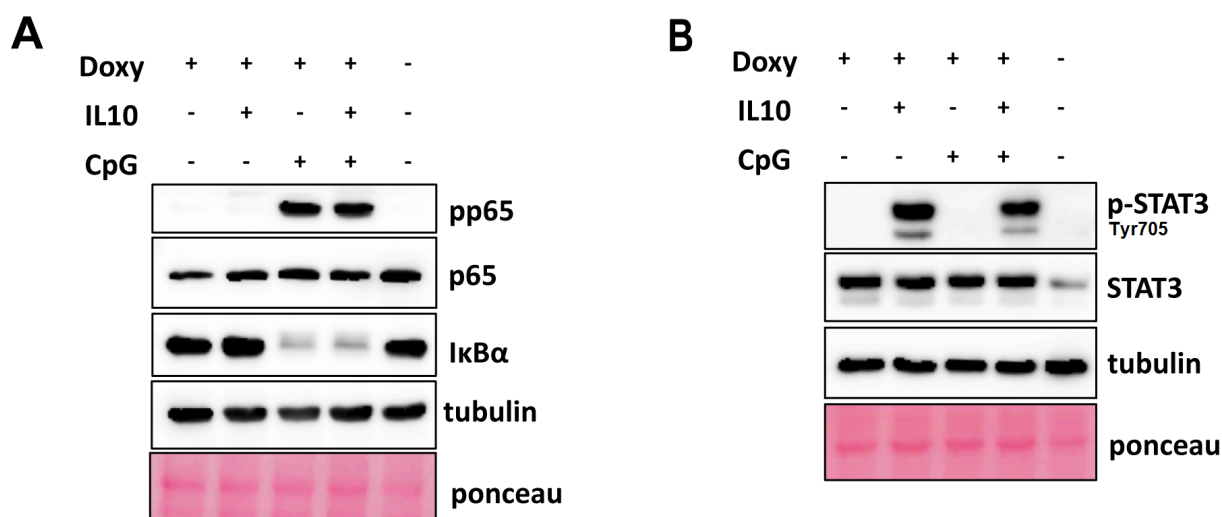


Figure 21: IL10+CpG stimulation synchronously activates STAT3 and NF- κ B signaling in Myc^{low} cells.

Immunoblot analysis of NF- κ B (**A**) and STAT3 (**B**) signaling in single IL10 and CpG and double stimulated Myc^{low} and unstimulated Myc^{high} cells. Myc^{low} cells (Doxy +) were treated with either IL10, CpG or both for 1 h. NF- κ B activation is shown by p65 phosphorylation and I κ B α degradation, STAT3 activation by Tyr705 phosphorylation. Equal loading is indicated by tubulin and ponceau staining. One representative blot out of three is shown.

p65 phosphorylation accompanied by a decrease in $\text{I}\kappa\text{B}\alpha$, while both, IL10 and IL10+CpG stimulation, induce STAT3 phosphorylation. In contrast none of these pathways was active in Myc^{high} cells. Since NF- κ B and STAT3 are important mediators of normal and transformed B cell proliferation (Ding *et al.*, 2007; McCarthy *et al.*, 2012) their involvement in IL10+CpG stimulation mediated proliferation was further analyzed.

First, cell doubling after NF- κ B or STAT3 pathway inhibition was assessed (Figure 22A). To inhibit NF- κ B signaling two inhibitors against IKK, called ACHP and MLN120B, were used. Incubation with ACHP completely blocked cell proliferation, while the synergistic effect of IL10+CpG stimulation vanished after MLN120B treatment. Same reduction of cell doubling of IL10+CpG to only CpG stimulated levels could be observed after JAK inhibition by using the small molecule inhibitors Ruxolitinib and Pyridone 6. Importantly, Myc^{high} cell proliferation was only slightly effected by ACHP and Pyridone 6 treatment and not by MLN120B or Ruxolitinib. As an increase of *CDK4* expression was thought to be involved in IL10+CpG stimulation induced proliferation, its expression was analyzed after ACHP and Ruxolitinib treatment (Figure 22B). Like observed for cell doubling experiments, ACHP treatment completely blocked *CDK4* expression in stimulated Myc^{low} cells, but not in Myc^{high} cells, while Ruxolitinib reduced IL10+CpG stimulation induced expression to CpG stimulation alone.

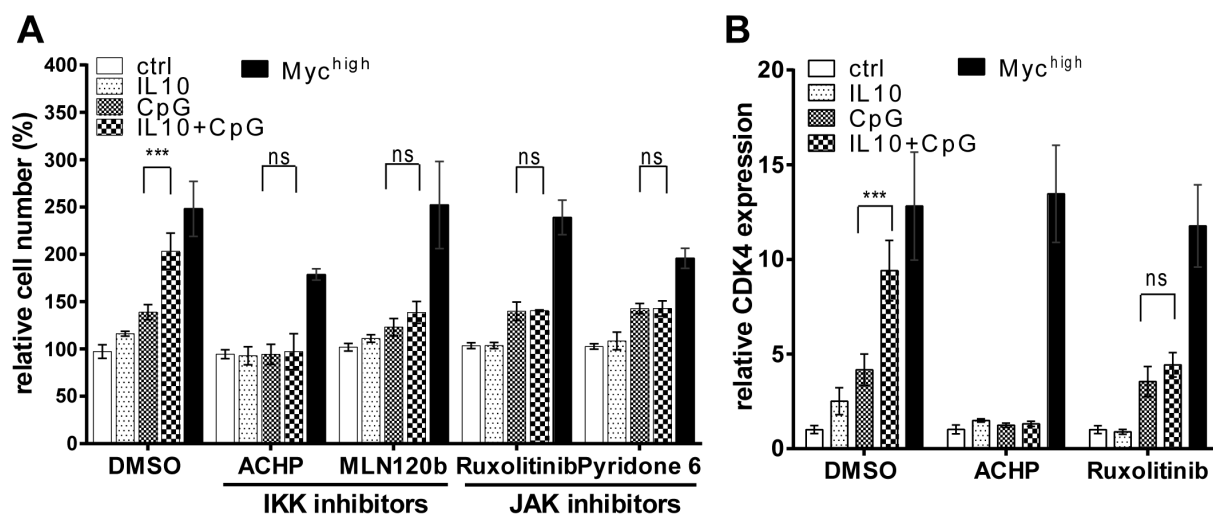


Figure 22: IL10+CpG stimulation mediated proliferation is NF- κ B and JAK/STAT dependent.

(A) Relative cell numbers of stimulated Myc^{low} and unstimulated Myc^{high} cells after IKK or JAK inhibition. Cells were preincubated for 3 h with IKK inhibitors (7 μM ACHP, 5 μM MLN120b) or JAK inhibitors (1 μM Ruxolitinib, 1 μM Pyridone 6), stimulated twice with IL10 and/or CpG as described before and total cell number was counted after 48 h. Data represent mean \pm SD of three independent experiments. Two-way ANOVA (Bonferroni's posttest) results are shown. (B) Relative *CDK4* expression of stimulated Myc^{low} and unstimulated Myc^{high} cells measured by qRT PCR 24 h after IKK and JAK inhibitor treatment. Expression was normalized on *drosophila ACT42A* expression and unstimulated DMSO treated Myc^{low} cells. Mean expression values and SD of three independent experiments and One-way ANOVA results are shown. (* $p < 0.05$, ** $p < 0.01$, *** $p < 0.001$).

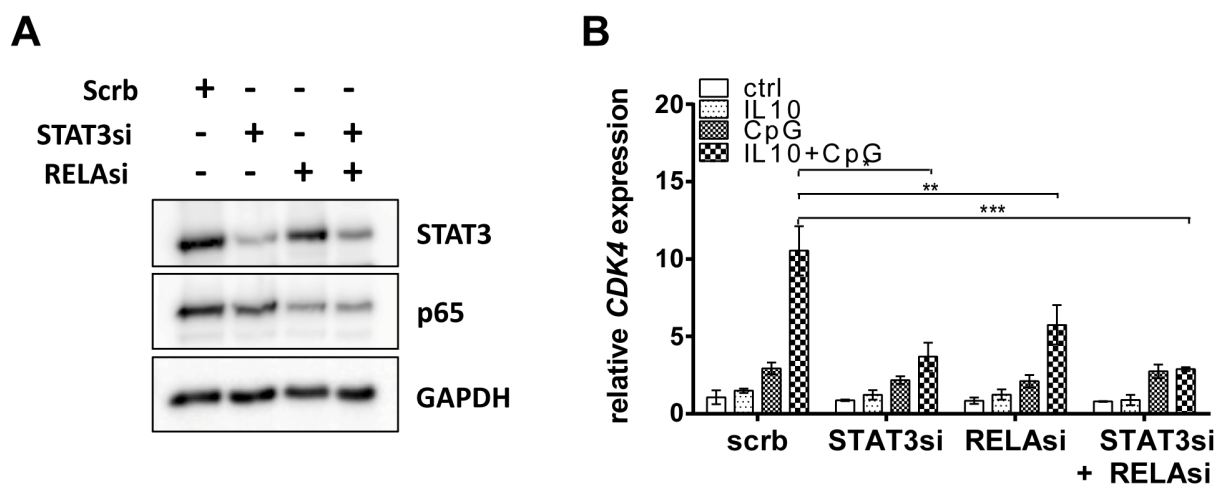


Figure 23: *CDK4* expression is STAT3 and p65/RELA dependent.

(A) Immunoblot analysis of STAT3 and p65 after *STAT3*, *RELA* or *STAT3* and *RELA* knockdown. GAPDH staining indicates equal protein loading. Figure is taken from MD thesis of Judith Kemper (Kemper, unpublished). (B) qRT analysis of *CDK4* mRNA expression of stimulated *Myc*^{low} cells after knockdowns shown in A. Analysis was performed 48 h after knockdown and 24 h after stimulation with IL10 and/or CpG. Results are shown relative to *drosophila ACT42A* and scrb transfected unstimulated *Myc*^{low} cells. Data represent mean \pm SD of three independent experiments. Two-way ANOVA (Bonferroni's posttest) results are shown.

To further support these observations, the involvement of NF- κ B/p65 and STAT3 in IL10+CpG stimulation induced proliferation was analyzed with support from Judith Kemper (Kemper, unpublished). She performed siRNA mediated knockdown of STAT3 and p65 (Figure 23A) and observed significantly reduced cell doubling in IL10+ CpG stimulated cells. To confirm the STAT3 and NF- κ B dependent regulation of *CDK4*, its gene expression was analyzed after STAT3 and/or p65 knockdown by qRT PCR (Figure 23B).

In line with the above described inhibitor experiments, *CDK4* mRNA expression was significantly reduced after STAT3 or NF- κ B knockdown, but double knockdown of both transcription factors showed strongest reduction of *CDK4* expression in IL10+CpG stimulated cells. In conclusion, synchronous STAT3 and p65 activation synergistically increases the expression of cell cycle regulators, for example *CDK4*, and thereby facilitates cell cycle entry and cell doubling in IL10+CpG stimulated *Myc*^{low} cells.

3.5.6 IL10 and CpG do not influence each other's STAT3 and p65 activation

While an important role of STAT3 and NF- κ B in IL10+CpG stimulated cells was confirmed, the mechanism underlying the synergistic effect of both pathways was still unknown. As described in the introduction, STAT3 and NF- κ B signaling can interact by modifying each other's signaling activity or duration (Liu *et al.*, 2013; Lee *et al.*, 2009). Therefore, pathway activation of NF- κ B and STAT3 signaling was monitored over time by immunoblotting and a flow cytometry based nuclear translocation assay. Immunoblot analysis with phosphospecific antibodies revealed no significant difference in STAT3 and p65 phosphorylation or I κ B α degradation over 2hrs (Figure 24A-C) or up to 24h (data not shown) between double or single stimulated *Myc*^{low} cells. In both cases STAT3 signaling was activated within 15 min,

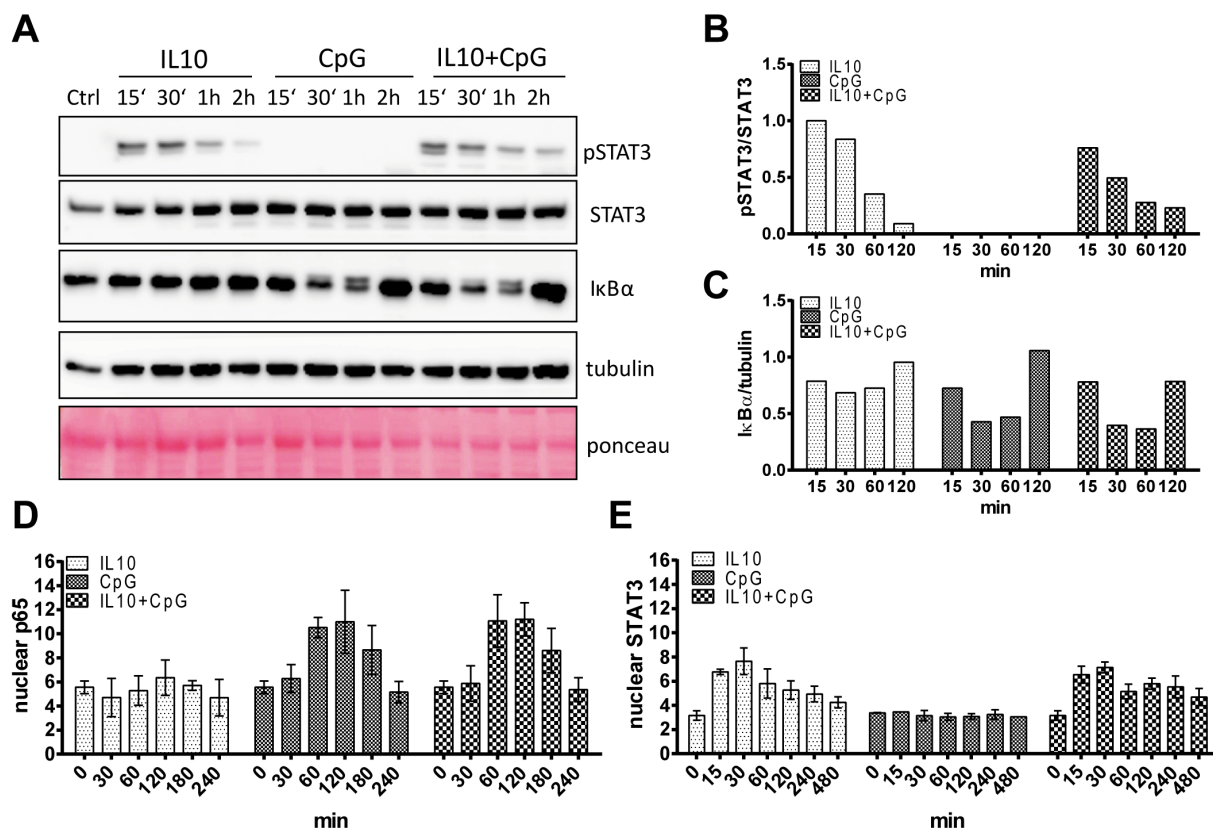


Figure 24: Comparable time course of STAT3 and NF- κ B activation after single and combined stimulation in *Myc*^{low} cells.

(A-C) Comparison of I κ B α degradation and STAT3 activation after single IL10 and CpG and double stimulation of *Myc*^{low} cells. Cells were stimulated with either IL10, CpG or both for indicated time points, followed by immunoblot analysis (A). Equal loading is shown by tubulin and ponceau staining. One representative blot out of three is shown. Activation of pSTAT3 (Tyr705, B) and degradation of I κ B α (C) of immunoblot shown in A were quantified using Image J. (D+E) Nuclear translocation time of p65 (D) and pSTAT3 (Tyr705, E) after IL10, CpG and IL10+CpG stimulation analysed by flow cytometry. Mean \pm SD of three independent experiments are shown.

followed by slow decrease of the signal. In contrast, I κ B α was degraded after 30 min and 1 h but again increased after 2 h in single as well as IL10+CpG stimulated cells. This time course was confirmed by nuclear staining of p65 and STAT3 by flow cytometry. No difference of p65 (Figure 24D) or STAT3 (Figure 24E) nuclear translocation was observed between 15 min and 8 h.

Therefore, differences in signaling strength or duration as a main reason for the synergistic effect of STAT3 and p65 on *CDK4* gene expression are excluded. Instead, it is suggested that a combined binding of STAT3 and NF- κ B to the *CDK4* promoter or a second unknown transcription factor regulated by both pathways is underlying the synergistic effect on gene expression.

3.5.7 STAT3 and NF- κ B directly bind to the *CDK4* promoter

It was shown that STAT3 and NF- κ B cooperatively induce gene expression (Kesanakurti *et al.*, 2013; Hagihara *et al.*, 2005). Therefore, STAT3 and NF- κ B were considered as direct regulators of *CDK4* expression in stimulated P493-6 Myc^{low} cells. To proof this hypothesis, IL10+CpG stimulation induced gene expression was analysed after 6 hrs of stimulation. An increase in the expression of the STAT3 target gene *SOCS3* and the NF- κ B target *NFKBIA*, coding for I κ B α , could be observed within this time frame (Figure 25A+B). Importantly, within 6 h also an increase in *CDK4* expression could be observed indicating a direct regulation by STAT3 and NF- κ B (Figure 25C).

To proof this hypothesis, chromatin immunoprecipitation of STAT3 and p65 after IL10 and/or CpG stimulation was performed. For this purpose, Myc^{low} cells were stimulated with single IL10 or CpG or both for 1 h. Proteins bound to the chromatin were fixed by double crosslinking and pulldown of STAT3 and p65 bound chromatin was performed by immunoprecipitation. After protein removal, the gene promoters fractions of *SOCS3*, *NFKBIA* and *CDK4* were identified in the isolated DNA by qPCR. A strong increase in STAT3 binding was observed on the *SOCS3* promoter after IL10 stimulation, while CpG treatment increased binding of p65 to the *NFKBIA* promoter (Figure 25D+E). Different primers amplifying regions between the transcription start side (TSS) and -1000bp of *CDK4* were used to screen for proximal binding site of STAT3 and p65 at *CDK4*. About 100bp from the TSS of *CDK4* a binding of STAT3 was detected after IL10 treatment accompanied by a weak p65 binding (Figure 25F). In contrast, after CpG treatment a strong p65 and a weak STAT3 binding was shown. Importantly, after IL10+CpG stimulation a strong binding of both STAT3 and p65 to the same promoter region was found. Interestingly, this dual binding of STAT3 and p65 was observed in the classical STAT3 and NF- κ B targets, *SOCS3* and *NFKBIA*. Both genes are synergistically upregulated after IL10+CpG stimulation. These data imply that strong dual binding of STAT3 and p65 to the same promoter region of a gene is involved in the synergistic increase in gene expression, including *CDK4*. Furthermore it is suggested, that this mechanism is important for IL10+CpG stimulation mediated proliferation.

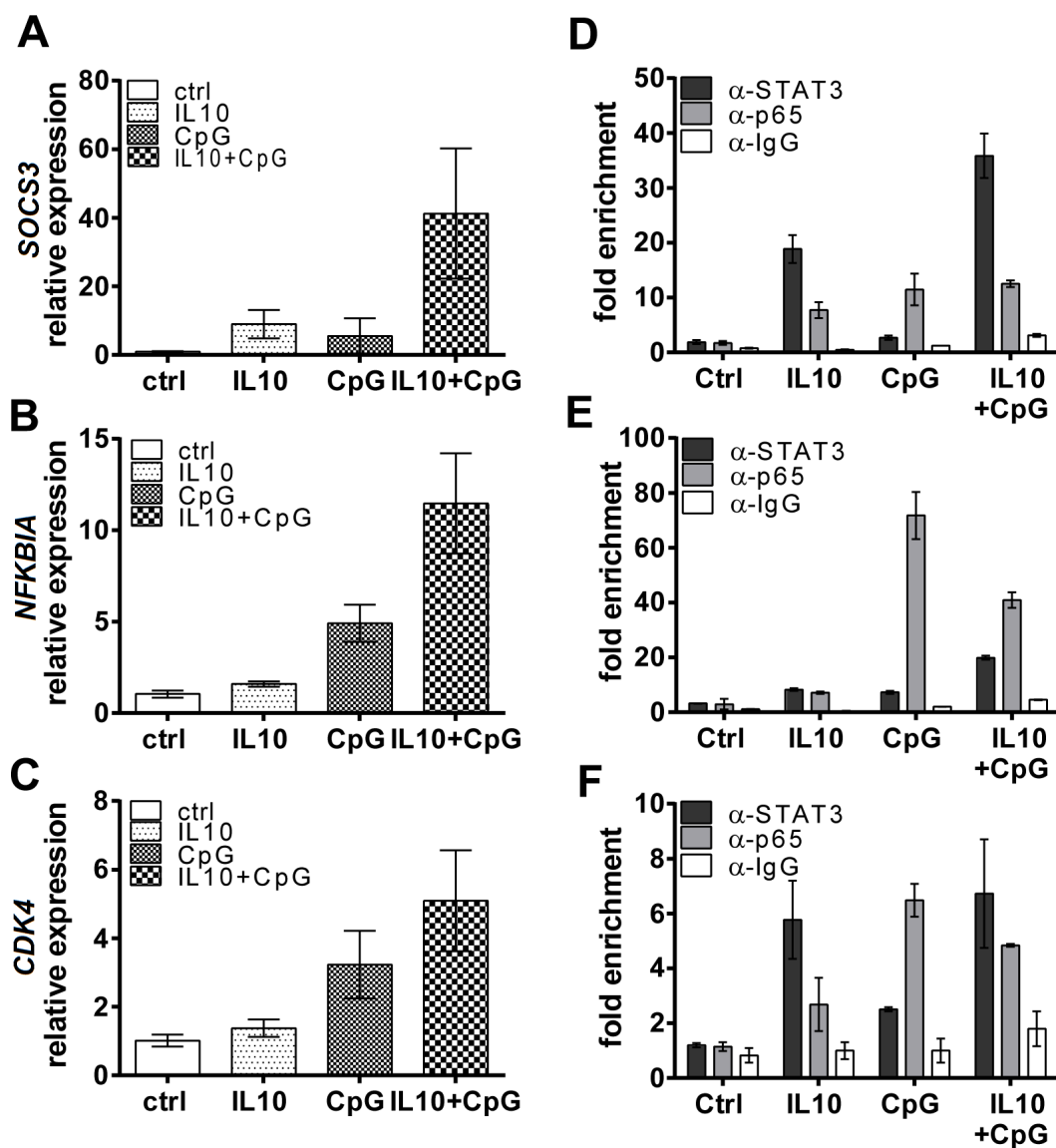


Figure 25: STAT3 and p65 bind to the proximal promoter of *CDK4*.

(A-C) Gene expression of *SOCS3* (A), *NFKBIA* (B) and *CDK4* (C) 6 h after IL10, CpG and IL10+CpG stimulation in *Myc*^{low} cells analyzed by qRT PCR. Expression was normalized on *drosophila ACT42A* and unstimulated *Myc*^{low} cells. Means±SD of three independent experiments are shown. (D-F) Chromatin Immunoprecipitation of STAT3 and p65 1 h after stimulation of *Myc*^{low} cells with IL10, CpG or IL10+CpG. qPCR analysis of proximal promoter regions of *SOCS3* (D), *NFKBIA* (E) or *CDK4* (F) of the pull down are shown. Fold changes were calculated relative to an inactive, closed intron region (*PRAME*) and unstimulated *Myc*^{low} cells. One representative precipitation out of three is shown. Error bars indicate SD of technical replicates.

3.6 Effects of IL10R and TLR9 signaling on cell metabolism

So far, a synergism of IL10R and TLR9 signaling on B cell proliferation and gene expression of cell cycle regulator was shown. However, beside the activation of specific cell cycle regulators, increasing evidence exist that changes in metabolism of the cell are important to provide energy and biomolecules for DNA replication and cell division (Vander Heiden *et al.*, 2011). First hints for these changes were shown above by a correlation of extracellular and intracellular metabolites and the number of cells in S-phase (Figure 12). More interestingly, these changes in proliferation and metabolism are often mediated by the same oncogenic pathways in cancer cells (Fritz & Fajas, 2010), indicating a possible role for STAT3 and NF- κ B in cell metabolism. However, metabolic and transcriptomic data obtained from the linear regression analysis have shown first possible differences between IL10+CpG stimulation and Myc induced proliferation (Figure 15). Therefore, the metabolic changes mediated by IL10+CpG stimulation or *MYC* overexpression and the molecular pathways underlying these changes were further analyzed in this study.

3.6.1 IL10+CpG stimulation synergistically induces expression of metabolic genes

Within the genes upregulated by IL10+CpG stimulation or *MYC* overexpression an enrichment of metabolism associated genes was observed (Figure 15D). Further gene set enrichment analysis revealed that these sets included genes associated with glycolysis or involved in glutaminolysis. Figure 26 shows log₂FC of important glycolysis and glutaminolysis genes in IL10+CpG stimulated Myc^{low} and Myc^{high} cells from the dataset shown in Figure 14. As shown above for genes involved in cell cycle regulation most glycolysis or glutaminolysis associated genes were significantly higher expressed in IL10+CpG stimulated Myc^{low} cells than single stimulated. This increase resulted in a comparable expression of genes after IL10+CpG stimulation as *MYC* overexpression. For example, Hexokinase 2 (*HK2*), the key enzyme of glycolysis, and the lactate dehydrogenase A (*LDHA*) are highly expressed in IL10+CpG stimulated Myc^{low} and Myc^{high} cells. This suggests a greater usage of glucose via anaerobic glycolysis. Key enzymes of glutaminolysis (including TCA cycle enzymes) are higher expressed in both proliferating cells under both conditions compared to unstimulated Myc^{low} cells. Importantly, expression of the glutaminase (*GLS*) and aspartate transaminases (*GOTs*) are increased in IL10+CpG stimulated Myc^{low} and Myc^{high} cells.

Therefore, an increase in glycolysis and glutaminolysis dependent genes in IL10+CpG stimulated Myc^{low} and Myc^{high} cells was observed that should facilitate the usage of glucose or glutamine as energy and biosynthetic sources in these cells. Notably, an increased usage of glucose and glutamine is resonable after IL10+CpG stimulation as depicted from the linear regression analysis (Figure 10, Supplemental Table 3, Appendix p. 119)

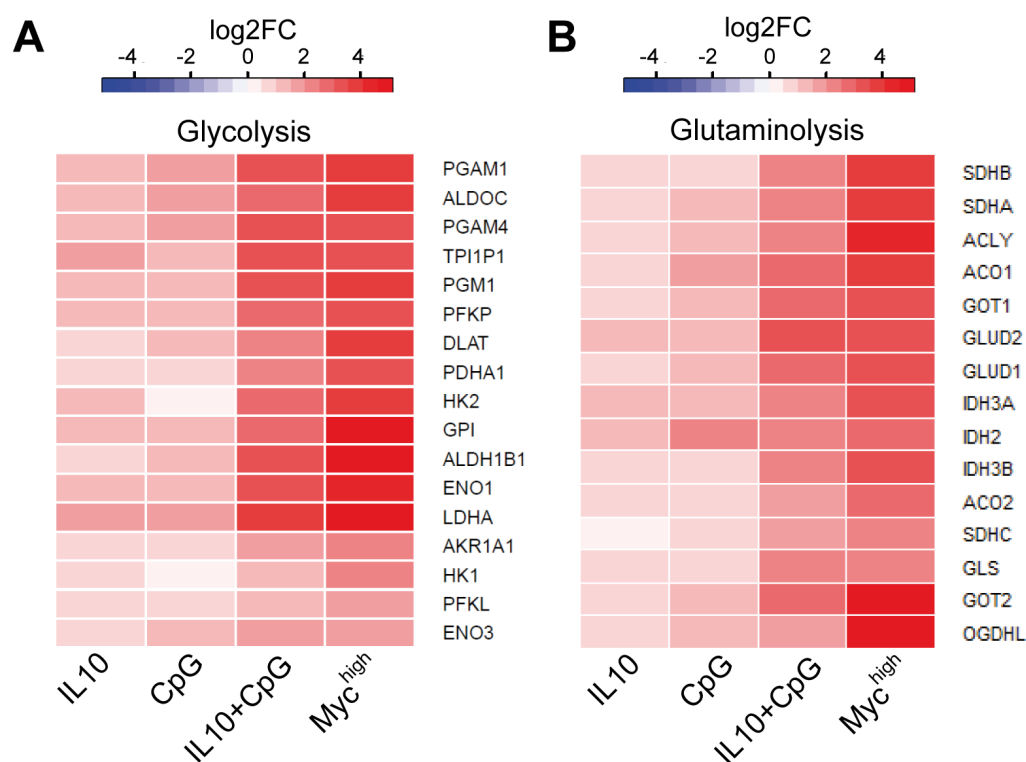


Figure 26: Synergistic upregulation of metabolic genes in IL10+CpG stimulated *Myc*^{low} cells. Heatmaps of log₂ gene expression changes induced by IL10, CpG, IL10+CpG stimulation and *MYC* expression relative to unstimulated *Myc*^{low} cells. Shown are genes of the IL10+CpG stimulation and *MYC* overexpression overlap presented in Figure 15, which are enriched for glycolysis (A) and glutaminolysis (B). Color codes used are shown above the figures. Log₂FC of the genes are provided digitally (Supplemental Table 4, Appendix p. 119).

3.6.2 Proliferation of IL10+CpG stimulated *Myc*^{low} and *Myc*^{high} cells is strictly glutamine dependent

The suggested increase in glucose and glutamine usage should be visible as a higher consumption rate of these metabolites from the media. Therefore, measurements of cell culture supernatants 24h after stimulation were performed by NMR spectrometry. A significant increase in the uptake of glucose and glutamine from the cell culture media in IL10+CpG stimulated *Myc*^{low} and *Myc*^{high} cells compared to untreated or single treated *Myc*^{low} cells was revealed (Figure 27A+B). Comparing IL10+CpG stimulation and *MYC* overexpression, a higher usage of glucose and glutamine was observed in *Myc*^{high} cells, consistent with the higher expression of TCA associated metabolic genes. Next it was analyzed, which of the metabolites, glucose or glutamine, was most important for IL10+CpG stimulation or *Myc* induced cell proliferation. Therefore, cells were grown in media depleted from either glucose or glutamine and cell numbers of IL10+CpG stimulated *Myc*^{low} and unstimulated *Myc*^{high} cells were defined. Depletion of glutamine from the media completely blocked IL10+CpG stimulation and *Myc* induced proliferation (Figure 27C). Glucose withdrawal resulted in a reduced proliferation rate under both conditions (Figure 27D).

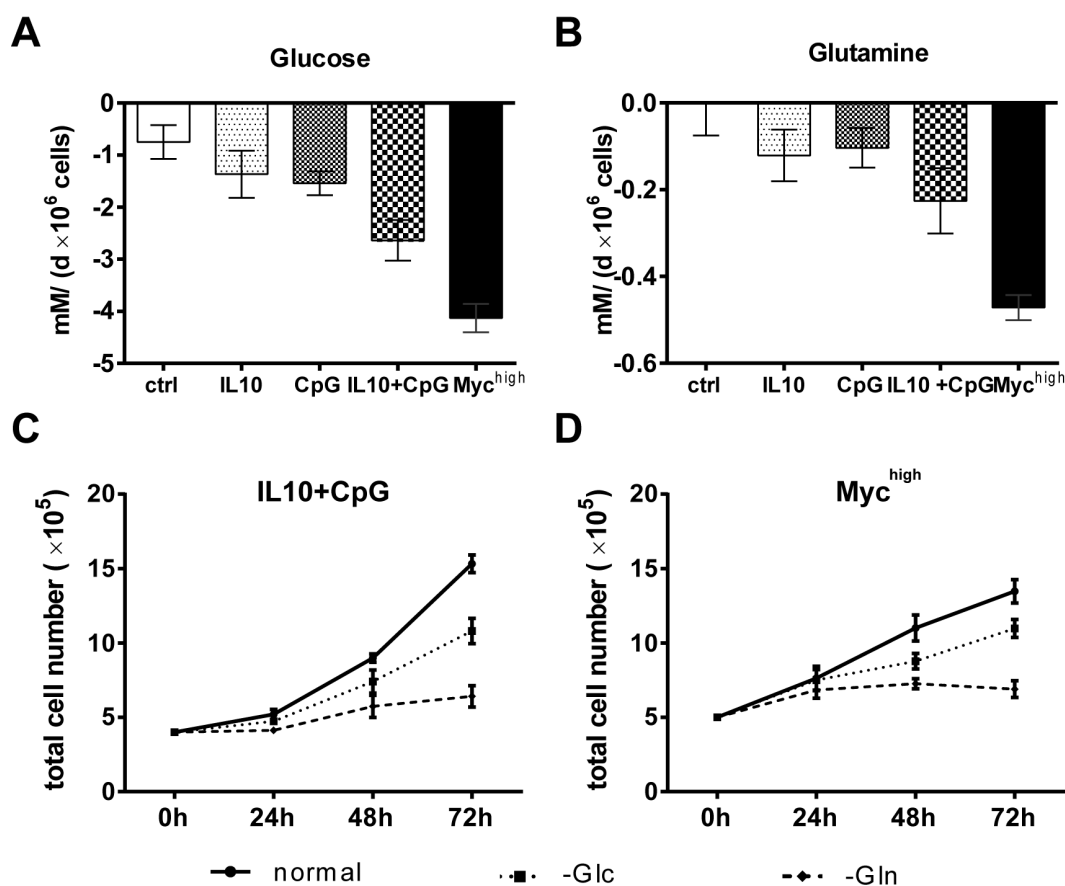


Figure 27: Increased glutamine consumption is important for proliferation of IL10+CpG stimulated Myc^{low} and Myc^{high} cells.

(A+B) Consumption of glucose (A) and glutamine (B) from cell culture media of IL10, CpG and IL10+CpG stimulated Myc^{low} and unstimulated Myc^{high} cells measured by NMR spectrometry. (C+D) Relative cell number of IL10+CpG stimulated Myc^{low} (C) and unstimulated Myc^{high} cells (D) grown in media depleted from glucose (-Glc) or glutamine (-Gln). Total cell number was counted every 24 h. Mean and SD of three independent experiments are shown.

To further support this observation the GLS inhibitor CB-839 was used. This inhibitor blocks the conversion of glutamine to glutamate (Figure 28A). Inhibiting the GLS blocked IL10+CpG stimulation and Myc mediated proliferation comparable to glutamine withdrawal, while untreated and single treated Myc^{low} cells were unaffected by this inhibitor (Figure 28B). Notably, the total cell number and viability of unstimulated or single stimulated Myc^{low} cells was not affected by either glutamine withdrawal or CB-839 treatment. Therefore, proliferation of both, IL10+CpG stimulated Myc^{low} and Myc^{high} cells, highly depends on glutamine metabolism.

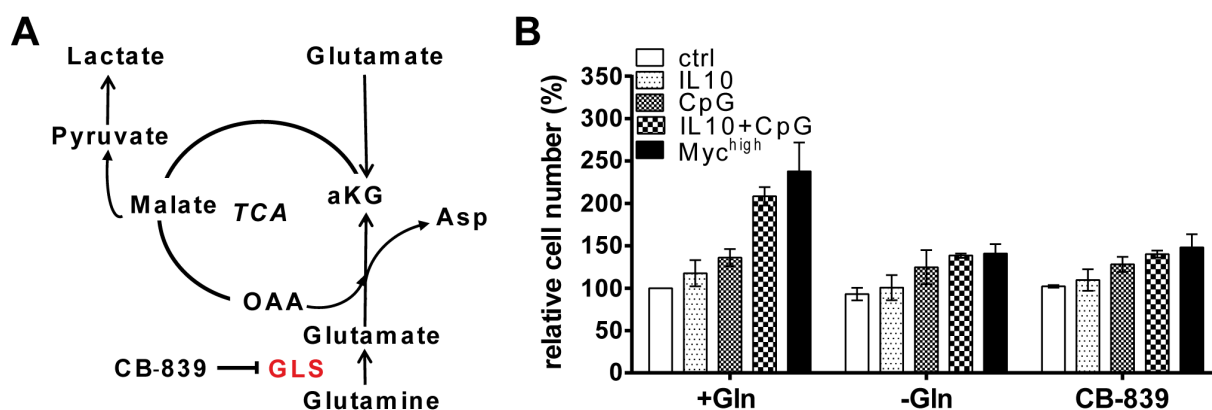


Figure 28: IL10+CpG stimulation and Myc induced proliferation is dependent on GLS.

(A) Scheme of selected pathway knots of glutaminolysis. Conversion of glutamine to glutamate by glutaminase (GLS) is blocked by the small molecule inhibitor CB-839. (B) Relative cell numbers of 1 μ M CB-839 treated Myc^{low} and Myc^{high} cells 48 h after treatment. Myc^{low} cells were simultaneously stimulated with IL10, CpG and IL10+CpG. Cells grown in media with glutamine (+Gln) and without glutamine (-Gln) were used as controls. Mean and SD of three independent experiments are shown.

3.6.3 Glutamine is incorporated into TCA intermediates and amino acids

To evaluate how glutamine is further metabolized, stable isotopic labeled glutamine was used. Myc^{low} and Myc^{high} cells were grown in media containing ubiquitous ¹³C-labeled glutamine and Myc^{low} cells were left unstimulated or stimulated with IL10+CpG and incubated at 37 °C for 18 h, 22 h, 24 h, 26 h, 30 h. Mass spectrometry of the cell lysate revealed no significant differences of ¹³C-enrichment in TCA metabolites or amino acids within these time points (data not shown). This indicates a steady state of metabolite labeling within this time frame. Therefore, an incubation time of 24 h was chosen for glutamine tracing of IL10+CpG stimulated Myc^{low} and Myc^{high} cells. Unstimulated Myc^{low} cells incorporated glutamine in about 20 to 30 % of each TCA metabolite within these 24 h (Figure 29A). In IL10+CpG stimulated cells a stronger enrichment of isotopic labeling of about 50 % was detected, while in Myc^{high} cells 60 to 65 % of each metabolite was derived from glutamine. In both, IL10+CpG stimulated Myc^{low} and Myc^{high} cells a small fraction (2-4 %) of lactate was glutamine derived, while nearly no glutamine was metabolized to lactate in unstimulated Myc^{low} cells (Figure 29B). In addition to TCA metabolites and lactate, a significant incorporation of glutamine into the amino acids aspartate, glutamate, proline and ornithine was observed (Figure 29C). Thereby, an equal distribution as TCA intermediates was observed for aspartate, glutamate and proline, while ornithine labeling was not increased by IL10+CpG stimulation or Myc induction compared to unstimulated Myc^{low} cells. Interestingly, only in Myc^{high} cells a small fraction about 2-3 % of alanine was glutamine derived. These results show, that both IL10+CpG stimulated Myc^{low} and Myc^{high} cells increase the incorporation of glutamine in metabolites involved in biosynthesis and energy production compared to unstimulated Myc^{low} cells. Nevertheless, Myc^{high} cells use more glutamine for this purpose consistent with a higher consumption rate of glutamine from the media observed in this (Figure 27) and published studies (Murphy *et al.*, 2013).

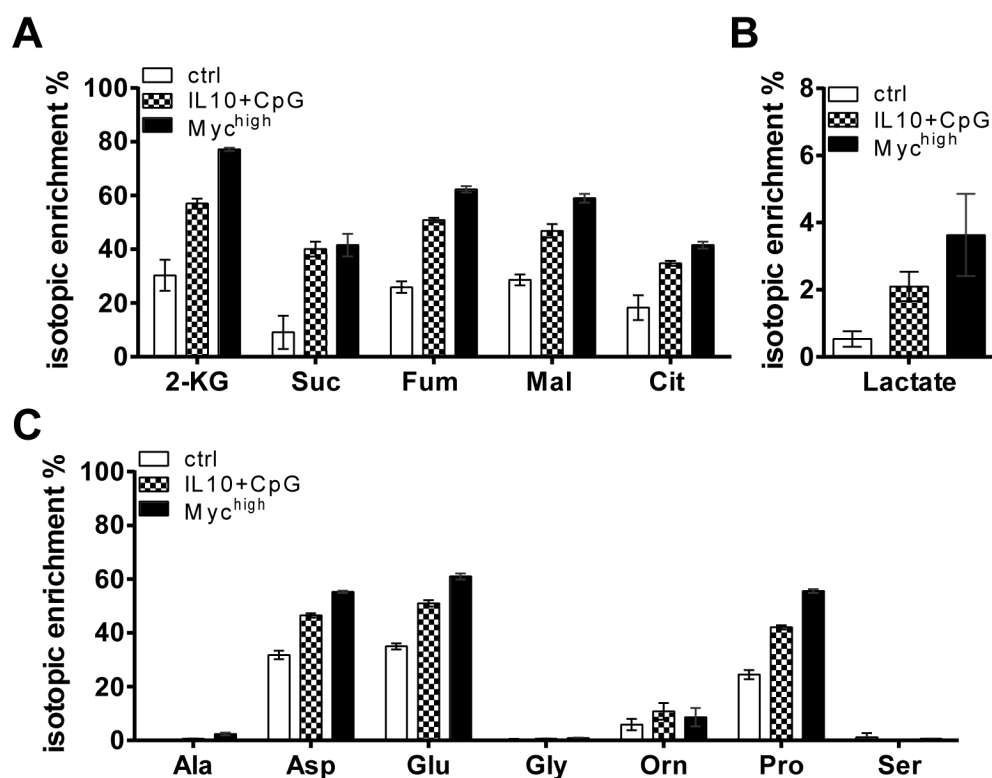


Figure 29: IL10+CpG stimulation and MYC overexpression are associated with an increase of glutamine incorporation into TCA intermediates and amino acids. (A-C) Isotopic enrichment of metabolites of unstimulated Myc^{low}, IL10+CpG stimulated Myc^{low} and Myc^{high} cells treated with ubiquitously labeled ¹³C-glutamine for 24h. TCA intermediates (A), intracellular lactate (B) and amino acids (C) were measured by mass spectrometry. In all plots mean \pm SD of three independent experiments are shown. 2-KG= α -ketoglutarate, Suc=succinate, Fum=fumarate, Mal=malate, Cit=citrate, Ala=alanine, Asp=aspartate, Glu=glutamate, Gly=glycine, Pro=proline, Ser=serine.

Glutamine derived metabolites can be metabolized via two different mechanisms in the TCA, oxidative decarboxylation or reductive carboxylation. These mechanisms can be distinguished by mass spectrometry due to different masses of the end products. These mass distributions were compared to answer the question if IL10+CpG stimulated Myc^{low} and Myc^{high} cells metabolize glutamine by equal mechanisms. In Figure 30 A an example of mass distribution for the synthesis of citrate is shown. First glutamine is converted to α KG via transaminases or deamination, which leads to labeling of all five carbons (m+5). During the oxidative carboxylation, which is part of the a respiration, one carbon is lost by the release of CO₂ leading to m+4 labeling of the following TCA intermediates. To generate citrate, glucose derived acetyl- CoA is added to the four carbons of OAA. Thus citrate is still m+4 labeling under this conditions. Lower levels of ¹³C-labeling indicate multiple rounds of oxidative TCA function as in each round an additional glutamine derived carbon will be removed as CO₂. In case of reductive carboxylation, one unlabeled CO₂ derived carbon is added to the five labeled carbons of α KG to build up citrate (m+5). Thus, the precise isotopic fractions (m+0 till m+6) of citrate were calculated for unstimulated Myc^{low}, IL10+CpG stimulated Myc^{low} and Myc^{high} cells. M+0 fraction was highest in unstimulated Myc^{low} cells, whereas IL10+CpG stimulated Myc^{low} and Myc^{high} cells a strong decrease in unlabeled cit-

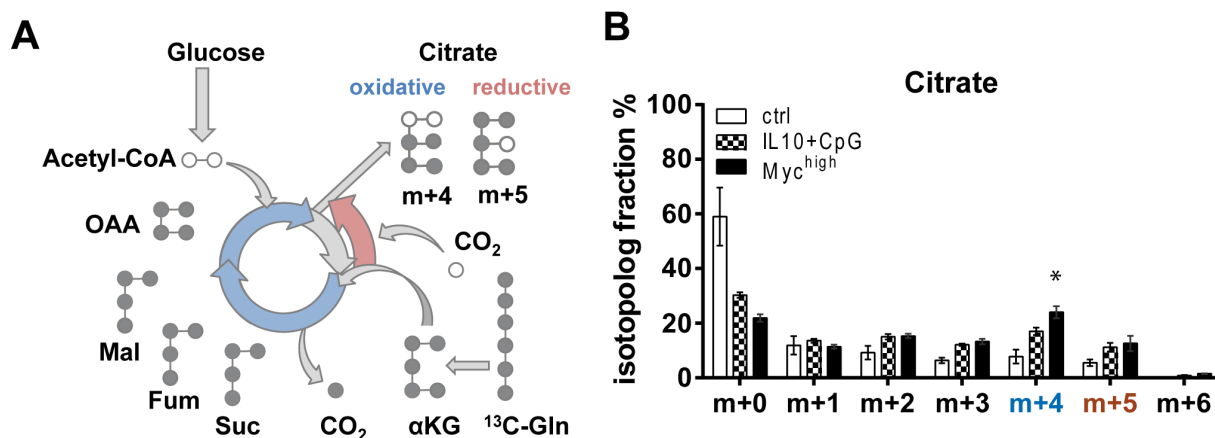


Figure 30: More citrate is oxidatively derived from glutamine in Myc^{high} cells.

(A) Oxidative decarboxylation (blue) and reductive carboxylation (red) can be distinguished by isotopic labeling and mass spectrometry. While oxidation of glutamine leads to m+4 labeled citrate, reductive generation of citrate is shown by m+5 labeling. α KG = α -ketoglutarate, Suc = succinate, Fum = fumarate, mal = malate, OAA = oxaloacetate. Glutamine derived carbons are shown in grey. (B) Isotopic fractions of citrate in IL10+CpG stimulated Myc^{low} and Myc^{high} cells. Mass spectra described in Figure 29 were analyzed according to the different masses of citrate. Mean \pm SD of three independent experiments and one-way ANOVA results are shown.

rate was observed. Furthermore, m+2, m+3 and m+5 fractions of IL10+CpG stimulated and Myc^{high} cells were equally increased compared to unstimulated Myc^{low} cells. However, the oxidative derived m+4 fraction was significantly increased in Myc^{high} cells compared to IL10+CpG stimulated Myc^{low} cells. Thus it is proposed, that both, IL10+CpG stimulated and MYC overexpressing cells, increase glutamine incorporation into TCA intermediates, but that Myc^{high} cells use more glutamine for aerobic respiration.

3.6.4 Myc^{high} but not IL10+CpG stimulated cells use glutamine for aerobic respiration

To further support that glutamine is used for aerobic respiration in Myc^{high} cells, the respiratory and glycolytic capacity of unstimulated Myc^{low}, IL10+CpG stimulated Myc^{low} and Myc^{high} cells was analyzed. Oxygen consumption rates (OCR) and extracellular acidification rates (ECAR) were simultaneously measured in the presence of glucose, glutamine or both. Figure 31A shown an example of OCR measurement in the presents of both glucose and glutamine. Adding oligomycin inhibits ATP synthase (complex V) and OCR decreases. This decrease correlates to the mitochondrial respiration associated with cellular ATP production. By adding Carbonyl cyanide-4 (trifluoromethoxy) phenylhydrazone (FCCP) the membrane potential of the mitochondrion is uncoupled from the proton gradient. Thereby, the electron flow through the ETC is uninhibited and maximally oxygen consumption is measured. Here, highest increase in CpG and IL10+CpG stimulated Myc^{low} and Myc^{high} cells is visible. At last rotenone, a complex I inhibitor, and antimycin A, a complex III inhibitor, are added. These inhibitors completely block mitochondrial respiration. From these inhibitor treatment the different respiratory parameters as basal respiration and maximal respiration can be calculated.

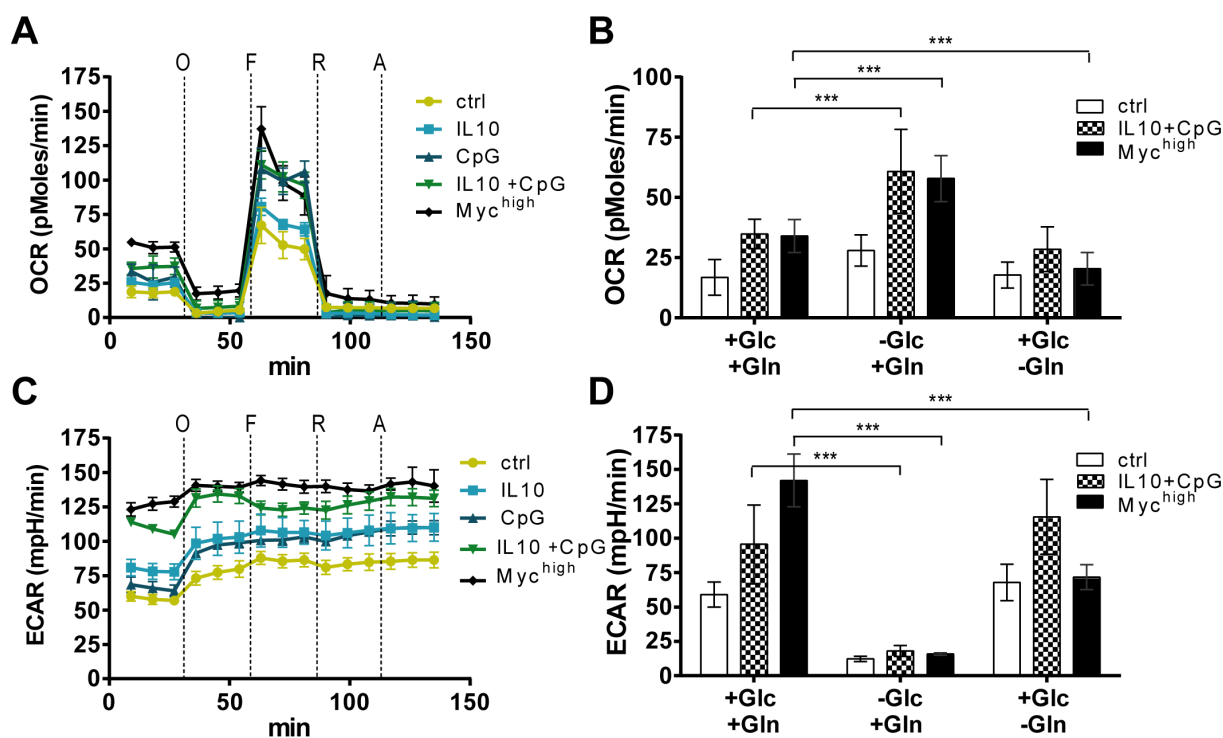


Figure 31: Respiration and acidification of Myc^{high} but not IL10+CpG stimulated Myc^{low} cells is glutamine dependent.

(A) Measurement of oxygen consumption rates (OCR) of 24 h IL10, CpG and IL10+CpG stimulated Myc^{low} and unstimulated Myc^{high} cells. Mean \pm SD of technical replicates of one representative experiment are shown. Respiratory parameters were calculated by inhibitor addition (O = 1.5 μ M Oligomycin, F = 0.5 μ M FCCP, A = 2 μ M antimycin A, R = 1 μ M rotenone) as described in section 2.2.2 (B) Basal OCR of IL10+CpG stimulated Myc^{low} and Myc^{high} cells under different media conditions. Cells were seeded in media with glucose and glutamine, without glucose and without glutamine and 24 h after seeding OCR was analyzed as shown in A. Basal respiration rates calculated from three independent biological replicates. (C+D) Extracellular acidification rates (ECAR) of samples described in A and B. Mean \pm SD of three independent experiments and one-way ANOVA (Bonferroni's posttest) results are shown (***) $p < 0.001$.

Calculation of these parameters are described in method section (page 29). Simultaneous to OCR the ECAR was measured at all time points (Figure Figure 31C). Notably, highest ECAR was observed in IL10+CpG stimulated Myc^{low} cells and Myc^{high} . Oligomycin treatment further increased the ECAR, due to a switch from aerobic respiration to anaerobic glycolysis and an increase in lactate production. Figure 31B shows basal respiration rates of triplicates of cells treated with glucose and glutamine or without glucose or glutamine. When both were present, comparable basal respiration rates of IL10+CpG stimulated Myc^{low} and Myc^{high} cells were observed. Without glucose respiration was equally increased, compensating for the loss of anaerobic glycolysis which reflected by a decrease in ECAR rates (Figure 31C+D). When glutamine was depleted from the media, however, no change in IL10+CpG stimulated cells was observed, while both, OCR and ECAR, significantly dropped in Myc^{high} cells (Figure 31B+D). Same effects were detected on ATP dependent and maximal respiration (data not shown). To further confirm the dependency of respiration on glutamine in Myc^{high} cells, OCR measurements were modified the following was. Cells were seeded in media without glucose and glutamine and instead adding respiratory inhibitors, glutamine

and glutaminolysis inhibitors (CB-839 and transaminase inhibitor aminooxyacetic acid) were added stepwise (Figure 32A). At the last step antimycin was added to enable the calculation of basal respiration. IL10+CpG stimulated cells showed higher respiration rates than Myc^{high} cells when glutamine was absent (Figure 32B). Adding glutamine increased OCR of Myc^{high} cells to levels comparable to IL10+CpG stimulated in Myc^{low} cells. This increase was reversed in Myc^{high} by addition of the transaminase inhibitor AOA, while IL10+CpG stimulation mediated respiration was unchanged. Treatment with the GLS inhibitor CB-839 did not further decrease respiration of Myc^{high} cells. In contrast a tendency towards even greater basal respiration rates was observed in IL10+CpG stimulated Myc^{low} cells. Considering both respiration experiments, only the respiration of Myc^{high} cells was dependent on glutamine, while IL10+CpG stimulated Myc^{low} cells seemed to use other fuels, most likely fatty acids, to increase respiration rates.

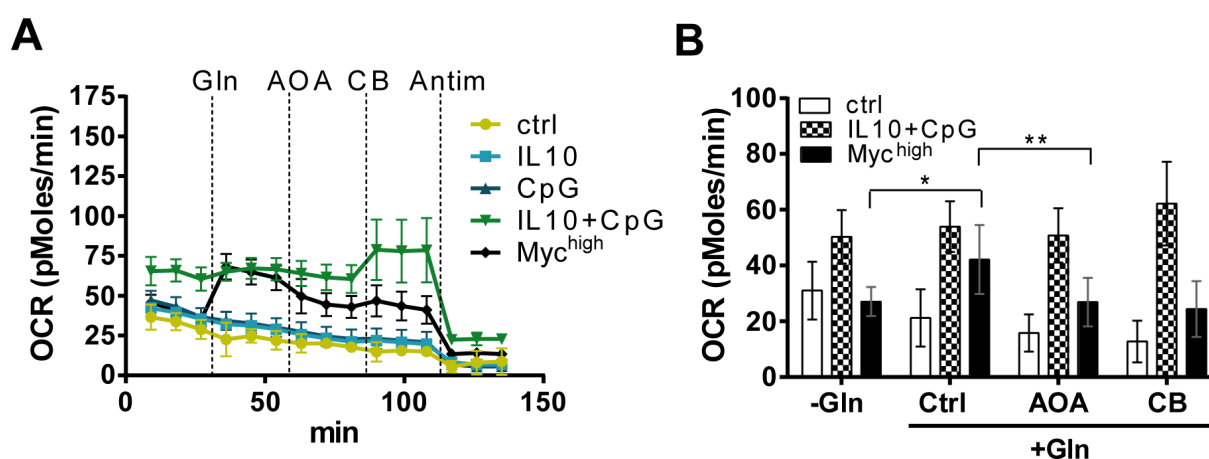


Figure 32: Respiration of Myc^{high} cells is dependent on glutaminolysis.

(A) OCR of IL10, CpG, IL10+CpG stimulated Myc^{low} and Myc^{high} cells seeded in media without glutamine and glucose. Glutamine and glutaminolysis inhibitors (500 μM AOA= aminooxyacetic acid, 1 μM CB=CB-839) were added stepwise. One representative analysis out of three is shown. Error bars indicate technical variations. (B) Basal respiration rates were calculated from three replicates of A as described before. Mean \pm SD of three independent experiments and one-way ANOVA (Bonferroni's posttest) results are shown (* $p < 0.05$, ** $p < 0.01$).

3.6.5 Glutamine derived aKG is important for proliferation of Myc^{high} cells

While the oxidation of glutamine via respiration is shown above for Myc^{high} cells and reported previously (Gao *et al.*, 2009), the importance of increased oxidative derived TCA intermediates and aerobic respiration for proliferation was still unknown. To analyze this, rescue experiments of cell proliferation were performed. Cells were grown in media without glutamine and TCA intermediates (Pyr, aKG, Mal, OAA) were added (Figure 33). Afterwards total cell numbers were counted 48 h after treatment. Proliferation of IL10+CpG stimulated Myc^{low} cells could only partially be rescued by the addition of oxaloacetate (OAA) to the media (Figure 33A) whereas Pyr, aKG or Mal showed no significant effects. In contrast, proliferation of Myc^{high} cells was partially restored by pyruvate and completely restored after aKG addition (Figure 33B), but neither Mal or OAA significantly increased cell doubling

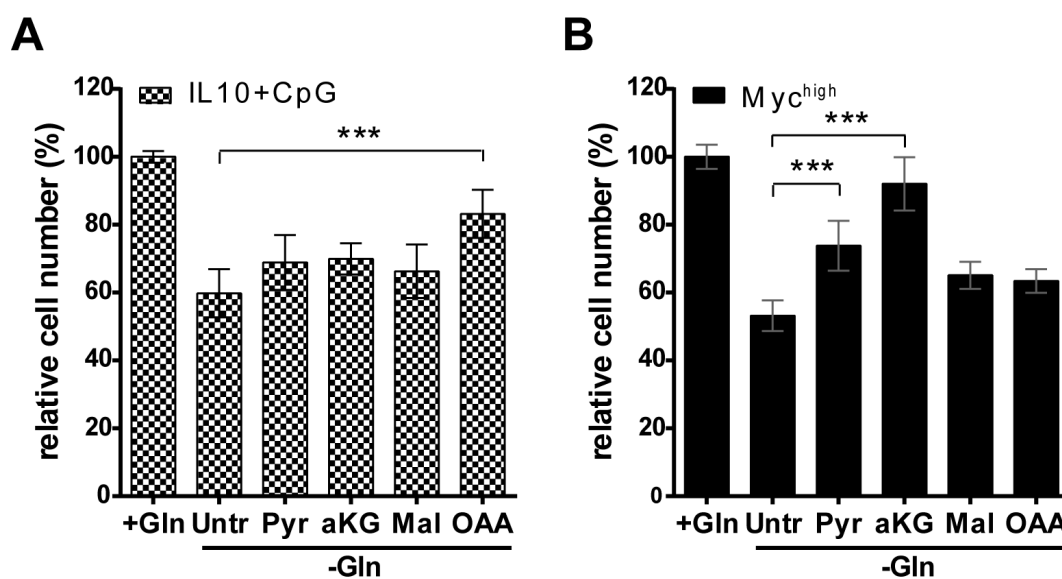


Figure 33: Proliferation of Myc^{high} cells but not IL10+CpG stimulated cells is aKG dependent. Cell numbers of glutamine deprived and metabolite treated IL10+CpG stimulated Myc^{low} and Myc^{high} cells relative to cells seeded in glutamine containing media. TCA intermediates were added as indicated to the glutamine deprived media (Pyr=pyruvate, aKG= α -ketoglutarate, Mal=malate, OAA= oxaloacetate) and cells were stimulated as described before. Cell number of IL10+CpG stimulated cells (**A**) and unstimulated Myc^{high} cells (**B**) was counted 48 h after treatment. Mean \pm SD of three independent experiments and one-way ANOVA results are shown (***) $p < 0.001$.

of Myc^{high} cells over time. Importantly, proliferation of unstimulated Myc^{low} cells was not increased by any of the metabolites (data not shown).

The fact that only aKG, but not Mal or OAA, is able to rescue Myc^{high} cells from glutamine dependent proliferation block, supports that the oxidation of glutamine derived TCA metabolites and therefore energy and reduction equivalent production is most important for proliferation in Myc^{high} cells. However, although proliferation of IL10+CpG stimulated Myc^{low} cells was equally glutamine dependent, other glutamine dependent pathways than respiration must play an important role for proliferation in these cells.

3.6.6 Proliferation of IL10+CpG stimulated Myc^{low} cells depends on aspartate and nucleotides synthesis

Only OAA, but not other TCA intermediates, was able to rescue IL10+CpG stimulation induced proliferation from glutamine deprivation and OAA is an important precursor for aspartate. Therefore the role for glutamine derived aminoacids, observed by glutamine tracing (Figure 29), was further analyzed in IL10+CpG stimulated Myc^{low} and Myc^{high} cells. Glutamine is not only incorporated in the carbon backbone of amino acids, but is also an important donor for amino groups, a process which is catalyzed by aminotransferases. To block enzyme activity of aminotransferase, cells were treated with aminooxyacetic acid (AOA) and cell doubling was analyzed. Treatment with AOA blocked proliferation of IL10+CpG stimulated and *MYC* overexpressing cells comparable to glutamine withdrawal (Figure 34A).

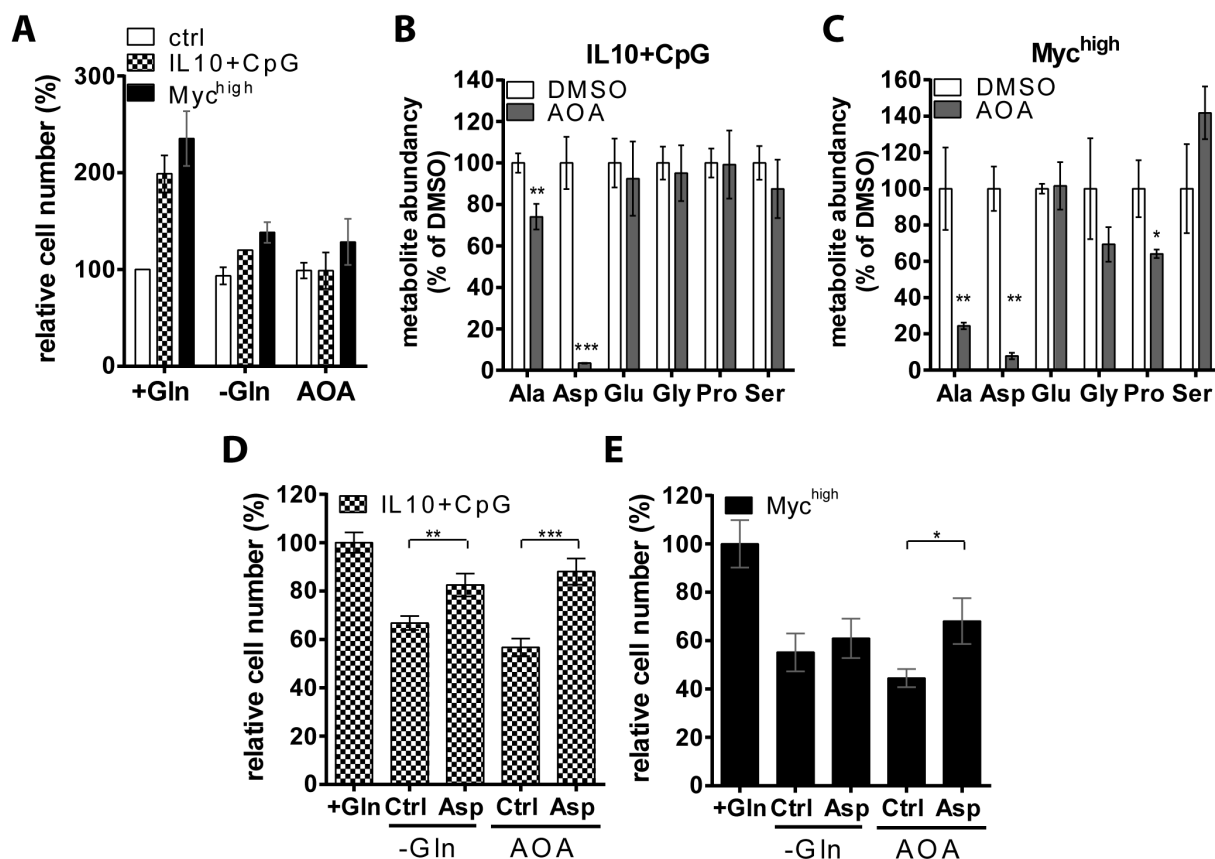


Figure 34: IL10+CpG stimulation induced proliferation is dependent on glutamine derived aspartate.

(A) Relative cell numbers of IL10+CpG stimulated Myc^{low} and unstimulated Myc^{high} cells after transaminase inhibition with 500 μ M AOA. IL10+CpG stimulation was performed as described before and cells were counted 48 h after treatment. (B+C) Intracellular amino acid abundance of IL10+CpG stimulated Myc^{low} (B) and Myc^{high} cells (C) 24 h after AOA treatment and stimulation measured by mass spectrometry. Percentage of DMSO treated cells are shown for each amino acid. (D+E) Relative cell numbers of IL10+CpG stimulated Myc^{low} (D) and unstimulated Myc^{high} cells (E) after glutamine withdrawal or 500 μ M AOA treatment and simultaneous 10 mM aspartate addition. Cells were stimulated as described before and numbers were counted 48 h after treatment. All experiments in this figure were performed in triplicates. Numbers were calculated relative to glutamine containing sample. Mean \pm SD and one-way ANOVA (Bonferroni's posttest) results are shown (* $p < 0.05$, ** $p < 0.01$, *** $p < 0.001$).

This supports the view that aminotransferases are important for proliferation of IL10+CpG stimulated Myc^{low} and Myc^{high} cells.

To answer the question which glutamine derived amino acid was most important for IL10+CpG stimulation or Myc induced proliferation, intracellular amino acid abundance after AOA treatment was measured by mass spectrometry (Figure 34B). In IL10+CpG stimulated Myc^{low} cells a 30% reduction of alanine levels was observed, while aspartate levels were nearly vanished. In contrast, in Myc^{high} cells a strong reduction of both alanine and aspartate was detected accompanied by a significant reduction of proline levels (Figure 34C). Since both, IL10+CpG stimulated Myc^{low} and Myc^{high} cells, showed strong decrease in aspartate levels, the role of aspartate for IL10+CpG stimulation and Myc mediated proliferation was analyzed. Cells were grown in glutamine deprived media or treated with AOA. To test the ability of aspartate to rescue cell proliferation, aspartate was added to the cells prior to stim-

ulation. Supplementing glutamine deprived media with aspartate significantly increased the total cell number after IL10+CpG stimulation (Figure 34D). The same rescue of proliferation was observed after aspartate addition to AOA treated IL10+CpG stimulated Myc^{low} cells. In contrast, no significant rescue of Myc induced proliferation was observed after aspartate treatment of glutamine deprived Myc^{high} cells and only a partial rescue of proliferation after AOA treatment could be achieved by aspartate addition (Figure 34E).

Aspartate is an important precursor for nucleotide synthesis (Lane & Fan, 2015). Thereby, carbon and nitrogen atoms of the aspartate are incorporated into the backbone of pyrimidines, while aspartate derived nitrogen is important for purine synthesis (Figure 35A). Importantly, also glutamine is a nitrogen donor for both nucleotides. To test if nucleotide synthesis is the main function of glutamine and glutamine derived aspartate in IL10+CpG stimulated cells, the nucleotide bases thymine (T) and adenine (A) were added to glutamine deprived and AOA treated cells (Figure 35B). Only in IL10+CpG stimulated Myc^{low} cells a complete rescue of proliferation was achieved by nucleotide base addition, while no significant increase in cell numbers was observed in Myc^{high} cells neither after glutamine deprivation nor AOA treatment (Figure 35C).

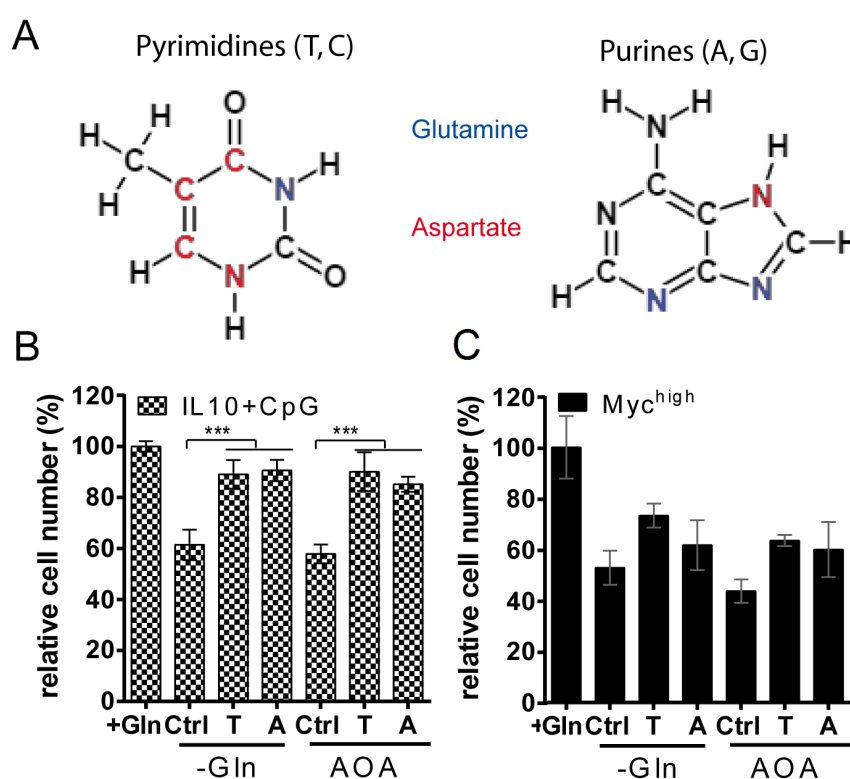


Figure 35: IL10+CpG stimulation induced proliferation depends on glutamine derived nucleotides.

(A) Aspartate and glutamine are important precursors for pyrimidine and purine base synthesis. Glutamine derived nitrogen are shown in blue, aspartate derived carbons and nitrogen in red. (B+C) Relative cell numbers of glutamine deprived (-Gln) and 500 μM AOA treated IL10+CpG stimulated Myc^{low} (B) and Myc^{high} cells (C) after 100 μM thymine (T) and 100 μM adenine (A) addition. Percent of glutamine treated positive control are shown. Experiment was performed in triplicates. Mean \pm SD and one-way ANOVA (Bonferroni's posttest) are shown.

Therefore a model is proposed in which glutamine derived aspartate is important for nucleotide synthesis and thus cell proliferation in IL10+CpG stimulated Myc^{low} cells. In contrast, aspartate and nucleotides are not sufficient to rescue Myc^{high} cells proliferation block mediated by glutamine deprivation. Furthermore, not only aspartate but also alanine is glutamine derived in Myc^{high} cells. Therefore, different dependencies of cell proliferation on glutamine is proposed for IL10+CpG stimulated and Myc^{high} cells.

3.6.7 GOT2 is important for aspartate and nucleotide synthesis in IL10+CpG stimulated Myc^{low} cells

Both, aspartate and aKG, are end products of the transamination from glutamine to oxaloacetate. This reaction is catalyzed by the aspartate aminotransferases, also known as glutamic-oxaloacetic transaminase (GOT). There are two isoforms of GOT, the cytosolic form GOT1 and the mitochondrial form GOT2 (Panteghini, 1990). To investigate their role in IL10+CpG stimulation and Myc induced proliferation, siRNA mediated knockdown of both was performed (Figure 36A) and cell doubling after two days was analyzed. Knockdown of *GOT1* reduced proliferation of Myc^{high} cells about 25 %, but did not affect cell doubling of IL10+CpG stimulated Myc^{low} cells. In contrast, knockdown of *GOT2* affected proliferation of both, IL10+CpG stimulated and Myc^{high} cells. Thereby, proliferation of IL10+CpG stimulated cells was reduced about 30 % (Figure 36B).

Next, it was tested whether GOT2 derived aKG or aspartate and nucleotide synthesis was important for cellular proliferation. After *GOT2* knockdown cells were treated with aKG, aspartate, adenine or thymine and cell numbers were counted after 48 h. In IL10+CpG stimulated cells a partial rescue by aspartate and a complete rescue of proliferation by nucleotide supplementation was observed (Figure 36C). Importantly, these metabolites were not able to rescue *GOT2* knockdown in Myc^{high} cells (Figure 36D). Instead, supplementation with aKG was needed to completely restore proliferation in Myc^{high} cells as already observed after glutamine deprivation. Therefore, glutamine is needed for aspartate and following nucleotide synthesis in IL10+CpG stimulated cells to support proliferation, while Myc^{high} primarily seems to rely on glutamine dependent aKG production, but in both cases generation of these metabolites is GOT2 dependent.

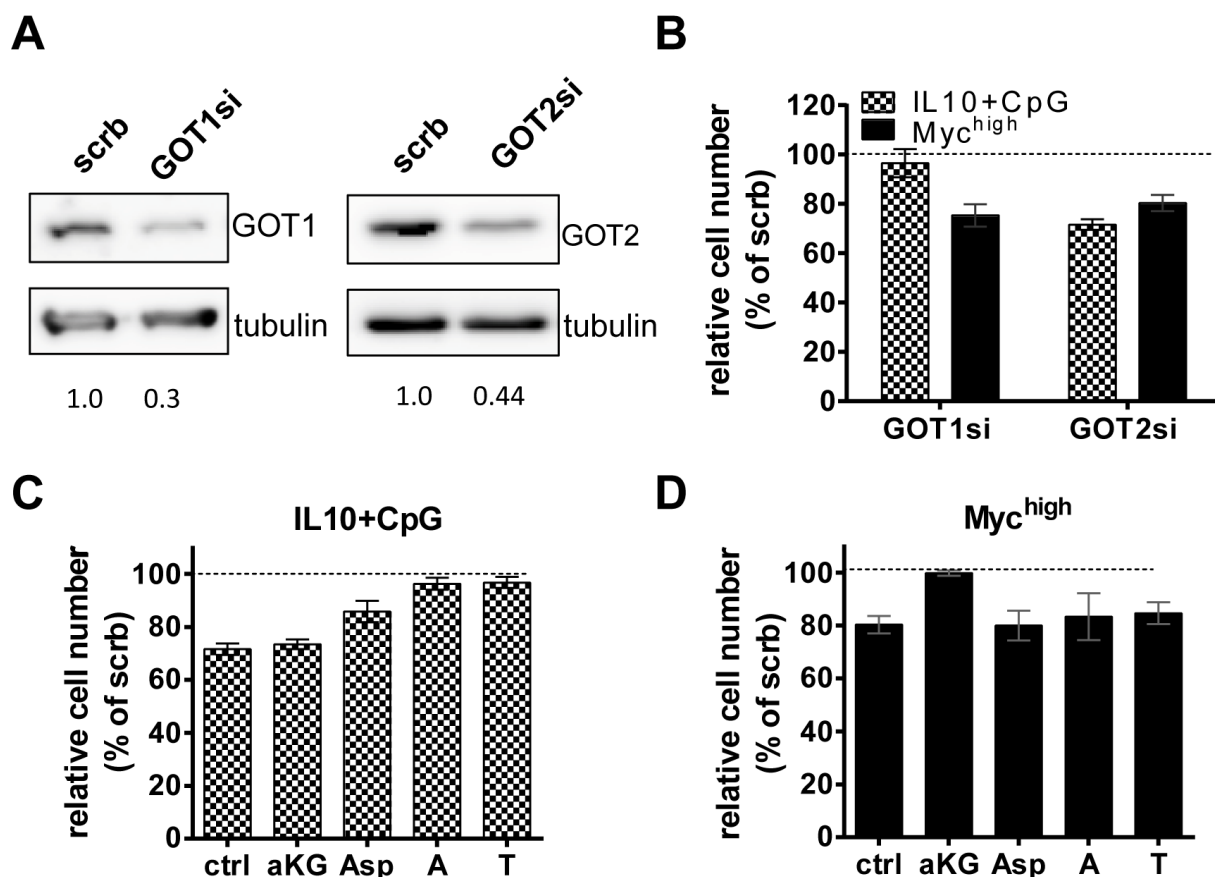


Figure 36: IL10+CpG stimulation induced proliferation is dependent on GOT2 mediated aspartate and following nucleotide synthesis.

(A+B) Transient knockdown of *GOT1* and *GOT2* in P493-6 cells performed by siRNA transfection. Knockdown efficiency was checked 24 h after knockdown by immunoblot (A). Knockdown efficiency (GOT/tubulin ratio) relative to scrb sample is shown below the images. 24 h after knockdown cells were seeded in fresh media and Myc^{low} cells were stimulated daily with IL10+CpG. After 48 h cells were counted and relative cell number was normalized on non-target (scrb) control (B). (C+D) Relative cell number after *GOT2* knockdown and indicated 1 mM aKG, 10 mM aspartate (Asp), 100 μ M adenine (A) or 100 μ M thymine (T) addition in IL10+CpG stimulated Myc^{low} (C) and Myc^{high} cells (D). All experiments were performed in triplicates. Mean and SD are shown.

3.6.8 *GOT2* is a target of Myc and STAT3/NF- κ B

GOT2 was shown above to be important for cell proliferation of IL10+CpG stimulated Myc^{low} and Myc^{high} cells. Furthermore, RNASeq data revealed an increase in *GOT2* expression after IL10+CpG stimulation and *MYC* overexpression (Figure 26B). Since STAT3 and NF- κ B were main mediators of *CDK4* expression after IL10+CpG stimulation (Figure 23), an additional role for these transcription factors in *GOT2* gene expression regulation was supposed. Therefore, cells were treated with ACPH and Ruxolitinib and *GOT2* gene expression of unstimulated, single stimulated, IL10+CpG stimulated Myc^{low} and Myc^{high} cells were compared by qRT PCR. After DMSO treatment a strong upregulation of *GOT2* expression in Myc^{high} cells was observed (Figure 37A). In addition, a synergistic upregulation of *GOT2* was observed in IL10+CpG stimulated Myc^{low} cells and this expression was, as *CDK4* before, dependent on IKK and JAK/STAT signaling. Importantly, none of these inhibitors affected Myc mediated *GOT2* expression. The dependency of *GOT2* expression on STAT3 and p65

in IL10+CpG stimulated Myc^{low} cells was further confirmed by Judith Kemper (Kemper, unpublished).

Furthermore a binding of STAT3 and p65 to the proximal promoter of *GOT2* was shown by chromatin immunoprecipitation (Figure 37B). It is supposed, that a combined binding of STAT3 and p65 is not only involved in *CDK4* regulation, but plays a role in the regulation of *GOT2*. However, the detailed mechanism that leads to an synergistic increase in gene expression needs to be analyzed in future experiments.

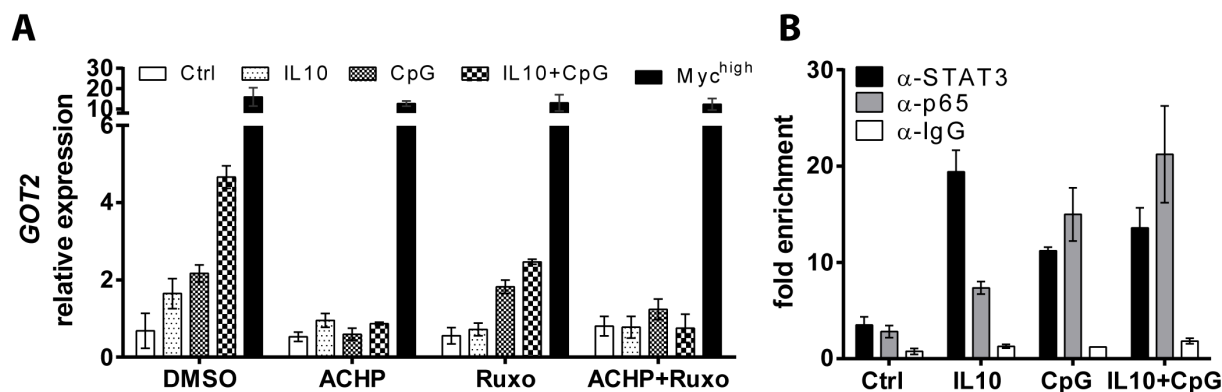


Figure 37: *GOT2* expression is directly regulated by STAT3 and NF- κ B.

(A) qRT analysis of *GOT2* expression of samples described in Figure 22 (p.62). Expression was normalized on *drosophila ACT42A* and unstimulated Myc^{low} cells. Mean \pm SD of three independent experiments are shown. (B) ChIP analysis of the *GOT2* promoter of samples described in Figure 25 (p.66). Pull down of chromatin fragments was quantified by qPCR. Enrichment was calculated relative to an inactive, closed intron region (*PRAME*) and unstimulated Myc^{low} cells. One representative precipitation out of three is shown. Error bars represent technical variance

3.7 Comparison of glutamine metabolism in lymphoma cell lines

A GOT2 dependent differential usage of glutamine in Myc and STAT3/NF- κ B dependent B cell proliferation was shown in P493-6 cells. Importantly, *MYC* overexpression, aberrant STAT3 and NF- κ B activation are known to be main drivers of lymphomagenesis. While Myc deregulation is a hallmark of Burkitt lymphoma (Dave *et al.*, 2006), a subtype of Diffuse Large B cell Lymphoma (DLBCL) was shown to be dependent on cooperative STAT3 and NF- κ B signaling (Lam *et al.*, 2008). Furthermore Hodgkin lymphoma cells were also shown to be dependent on NF- κ B signaling and additional STAT3 or STAT5 activation (Wood *et al.*, 1998; Küppers, 2009). By using cell lines representing these types of lymphoma, the pathway dependent usage of glutamine observed in P493-6 cells was investigated.

3.7.1 B cell lymphoma cell lines dependent on different signaling pathways

CA-46, OCI-Ly3 and L-428 cells were chosen to represent Burkitt, DLBCL and Hodgkin lymphoma, respectively. First, *MYC* expression and activation of STAT3 and NF- κ B signaling was confirmed in these cell lines by immunoblot (Figure 38A). While neither STAT3 nor p65 were active in CA-46 cells, OCI-Ly3 cells showed strong STAT3 and p65 phosphorylation. In L-428 cells a weak STAT3 and p65 phosphorylation was detected, but a complete deletion of the NF- κ B inhibitor I κ B α , which was mediated by non-sense mutation in I κ B α in this cell line (Wood *et al.*, 1998). Myc levels were strongest in CA-46 cells, followed by a moderate protein level in the other two cell lines. To analyze the dependency of OCI-Ly3 and L-428 cells on active STAT3 and NF- κ B signaling, the previously described small molecule inhibitors AHP and Ruxolitinib were used. In CA-46 cells no effect of these inhibitors on any of the investigated pathways was detected in immunoblot analysis and proliferation of these cells was not significantly affected by STAT3 or NF- κ B inhibition (Figure 38B). A strong reduction of p65 phosphorylation accompanied by an increase in I κ B α by AHP and a decrease in STAT3 phosphorylation by Ruxolitinib were observed in OCI-Ly3. Importantly, these inhibitions correlated with a complete loss of cell doubling over two days in this cell line (Figure 38B). In contrast, L-428 cells only mildly responded to both inhibitors, which was reflected in lower STAT3 and p65 signaling pathway activations, that were only slightly affected by AHP or Ruxolitinib treatment. This might be due to the published mutations in this cell line.

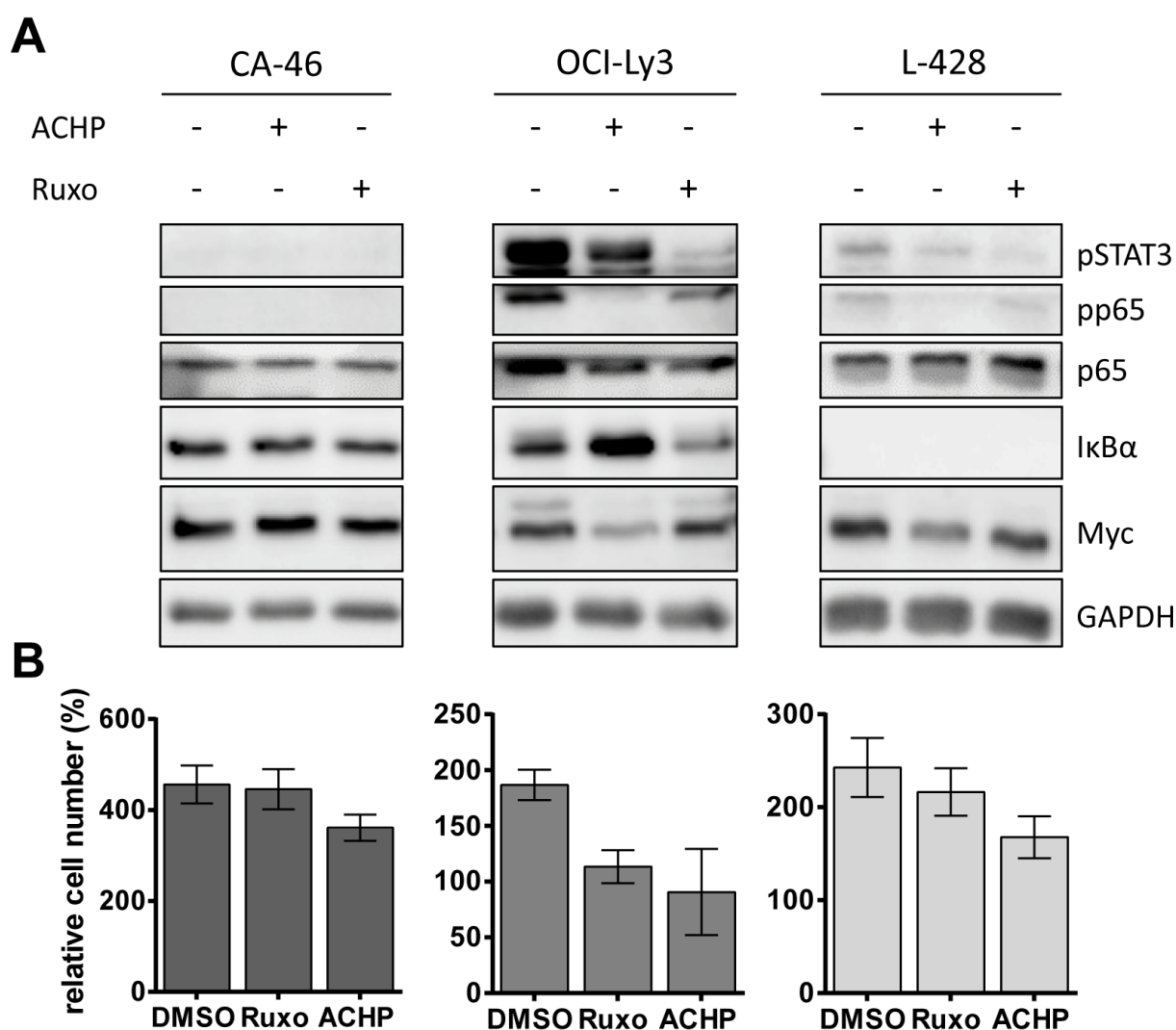


Figure 38: Proliferation of B cell lymphoma cell lines relies on different pathway activations. (A) Immunoblot of signaling pathway activations in CA-46 Burkitt, OCI-LY3 DLBCL and L-428 Hodgkin cell lines. STAT3 activity is shown by Tyr705 phosphorylation, NF- κ B signaling by p65 phosphorylation and I κ B α degradation. Signaling was blocked by inhibitors against IKK (7 μ M ACHP) or JAK (1 μ M Ruxolitinib). Equal protein loading is indicated by GAPDH staining. (B) Cell number of 1 μ M Ruxolitinib and 7 μ M ACHP treated cell lines in A relative to initial cell number 48 h after seeding. Mean and SD of three independent experiments are shown.

3.7.2 Differential usage of GOT2 derived metabolites in B cell lymphoma cell lines

As above shown P493-6 cells can proliferate either when overexpressing exogenous *MYC* or when Jak/STAT and NF- κ B signaling is activated in a way were global gene expression is affecting both cell cycle regulators but also metabolic enzymes. Therefore, one question was, whether in lymphoma cell lines a comparable dependency between Myc or Jak/STAT and NF- κ B, glutamine and proliferation can be observed. CA-46 BL cells, OCI-LY3 DLBCL and L428 HL cells were used. Cells were grown for 48 h in glutamine free media and cell doubling was defined. As shown in Figure 39 the cell doubling (and thus proliferation) in all three cell lines was reduced by 50% after glutamine withdrawal, confirming the importance of glutamine metabolism in B cell proliferation. In previous chapters clear evidence was provided that the inhibitor AOA affecting aminotransferase reduces both, Myc or IL10+CpG stimu-

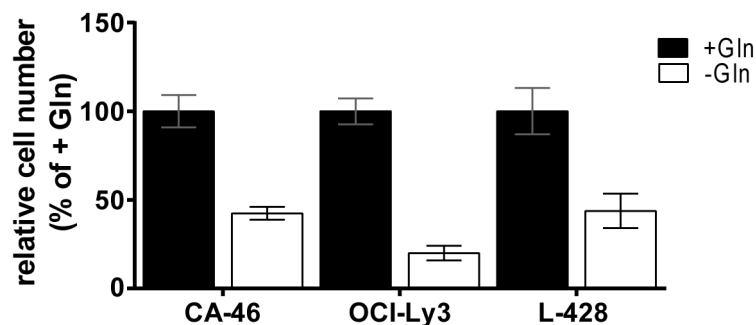


Figure 39: Proliferation of B cell lymphoma cell lines is glutamine dependent.

Cell number of CA-46, OCI-Ly3 and L-428 cells 48 h after seeding in glutamine media relative to glutamine containing media (+Gln). Mean and SD of three independent experiments are shown.

lation, driven proliferation through interrupting metabolic support of cell cycle progression. Therefore, CA46, OCI-LY3 and L-428 cells were treated with AOA (Figure 40). A strong reduction in cell doubling as for Glu deprivation was observed and was also comparable to the reduction of proliferation by AOA treatment in P493-6 cells (Figure 40A). Importantly, when adding aspartate or adenine to AOA treated CA-46 cells a twofold increase in the relative cell number was detected. In contrast in OCI-Ly3 and L-428 cells aspartate and to some extent also adenine was rescuing proliferation of AOA treated cells (Figure 40). 90% of OCI-Ly3 proliferation could be rescued by aspartate and over 60% by adenine addition (Figure 40B). L-428 cells could nearly be rescued from AOA induced proliferation block by aspartate or adenine addition (both > 80%, Figure 40C).

As GOT2 was important for aspartate synthesis and proliferation in P493-6 cells (Figure 34, Figure 36), its role in the other cell lines was further analyzed. The *GOT2* knockdown of about 40% resulted in a reduced proliferation in all three lymphoma cells lines at about 20-35% (Figure 41B). Importantly, in CA-46 cells the GOT2 mediated proliferation was rescued by aKG, while the reduced cell proliferation under lower *GOT2* gene expression in L-428 and OCI-LY3 cells was reverted by adding aspartate or adenine.

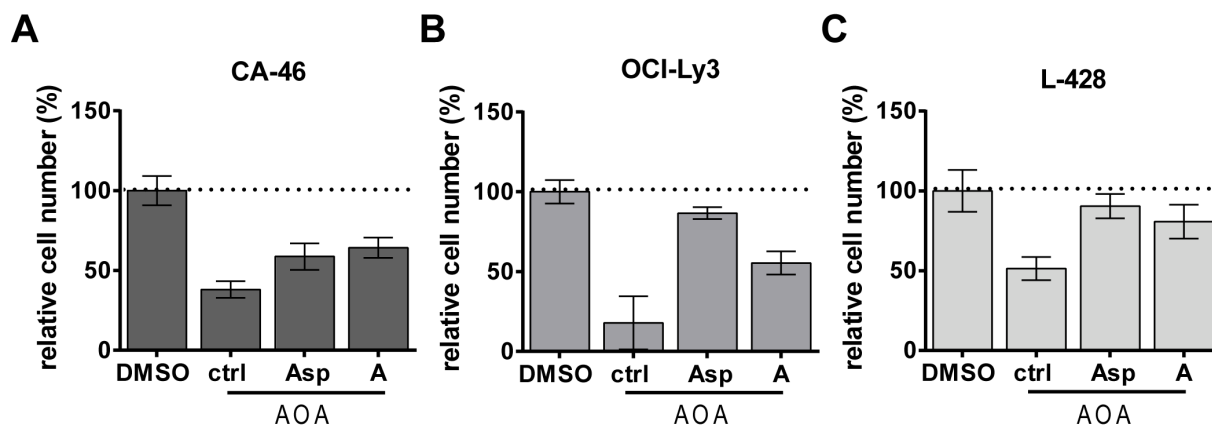


Figure 40: Proliferation of lymphoma cells is amino transaminase dependent.

Cell numbers of 500 μ M AOA treated CA-46 (A), OCI-Ly3 (B) and L-428 cells (C) relative to DMSO control. For rescue 10 mM aspartate (Asp) or 100 μ M adenine (A) was added simultaneously to the cells. Cell numbers were counted 48 h after treatment. Mean and SD of three independent experiments are shown.

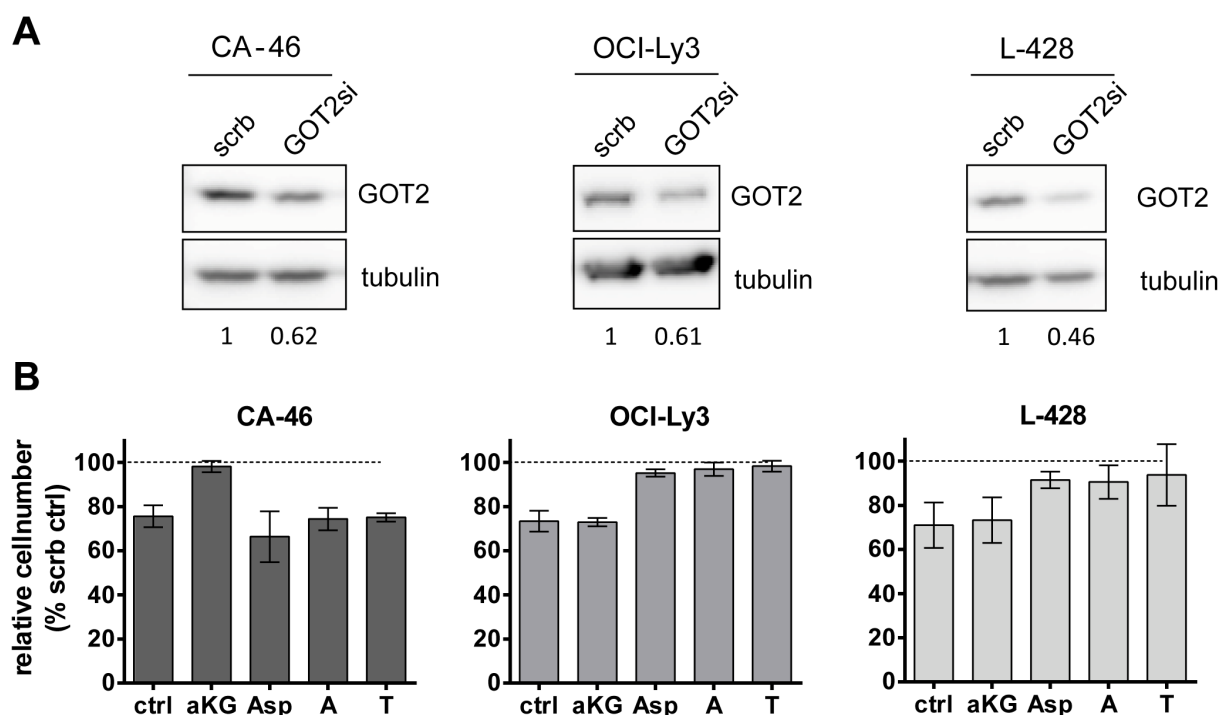


Figure 41: Pathway dependent usage of GOT2 derived metabolites in lymphoma cells.

(A) Immunoblot of GOT2 in CA-46, OCI-Ly3 and L-428 cells 24 h after siRNA mediated knockdown. Knockdown efficiencies (GOT2/tubulin) relative to scrb control are shown under the images. (B) Relative cell number of CA-46, OCI-LY3 and L-428 cells after *GOT2* knockdown and metabolite treatment. 24 h after transfection cells were seeded in fresh media as indicated 1 mM α -ketoglutarate (aKG), 10 mM aspartate (asp) or 100 μ M nucleotide bases adenine (A) and thymine (T) were added to the media and cell number was calculated after 48 h. Mean and SD of cell numbers relative to non-target siRNA (scrb) are shown. All experiments were performed in triplicates.

Summing these data, a comparable dependency on glutamine for aKG synthesis for proliferation could be shown for CA-46 cells as well as P493-6 Myc^{high} cells. Also OCI-Ly3 cells showed a comparable dependency on glutamine for aspartate and nucleotide synthesis as IL10+CpG stimulated P493-6 Myc^{low} cells. However, L-428 cells showed an equal dependency on aspartate and nucleotides for proliferation as OCI-Ly3. This could be explained by the well known deregulated Jak/STAT and Nf- κ B pathways in both cell lines, although mainly for HL cells a more comprehensive analysis of involved pathways is necessary. Importantly, GOT2 was identified as a central player also in lymphoma cell lines *in vitro*. Furthermore, either aKG or aspartate and nucleotides can rescue aminotransferase deficiency in these cells depending on the signaling network active in the corresponding cell line mediated either by Myc or NF- κ B/STAT3.

3.7.3 *GOT2* expression is upregulated in Burkitt and ABC DLBCL patients

To answer the question about *GOT2* gene expression in primary lymphoma samples microarray based GE data from Oncomine were used (Rhodes *et al.*, 2004) (Figure 42). In a dataset published by Basso *et al.* (2005) increased expression of *GOT2* in Burkitt ($n = 17$, $p = 4.9E-9$) and DLBCL ($n = 32$, $p = 7.6E-7$) samples compared to normal B cell controls was observed (Figure 42A). Interestingly highest expression of *GOT2* in normal controls

was detected in proliferating centroblast. A higher expression of *GOT2* was also observed in HL, however, in this dataset only data from three different cell lines were included. Therefore, a second dataset from Brune *et al.* (2008) was analyzed (Figure 42B). In this dataset a higher expression of *GOT2* was observed for in BL and DLBCL in comparison to pre-GC B cells and memory B cells but not normal circulating B cells. Thereby the latter again were characterized by the highest expression in control cells. Notably, expression of *GOT2* in both subgroups of HL was less pronounced as in the Basso data set. Therefore, it is stated that *GOT2* seems to be highly expressed in proliferating B cells or aggressive NHL but also in subsets of HL which needs to be further defined.

In addition to different expression between normal B cells and lymphoma, it is obvious that the different lymphoma subtypes and most notably DLBCL are heterogenic in their *GOT2* expression. Therefore it was suggested that further molecular subgroups with different *GOT2* expression exist. As described in the introduction DLBCL can be distinguished in so called ABC-like and GCB like DLBCL. Expression analysis of primary lymphoma with ABC-like and GCB-like DLBCL subgrouping but also clinical data for R-CHOP treated DLBCL patients are only available from Lenz *et al.* (2008) which was analyzed using the LYMMML web based analysis tool (<http://lymmml.ur.de/>). Within this DLBCL cohort 93 ABC-like and 117 GCB-like DLBCL cases but also 33 unclassified DLBCL were analyzed. A higher expression of *GOT2* in ABC patients compared to GCB or unclassified DLBCL was observed. Importantly, *GOT1* was not differential expressed in any of these datasets (data not shown). The high expression of *GOT2* in ABC-DLBCL underlines the important role for *GOT2* in OCI-Ly3 cells, as OCI-Ly3 cells are molecular classified as ABC-like DLBCL.

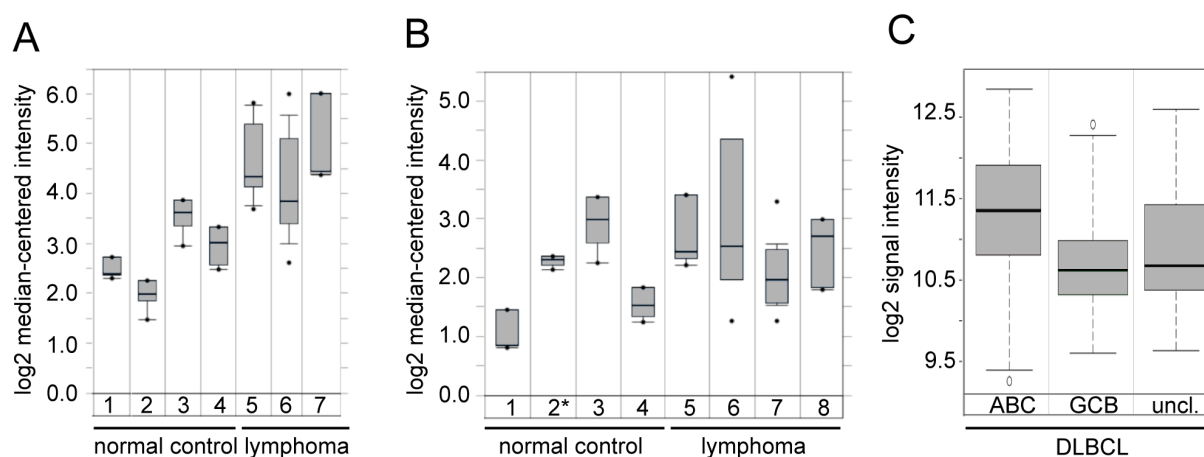


Figure 42: High expression of *GOT2* in BL and ABC DLBCL patients.

(A+B) Microarray gene expression data of *GOT2* from Basso *et al.* (2005) (A) and Brune *et al.* (2008) (B) taken from oncomine.org. Expression of normal B cell controls (1 = naive pre-germinal B cell, 2 = B lymphocyte, 2 = plasma cell, 3 = centroblast, 4 = memory B cell) and lymphoma samples (5 = Burkitt, 6 = DLBCL, 7/8 = Hodgkin lymphoma (classical/nodular lymphocyte predominant)) is shown. Shown are minimum and maximum values (dots), 10% and 90% percentile (outer whiskers), 25% and 75% percentile (outer edges of the box) and median value (middle lane). (C) Differential expression of *GOT2* in molecular DLBCL subtypes. Patient data from Lenz *et al.* (2008) were analyzed using the MMLymphoma Miner (lymmml.ur.de). Shown are minimum and maximum values (whiskers) upper and lower quantile (outer edges of the box) and median value (middle lane).

Importantly, it also connects ABC DLBCL to the observed STAT3/NF- κ B regulation of *GOT2* in IL10+CpG stimulated P493-6 as ABC DLBCL are defined by aberrant activated STAT3 and NF- κ B signaling (see introduction).

Next it was analyzed, whether high *GOT2* expression is also prognostic in DLBCL. This is most likely as in a number of studies for ABC-like DLBCL a worse clinical outcome has been shown (Lenz *et al.*, 2008).

3.7.4 High *GOT2* expression is a negative prognostic factor in DLBCL

To analyze if high *GOT2* expression affects lymphoma aggressiveness or progression *in vivo*, R-CHOP treated DLBCL patients from Lenz *et al.* (2008) were classified according to their *GOT2* expression. Thereby, patients with a *GOT2* expression higher than the median expression of the group were defined as GOT2^{high} whereas patients with an expression level lower than the median were classified as GOT2^{low}. For both groups Kaplan-Meier curves were calculated in R and survival curves were compared (Figure 43). A significant difference in the survival of GOT2^{high} and GOT2^{low} expressing patients was observed in a univariate model (survdif: $p=0.00255$) but also an effect of *GOT2* on patient survival in a multivariate model could be proved (Cox: $p=0.03756$). Thereby, a high *GOT2* expression was associated with a worse clinical outcome compared to low expression. About 80% of GOT2^{low} patients lived for 5 or more years after diagnosis, whereas less than 50% of patients with high *GOT2* expression survived during this time frame. From this retrospective

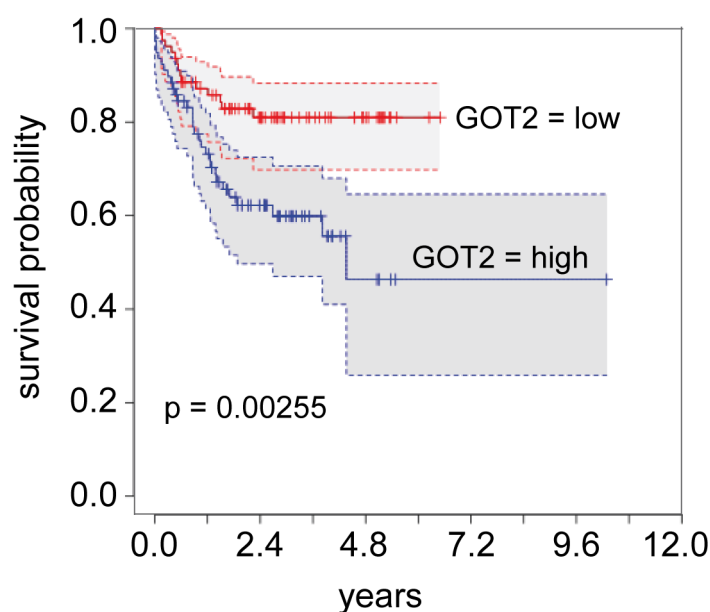


Figure 43: High *GOT2* expression is associated with decreased survival rates DLBCL patients. Kaplan-Meier curves of R-CHOP treated DLBCL patients from Lenz *et al.* (2008) ($n=157$). Patients were grouped according to their *GOT2* expression relative to the median of the group (high $>$ median, low \leq median). GOT2 low is shown as red, GOT2 high as blue line. Grey areas and dashed lines indicate 95% confidence intervals. P value shown was calculated using the 'survdif' function in R.

DLBCL cohort, although not derived from a clinical trial, first evidence is provided that GOT2 might play an important role in subtypes of lymphoma and also in their clinical outcome. Thus GOT2 is suggested a promising drug target or therapeutic predictive marker in DLBCL. However, additional *in vitro* analysis and data from patients cohort of different retrospective and prospective clinical trials are necessary to further support this assumption in the future.

4 Discussion

The aim of the study was to investigate the impact of combinations of microenvironmental stimuli on global gene expression, proliferation and metabolism in resting B cells. Thereby, a new regulatory circuit of IL10R and TLR9 stimulation was found that involved interactions of the transcription factors STAT3 and NF- κ B. The proposed gene expression regulatory mechanisms of STAT3 and NF- κ B interaction, the impact of the increased gene expression on proliferation and metabolism and its supposed role in B cell lymphomagenesis are discussed below.

4.1 Global gene expression amplification is not limited to *MYC* overexpression

A major question of this study was how signaling pathways activated by single or combinations of stimuli affect B cell proliferation by global gene expression. It could be shown, that α -IgM, CD40L, IGF-1, CpG and IL10 activate different signaling pathways in *Myc*^{low} P493-6 cells and that these stimulations vary in their capacity to induce S-phase entry in these cells. Previous publications have shown that perturbations that induce cell cycle changes can also affect total RNA amounts (Darzynkiewicz *et al.*, 1979). More importantly, comparison of different samples with varying RNA amounts have been shown to result in hampered gene expression interpretation (Lovén *et al.*, 2012). By using cell number based normalization and a newly developed spike-in method, a RNA amount unaffected comparison of gene expression in unstimulated *Myc*^{low}, stimulated *Myc*^{low} and *Myc*^{high} cells could be performed in this study. Thereby, a global amplification of RNA expression after *Myc* induction could be confirmed in the P493-6 cell line (Lin *et al.*, 2012; Nie *et al.*, 2012). Interestingly, stimulating the P493-6 *Myc*^{low} cells with factors derived from the microenvironment also increased global gene expression. Thereby, the same set of genes was affected by all stimuli and differences between the stimuli were mainly quantitative and not qualitative, indicating an important role for gene expression amplification in normal B cell activation as well. Importantly, stimulation of lymphocytes with the TLR agonist lipopolysaccharide (LPS) was reported to increase global RNA levels in a *Myc* dependent fashion (Nie *et al.*, 2012). In contrast, data published during the time course of this study showed that the increase in total RNA in LPS stimulated lymphocytes was largely independent from endogenous *MYC* expression after longer time periods (24-48 h) (Sabò *et al.*, 2014). The concept of a *Myc* independent

amplification of global RNA is also supported from data in this thesis. *CDK4* and *GOT2* expression was dependent on STAT3 and NF- κ B activation but largely unaffected by Myc inhibition after IL10+CpG stimulation. In B cells more than 10.000 STAT3 and 20.000 p65 binding sites could be found by ChIP Seq and about one-third of the NF- κ B binding sites lacked the canonical binding motifs (Hardee *et al.*, 2013; Zhao *et al.*, 2014). Due to the large number of binding sites, it is therefore likely that a majority of genes consists both, STAT3 and NF- κ B, binding sites and that the observed global upregulation of gene expression is also largely mediated by simultaneous STAT3 and NF- κ B binding.

To confirm this Myc independent gene expression amplification after IL10+CpG stimulation, RNASeq of stimulated samples could be performed after *MYC* knockdown. However, the present study shows that endogenous *MYC* expression can be reduced by RNAi but not completely diminished. To completely knockout *MYC* expression the clustered regularly interspaced short palindromic repeats (CRISPR)/CRISPR-associated (Cas) system might be applicable (Jinek *et al.*, 2012). By these means an involvement of Myc in the global gene expression increase after IL10+CpG stimulation could be completely excluded.

4.2 Synergy in gene expression changes by STAT3 and NF- κ B pathway activity

The most important observation in this study was that simultaneous stimulation with IL10 and CpG synergistically increased global gene expression in Myc deprived cells. Moreover, on the example of *CDK4* and *GOT2* it was shown that this synergistic effect was not mediated by an increase in *MYC* expression but that a simultaneous activation of STAT3 and NF- κ B was underlying this gene expression increase.

4.2.1 Simultaneous binding of STAT3 and NF- κ B to target gene promoters

While there is just one publication about the role of combined STAT3 and NF- κ B in B cells, their cooperation was extensively studied in solid tumors and inflammation (Lam *et al.*, 2008; Grivennikov & Karin, 2010). One theory states that the interaction of STAT3 recruits the histone acetylase p300, which acetylates p65 and increases nuclear retention (Lee *et al.*, 2009). However, prolonged nuclear retention can be excluded based on nuclear staining of p65.

In a second study, direct interaction of STAT3 and NF- κ B and combined binding at the ICAM-1 were found (Kesanakurti *et al.*, 2013). Using chromatin immunoprecipitation combined binding of STAT3 and NF- κ B to the proximal promoters of *CDK4* and *GOT2* were also found this study. Based on these ChIP data, a model of STAT3 and NF- κ B binding after IL10+CpG stimulation is suggested that is involved in gene expression after IL10+CpG stimulation (Figure 44).

While single stimulation of Myc^{low} cells with IL10 or CpG results in moderate binding of either STAT3 or p65 and only weak binding of the corresponding other, combined stimulation with IL10+CpG leads to strong, simultaneous binding of STAT3 and p65 to the same promoter region. This increased combined binding is then thought to be involved in the increased gene expression by so far unknown regulatory mechanisms. Possible mechanisms involved in the observed increased transcription are further discussed below.

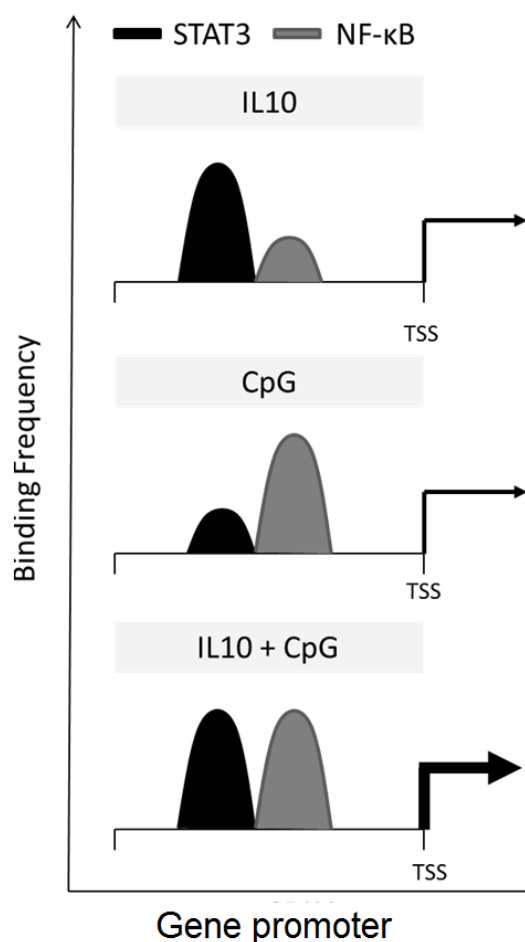


Figure 44: Scheme of STAT3 and NF- κ B binding to target gene promoters.

Arrows indicate gene expression value.
TSS = transcription start site.

There are no known canonical STAT3 or NF- κ B binding sites in the investigated promoter regions of *CDK4* and *GOT2*. Nevertheless, it was shown that STAT3 and p65 directly interact and together bind sequences that differ from the canonical binding sites (Kesanakurti *et al.*, 2013; Hagihara *et al.*, 2005). Furthermore, binding of STAT3 to the *CDK4* and *GOT2* promoters (*CDK4* -200 bp, *GOT2* -32 bp) can be concluded from DLBCL cell line ChIP-Seq data, and a binding of NF- κ B next to these sites (*CDK4* -125 bp, *GOT2* -7 bp) can be found in the ChIPbase database of the lymphoblastoid cell line GM12878 (Hardee *et al.*, 2013; Yang *et al.*, 2013). Importantly, these data correspond with the increased STAT3/NF- κ B binding at the proximal promoter regions found in this study (*CDK4* -88 bp, *GOT2* -13bp), confirming the existence of these binding sites. It has to be mentioned, that due to a strong sequence conservation of the proximal *CDK4* and *GOT2* promoter regions no specific PCR primer could be designed that exactly matched the binding sites found in the ChIP Seq data. However, these conserved promoter regions also imply a common sequence pattern for combined STAT3 and NF- κ B binding within gene promoters.

ChIP Seq analysis of STAT3 and NF- κ B binding in IL10+CpG stimulated P493-6 and OCI-Ly3 cells might be able to reveal this patterns. Although combined binding of STAT3 and p65 to promoters could be shown, the presented experimental approach was unable to discriminate whether STAT3 binding is a prerequisite for NF- κ B binding (or vice versa) as it was also recently shown (Lee *et al.*, 2011). Therefore, future co-precipitation experiments and corresponding time series analysis have to reveal additional mechanistic details of the described synergistic gene activation.

4.2.2 Supposed gene regulatory mechanisms of STAT3 and NF- κ B

As described above, the precise mechanism of STAT3/p65 mediated transcription increase was not investigated so far. However, combining experimental and literature based knowledge possible mechanisms are supposed.

The fact that the expression of the same genes is increased by IL10, CpG or IL10+CpG stimulation resembles the gene expression observed in cells with different Myc levels (Nie *et al.*, 2012; Lin *et al.*, 2012). By combination of IL10+CpG an increase in the expression of already single stimulation increased genes is achieved, but no additional genes is activated compared to single stimuli alone. The same activation pattern was observed in case of Myc. Increasing the Myc level only increased the expression of already active genes, but not of new ones. A mechanism, called transcriptional pause release is believed to be underlying this effect in case of varying Myc levels (Nie *et al.*, 2012; Rahl *et al.*, 2010). After recruitment of the RNA polymerase II by initiation complexes, the elongation of the transcription can be blocked by DRB-sensitivity inducing factor (DSIF) and negative elongation factor (NELF). In case of Myc binding, the positive transcription elongation factor b (P-TEFb) is recruited, which releases the polymerase from these blocking factors and promotes transcriptional elongation and thereby increases transcription rates. As both, STAT3 and NF- κ B, were shown to be able to recruit P-TEFb, the synergistic effect of combined binding of these transcription factors could be mediated by an increased P-TEFb recruitment and therefore increased transcriptional elongation instead of initiation (Barboric *et al.*, 2001; Hou *et al.*, 2007). Thereby the expression of under single stimulation already active genes is further increased by the combination of IL10+CpG. Future localization and phosphorylation analysis of the RNA polymerase II are needed to prove this assumption.

Second, posttranslational modifications of STAT3 and p65 might be involved in the synergistic effect of IL10+CpG stimulation on gene expression. While a mutual modification of tyrosine STAT3 and p65 phosphorylation could be excluded, other phosphorylation or acetylation sites could differ between single and double stimulations. One example is an additional serine 727 phosphorylation of STAT3, which was shown to modulate STAT3 transcriptional activity before (Andrés *et al.*, 2013). Importantly, TLR signaling is able to induce this serine phosphorylation via a mTOR dependent mechanism (Dreher, 2009). Future proteomic approaches have to reveal if such mutual modifications might occur in IL10+CpG stimulated cells and how they are connected the synergistic increase in gene expression.

4.3 Effects of gene expression changes on proliferation and metabolism

A further question of this study was how global gene expression changes due to *MYC* overexpression or stimulation effects proliferation and metabolism in B cells. Thereby, it was found that most importantly gene expression of G1/S cell cycle regulators (e.g. *CDK4*) and glutaminolysis associated enzymes (e.g. *GOT2*) were synergistically increased by combined STAT3 and NF- κ B activation and important for Myc as well as IL10+CpG stimulation induced proliferation.

4.3.1 Overexpression of G1/S cell cycle regulator genes induces proliferation

The importance of *CDK4* overexpression for B cell proliferation was confirmed by inhibition of the CDK4/6 complex, which completely blocked cell doubling over time. Importantly, beside posttranslational regulation of CDK4 activity, *CDK4* overexpression was shown to be sufficient to overcome cell cycle arrest of serum starved cells (Latham *et al.*, 1996). Furthermore, gene amplification of *CDK4* correlates with high proliferation rates in breast cancer (Ewen *et al.*, 1993; An *et al.*, 1999). As the expression of negative cell cycle regulators (*CDKN1A*, *CDKN1B*) was not affected by IL10+CpG stimulation, overexpression of *CDK4* and *CDK6* shifts the ratio of kinases to inhibitors, thereby leading to more activated CDK/cyclin complexes than in unstimulated cells and increased cell cycle entry (Harper *et al.*, 1995; Hengst *et al.*, 1998). The activity of CDK4/CDK6 complexes is further increased by the expression of *CCND2* and *CCND3*, while *CCND1* was not detected in any of the samples. Beside their classical role as cofactors for CDKs, cyclin D's were shown to sequester the negative regulators p21 and p27, thereby leading to more active CDK complexes (Quintanilla-Martinez *et al.*, 2003). Therefore, cell cycle progression is not solely mediated by posttranslational modifications, but overexpression of genes coding for activating cell cycle regulators is sufficient to induce proliferation.

4.3.2 Increased gene expression of glutaminolysis enzymes supports transformation processes

Beside gene expression of cell cycle regulators, the gene expression of metabolic enzymes is increased in proliferating cells (Whitfield *et al.*, 2006). In line with these observations, gene expression of glucose and glutamine metabolism regulating enzymes was increased by either IL10+CpG stimulation or *MYC* overexpression. However, only glutamine deprivation completely blocked proliferation of IL10+CpG stimulated Myc^{low} and unstimulated Myc^{high} cells. These data correlate with previous findings showing that most cancer types are highly glutamine dependent (Hensley *et al.*, 2013). The dependency on glutamine is often reflected in an increased expression of *GLS* isoforms in different cancer entities, which is also associated with an increased invasiveness or poor clinical prognosis (van den Heuvel *et al.*, 2012; Pan *et al.*, 2015; Huang *et al.*, 2014). Nevertheless, an important role for increased *GLS* expression in lymphoma is so far only provided by *in vitro* data and mouse models (Xiang *et al.*,

2015; Gao *et al.*, 2009). The current study shows that high *GOT2* expression, is equally important for glutaminolysis and proliferation in lymphoma. Most importantly high *GOT2* expression was shown to be associated with worse prognosis in DLBCL patients.

GOT2 was described to be a potential Myc target genes before (Korangath *et al.*, 2015). In line with these data, *MYC* expression was increased in Myc^{high} P493-6 cells as well as BL patient samples. Additionally, a regulation by and simultaneous binding of STAT3 and NF- κ B to the promoter of *GOT2* could be shown. The supposed regulation of *GOT2* expression by STAT3 and NF- κ B was further confirmed by an increased expression in ABC DLBCL patients, the subgroup of DLBCL described to rely on deregulated STAT3 and NF- κ B signaling (Lam *et al.*, 2008).

Expression of transaminases, including *GOT2*, was shown to be increased in glutamine dependent breast cancer cell lines and treatment with AOA decreased tumor growth concurrent xenograft models (Korangath *et al.*, 2015). Also in pancreatic tumors a role for GOT1 and GOT2 was described. Here an increased glutamine metabolism and high *GOT1* expression were necessary to provide reducing equivalents for redox homeostasis in the cell. The importance of transaminases is further supported by a recent publication, showing that quiescent fibroblasts metabolize glutamine via GLUD's, while proliferating cells rely on transaminases to provide both aKG for energy and amino acids for biosynthetic demands (Coloff *et al.*, 2016). Considering these data altogether, specific transaminase inhibitors could be a promising therapeutic target for STAT3/NF- κ B and Myc dependent lymphoma while non proliferating naive B cells should be not affected.

4.4 Different glutamine usage in B cell lymphoma

Inhibitor and knockdown experiments revealed an important role for GOT2 in proliferation of *MYC* overexpressing and STAT3/NF- κ B activated cells. However, rescue experiments with different glutamine derived metabolites showed that the proliferation of these cells relied on different GOT2 derived metabolites. While *MYC* overexpressing cells needed glutamine and aKG, STAT3/NF- κ B activated cells were dependent on aspartate for nucleotide biosynthesis. These differences in glutamine usage and the supposed underlying mechanisms are discussed below und summarized in Figure 45.

4.4.1 Using glutamine as a energetic fuel

Different energetic dependencies were observed for P493-6 Myc^{high} and IL10+CpG stimulated Myc^{low} cells. While *MYC* overexpressing cells used glutamine for respiration and lactate production, oxygen consumption and extracellular acidification of IL10+CpG stimulated Myc^{low} cells was independent from glutamine. *MYC* overexpression was shown to increase mitochondrial function and glutamine respiration before (Li *et al.*, 2005). It was also shown that the usage of glutamine for TCA function and respiration is independent from glucose metabolism (Le *et al.*, 2012). Importantly, both studies focused on increased

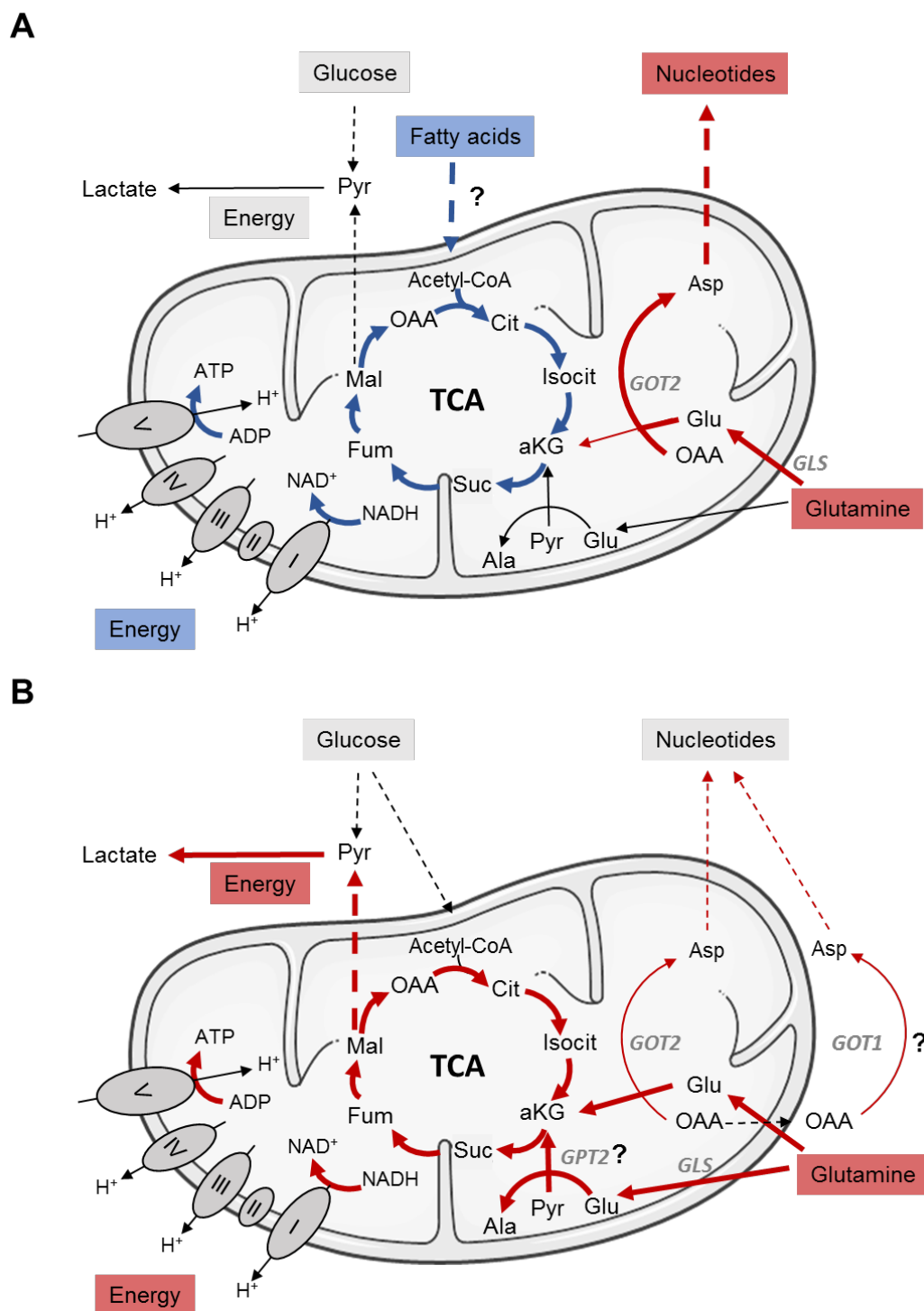


Figure 45: Supposed metabolism in STAT3/NF- κ B and Myc mediated proliferation.

(A) STAT3/NF- κ B dependent cells do not rely on glutamine or glucose for cellular respiration, therefore a dependency of fatty acid oxidation (blue) is supposed. In contrast, the majority of glutamine (red) is needed for aspartate and nucleotide synthesis. (B) Myc dependent cells use more glutamine for TCA function, respiration and lactate production possibly mediated by the additional usage of GPT2. Aspartate is most likely derived from both GOT1 and GOT2. Note, that narrow or missing arrows do not indicate that these pathways are not active in these cells, but only that they are not that important for the proliferation of the depicted model. Gene names of important enzymes are shown in grey and italic letters. Gln = glutamine, Glu = glutamate, Ala = alanine, Asp = aspartate, aKG = α -ketoglutarate, Suc = succinate, Fum = fumarate, Mal = malate, OAA = oxaloacetate, Cit = citrate, Isocit = Isocitrate, Pyr = pyruvate.

GLS activity as a major reason for increased usage of glutamine in respiration. However, the expression of *GLS* was also increased in IL10+CpG stimulated Myc^{low} cells in this study. In contrast, a major difference in the expression of the alanine aminotransferase (*GPT2*) was observed between both samples (Table 28, Appendix p. 114). Expression of *GPT2* was only increased in Myc^{high} cells. Furthermore high levels of alanine were found in Myc^{high} cells but not in any of the stimulations performed on Myc^{low} cells. *GPT2* uses glutamate and pyruvate to synthesize alanine and aKG. Therefore, Myc^{high} cells could use *GPT2* in conjunction with *GOT2* to synthesize aKG from glutamate therefore fueling the TCA and respiration with glutamine. As pyruvate is the acceptor of the amino group of glutamine, usage of *GPT2* would explain the high levels of alanine in Myc^{high} cells. This hypothesis is further supported by a higher percentage of glutamine derived TCA metabolites and a dependency of respiration and acidification on glutamine. Future knockdown experiments will prove the dependency of glutamine respiration on *GPT2* in Myc^{high} cells, which would then be a promising target for Myc dependent cancer.

Since oxygen consumption of IL10+CpG stimulated Myc^{low} cells was neither glutamine nor glucose dependent, STAT3/NF- κ B activated cells are supposed to use fatty acids for cellular respiration. This hypothesis is further supported by a recent publication showing that another B cell derived malignancy, chronic lymphocytic leukemia, oxidize free fatty acids in a STAT3 dependent manner (Rozovski *et al.*, 2015). It was also shown, that STAT3 activation in general regulates ETC function (Wegrzyn *et al.*, 2009). Therefore, respiration of STAT3 and NF- κ B activated cells might be independent from glutamine due to a oxidation of free fatty acids. Further respiratory analysis with inhibitors affecting fatty acid oxidation will test this hypothesis in future. If validated positively, inhibiting fatty acid oxidation could be a promising tool for the treatment of STAT3/NF- κ B dependent lymphoma.

4.4.2 The role of glutamine in aspartate and nucleotide synthesis

Finally an important role for aspartate in proliferation of STAT3/NF- κ B dependent P493-6 and OCI-Ly3 cells was shown. Importantly, the synthesis of aspartate is highly linked to cellular respiration. Two recent publication showed that the main function of the ETC is to provide reduction equivalents for biosynthesis mainly including aspartate and nucleotides synthesis (Birsoy *et al.*, 2015; Sullivan *et al.*, 2015). In line with these findings, knockdown of *GOT2* in STAT3/NF- κ B dependent cells was completely rescued by nucleotide bases confirming the important role aspartate and nucleotides for proliferation.

Nevertheless, proliferation of *MYC* overexpressing P493-6 Myc^{high} and Burkitt CA-46 cells was not rescued by aspartate and nucleotides after *GOT2* knockdown. While cellular respiration is supposed to be mediated by a glutamine independent process in STAT3/NF- κ B dependent B cells, this thesis and other studies show that glutamine is a major source for both, reduction equivalents and energy, in Myc dependent cells (Gao *et al.*, 2009). Due to the connection of ETC and biosynthesis, it is proposed that providing reduction equivalents and

energy is a prerequisite for biosynthesis and proliferation in these cells. Therefore, without the addition of aKG for fueling the TCA and respiration neither addition of aspartate nor nucleotides is able to rescue Myc dependent proliferation as energy and reduction equivalents are missing to support the further biosynthetic processes.

Nevertheless, it is still not known how solely aKG addition can be sufficient to rescue proliferation of Myc^{high} cells under glutamine deprived conditions. Glutamine is necessary for nucleotide synthesis and nucleotides themselves are mandatory for cell proliferation. In contrast, aKG cannot be used for nucleotide *de novo* synthesis. Therefore it is still unknown how Myc^{high} cells synthesize nucleotides without glutamine.

Myc^{high} cells show an increased glutaminolysis rate and large glutamate pools. It can be supposed that the increased glutamate pool in Myc^{high} is able to support nucleotide synthesis for at least one more cell doubling. Another hypothesis would be that Myc^{high} cells could use the excess of intracellular alanine and the addition of aKG to synthesize glutamate in a GPT2 dependent manner. Glutamate can then be converted to glutamine by the glutamine synthetase also known as glutamate-ammonia ligase (*GLUL*). Importantly *GLUL* expression was only increased in Myc^{high} cells but not in IL10+CpG stimulated cells (Table 28, Appendix p. 114). Thereby, Myc^{high} cells could use the intracellular alanine pool to generate glutamate and glutamine for nucleotide synthesis. These assumptions are further supported by a recent publication showing that Myc is directly regulating *GLUL* expression by promoter demethylation (Bott *et al.*, 2015). Future assays have to reveal, if GPT2 and *GLUL* might be involved in the proliferation rescue after aKG addition in Myc^{high}.

In summary, new metabolic differences between Myc and STAT3/NF- κ B activated B cells were found that, when further investigated, could lead to the development of new lymphoma subtype specific therapy.

4.5 IL10R and TLR9 signaling in B cell lymphoma development and progression

Since IL10R and TLR9 signaling are involved in GC formation, the supposed mechanism of IL10 and CpG stimulation and the synergy of STAT3 and NF- κ B might be involved in B cell activation. Moreover, as lymphoma cells rely on different mutations that aberrantly activate these pathways, it can be proposed that comparable mechanisms are not only observed in normal B cell physiology but also in transformed B cells. This hypothesis is further supported by studies providing first evidence that also the B cell microenvironment might play a role in lymphoma development and progression (Lenz *et al.*, 2008; Aldinucci *et al.*, 2010).

4.5.1 The role of IL10 and CpG in B cell lymphoma

During the last years, multiple studies have shown an impact of either IL10 or CpG signaling on lymphomagenesis. For example, deregulated *IL10* gene expression is thought to increase lymphoma susceptibility and risk (Cao *et al.*, 2013; Edlefsen *et al.*, 2014). IL10 also was shown to be involved in lymphoma progression, as high IL10 serum levels are associated with worse clinical outcome in DLBCL patients (Lech-Maranda *et al.*, 2006; Gupta *et al.*, 2012). Furthermore, gene amplifications of *IL10RA* and *IL10RB* can be found in DLBCL (Béguelin *et al.*, 2015). While IL10 signaling is thought to mainly induce antiapoptotic processes in these studies, data from this thesis imply that a prominent role for IL10 in lymphomagenesis might be the promotion of proliferation and metabolism in B cells with additional activated NF- κ B signaling.

In contrast to IL10, less evidence exists about a direct role for CpG in lymphoma development. Only in BL an activation of TLR9 signaling by malaria parasites is discussed (Torgbor *et al.*, 2014). However, in DLBCL mutations in *MYD88*, a key component of TLR signaling, were frequently reported (Ngo *et al.*, 2011; Choi *et al.*, 2013). In this study it is supposed that stimulation of P493-6 Myc^{low} cells with CpG can serve as a model for chronic TLR activation and canonical NF- κ B activation in lymphoma with these gene mutations.

4.5.2 STAT3 and NF- κ B are important factors in B cell lymphoma pathogenesis

While IL10 is mainly activating STAT3, CpG is a strong mediator of canonical NF- κ B signaling. In lymphoma aberrant activation of both pathways can be found: STAT3 is frequently activated in DLBCL or HL (Hu *et al.*, 2013; Kube *et al.*, 2001) and found to correlate with higher cell proliferation and worse clinical outcome in both (Ding *et al.*, 2007; Huang *et al.*, 2014). Additionally, constitutive NF- κ B signaling can be found in DLBCL and HL and phosphorylated p65 was shown to be an independent prognostic factor in DLBCL (Wood *et al.*, 1998; Davis *et al.*, 2001; Zhao *et al.*, 2015). Importantly, NF- κ B and STAT3 were shown to cooperate and promote the development and progression of glioma, colon, gastric and liver cancers (Grivennikov & Karin, 2010). Today, also growing evidence exists about a cooperative role of both transcription factors in lymphoma. In DLBCL with constitutive NF- κ B signaling phosphorylated STAT3 was found, activated by an interleukin dependent feed forward loop (Davis *et al.*, 2001). Importantly, Lam and colleagues showed that proliferation and survival is maintained by cooperation of both transcription factors in this subgroup of DLBCL (Lam *et al.*, 2008). These findings are further supported by a study that showed that STAT3 is important for ABC DLBCL pathogenesis, the subtype of DLBCL with highest NF- κ B activation (Scuto *et al.*, 2011). Therefore, simultaneous activation of the NF- κ B and STAT3 pathway might be a common feature in different B cell lymphoma. Importantly, the current thesis shows, that not solely mutations but continuous stimulation with factors of the GC environment are able to induce a proliferation comparable to

MYC overexpression in resting B cells. It also implies, that continuous activation of STAT3 and NF- κ B signaling by both, stimuli (IL10/CpG) or a mutation in one pathway combined with the stimulation of the corresponding other, might be sufficient for B cell transformation. Therefore, histologic analysis of STAT3 and NF- κ B pathway activations, also in lymphoma without known mutations, might be a suitable prediction tool for lymphoma outcome.

5 Summary and conclusion

Using a cell based normalization method, it was shown that different GC derived stimuli induce qualitative comparable but quantitative distinct global gene expression and metabolic changes in P493-6 Myc^{low} cells. Thereby, expression of the same set of genes was increased independently from the used stimuli, implying that global gene expression amplification, which was supposed for Myc before, might also be involved in other B cell activations.

Importantly, specific combination of stimuli resulted not only in additive but synergistic effects in global gene expression and metabolite abundance. Strongest synergistic global gene expression and metabolic reprogramming was observed by combined IL10 and CpG stimulation of Myc^{low} cells, leading to sustained cell doubling comparable to overexpression of *MYC*. Further mechanistic analyses revealed that the synergism of IL10 and CpG stimulation was mediated by NF- κ B and STAT3 signaling. Therefore, a model is presented in which the simultaneous binding of both transcription factors is involved in this synergistic increase in target gene expression, as for example *CDK4* and *GOT2*. While this new regulatory circuit of IL10R and TLR9 signaling in B cells is proposed, its detailed underlying mechanisms involved in gene expression regulation need to be elucidated in future experiments.

Importantly, IL10+CpG stimulation induced gene expression changes greatly resembled Myc mediated global amplification of gene expression, cell cycle changes and proliferation. Although proliferation of IL10+CpG stimulated Myc^{low} and Myc^{high} was strictly glutamine dependent and the aspartate aminotransferase *GOT2* was identified as a common regulator of glutaminolysis in both, the following differences were observed: proliferation of IL10+CpG stimulated Myc^{low} cells was dependent on glutamine derived aspartate and nucleotides whereas Myc induced proliferation was rescued by α -ketoglutarate addition under AOA treatment or glutamine deprivation. Equally, the STAT3/NF- κ B dependent lymphoma cells OCI-LY3 and L-428 relied on glutamine derived aspartate and nucleotides for proliferation, whereas proliferation of Myc associated CA-46 cells was dependent on glutamine derived α -ketoglutarate. Thus, first evidence for signaling pathway dependent regulation of glutamine metabolism was provided in this study.

In addition to *in vitro* data, *GOT2* could be shown to be strongly expressed in proliferating centroblasts but also in primary B cell lymphoma, where STAT3/NF- κ B dependent ABC-like DLBCL were characterized by higher *GOT2* expression as germinal centre like DLBCL. More importantly high *GOT2* expression was shown to be associated with a worse clinical outcome of R-CHOP treated DLBCL patients, showing that some of the found *in vitro* results might also be important for *in vivo* lymphomagenesis.

Therefore, from previously published and herein presented data, it is now proposed that simultaneous NF- κ B and STAT3 signaling, activated either by extracellular stimulation or already known pathway mutations as for example *MYD88*, *SOCS1* or *CARD11*, plays an important role in B cell proliferation and relies on a synergistic increase in global gene expression including key cell cycle and metabolism regulators. The presented data also highlight

the importance of factors of the B cell microenvironment in transformation processes of B cells. Additionally, for the first time evidence is provided that GOT2 plays an important role in STAT3/NF- κ B and Myc mediated transformation and that different glutamine dependent metabolism exist in lymphoma. However, future analyses are necessary to fully understand the mechanism behind and its functional role in lymphomagenesis but also normal homeostasis of mature B cells. Further investigating the mechanism underlying the synergistic effect of IL10R and TLR9 signaling as well as metabolic differences could help to reveal new prognostic or therapeutic targets for these NF- κ B/STAT3 dependent B cell lymphoma in the future.

6 References

- ADAMS, T. E., EPA, V. C., GARRETT, T. P., & WARD, C. W. 2000. Structure and function of the type 1 insulin-like growth factor receptor. *Cellular and molecular life sciences : Cmls*, **57**(7), 1050–93.
- ALDINUCCI, D., GLOGHINI, A., PINTO, A., DE FILIPPI, R., & CARBONE, A. 2010. The classical Hodgkin's lymphoma microenvironment and its role in promoting tumour growth and immune escape. *The journal of pathology*, **221**(3), 248–63.
- ALIZADEH, A. A., EISEN, M. B., DAVIS, R. E., *et al.* 2000. Distinct types of diffuse large B-cell lymphoma identified by gene expression profiling. *Nature*, **403**(6769), 503–11.
- ALTMAN, B. J., & DANG, C. V. 2012. Normal and cancer cell metabolism: lymphocytes and lymphoma. *The febs journal*, **279**(15), 2598–609.
- AN, H. X., BECKMANN, M. W., REIFENBERGER, G., BENDER, H. G., & NIEDERACHER, D. 1999. Gene amplification and overexpression of CDK4 in sporadic breast carcinomas is associated with high tumor cell proliferation. *The american journal of pathology*, **154**(1), 113–8.
- ANDERSON, J. R., ARMITAGE, J. O., & WEISENBURGER, D. D. 1998. Epidemiology of the non-Hodgkin's lymphomas: distributions of the major subtypes differ by geographic locations. Non-Hodgkin's Lymphoma Classification Project. *Annals of oncology : official journal of the european society for medical oncology / esmo*, **9**(7), 717–20.
- ANDRÉS, R. M., HALD, A., JOHANSEN, C., KRAGBALLE, K., & IVERSEN, L. 2013. Studies of Jak/STAT3 expression and signalling in psoriasis identifies STAT3-Ser727 phosphorylation as a modulator of transcriptional activity. *Experimental dermatology*, **22**(5), 323–8.
- BARBORIC, M., NISSEN, R. M., KANAZAWA, S., JABRANE-FERRAT, N., & PETERLIN, B. M. 2001. NF-kappaB binds P-TEFb to stimulate transcriptional elongation by RNA polymerase II. *Molecular cell*, **8**(2), 327–37.
- BARGOU, R. C., EMMERICH, F., KRAPPMANN, D., *et al.* 1997. Constitutive nuclear factor-kappab-rela activation is required for proliferation and survival of hodgkin's disease tumor cells. *The journal of clinical investigation*, **100**(12), 2961–9.
- BASSO, K., SCHNEIDER, C., SHEN, Q., *et al.* 2012. BCL6 positively regulates AID and germinal center gene expression via repression of miR-155. *The journal of experimental medicine*, **209**(13), 2455–2465.
- BASSO, KATIA, MARGOLIN, ADAM A, STOLOVITZKY, GUSTAVO, *et al.* 2005. Reverse engineering of regulatory networks in human B cells. *Nature genetics*, **37**(4), 382–90.
- BÉGUELIN, W., SAWH, S., CHAMBWE, N., *et al.* 2015. IL10 receptor is a novel therapeutic target in DLBCLs. *Leukemia*, **29**(8), 1684–94.

-
- BERNASCONI, N. L., ONAI, N., & LANZAVECCHIA, A. 2003. A role for Toll-like receptors in acquired immunity: up-regulation of TLR9 by BCR triggering in naive B cells and constitutive expression in memory B cells. *Blood*, **101**(11), 4500–4.
- BIRSOY, K., WANG, T., CHEN, W. W., *et al.* 2015. An Essential Role of the Mitochondrial Electron Transport Chain in Cell Proliferation Is to Enable Aspartate Synthesis. *Cell*, **162**(3), 540–551.
- BLAECHE, ALINE, DELNESTE, YVES, HERBAULT, NATHALIE, *et al.* 2002. Measurement of nuclear factor-kappa B translocation on lipopolysaccharide-activated human dendritic cells by confocal microscopy and flow cytometry. *Cytometry*, **48**(2), 71–9.
- BOTT, A. J., PENG, I.-C., FAN, Y., *et al.* 2015. Oncogenic Myc Induces Expression of Glutamine Synthetase through Promoter Demethylation. *Cell metabolism*, **22**(6), 1068–77.
- BOUCHARD, C., STALLER, P., & EILERS, M. 1998. Control of cell proliferation by Myc. *Trends in cell biology*, **8**(5), 202–6.
- BRUNE, V., TIACCI, E., PFEIL, I., *et al.* 2008. Origin and pathogenesis of nodular lymphocyte-predominant Hodgkin lymphoma as revealed by global gene expression analysis. *The journal of experimental medicine*, **205**(10), 2251–68.
- BUCALA, R. 1992. Polyclonal activation of B lymphocytes by lipopolysaccharide requires macrophage-derived interleukin-1. *Immunology*, **77**(4), 477–82.
- BURGER, J. A., GHIA, P., ROSENWALD, A., & CALIGARIS-CAPPIO, F. 2009. The microenvironment in mature B-cell malignancies: a target for new treatment strategies. *Blood*, **114**(16), 3367–75.
- CALADO, D. P., SASAKI, Y., GODINHO, S. A., *et al.* 2012. The cell-cycle regulator c-Myc is essential for the formation and maintenance of germinal centers. *Nature immunology*, **13**(11), 1092–100.
- CAO, H.-Y., ZOU, P., & ZHOU, H. 2013. Genetic association of interleukin-10 promoter polymorphisms and susceptibility to diffuse large B-cell lymphoma: a meta-analysis. *Gene*, **519**, 288–94.
- CARPENTER, R. L., & LO, H. W. 2014. STAT3 target genes relevant to human cancers. *Cancers*, **6**(2), 897–925.
- CARR, E. L., KELMAN, A., WU, G. S., *et al.* 2010. Glutamine uptake and metabolism are coordinately regulated by ERK/MAPK during T lymphocyte activation. *Journal of immunology (baltimore, md. : 1950)*, **185**(2), 1037–44.
- CASTILLO, J. J., WINER, E. S., & OLSZEWSKI, A. J. 2013. Population-based prognostic factors for survival in patients with Burkitt lymphoma: An analysis from the Surveillance, Epidemiology, and End Results database. *Cancer*, **119**(20), 3672–3679.

-
- CHIRON, D., BEKEREDJIAN-DING, I., PELLAT-DECEUNYNCK, C., BATAILLE, R., & JEGO, G. 2008. Toll-like receptors: lessons to learn from normal and malignant human B cells. *Blood*, **112**(6), 2205–13.
- CHOI, J.-W., KIM, Y.-S., & LEE, J.-H. 2013. MYD88 expression and L265P mutation in diffuse large B-cell lymphoma. *Human pathology*, **44**(7), 1375–81.
- COLOFF, J. L., MURPHY, J. P., BRAUN, C. R., *et al.* 2016. Differential Glutamate Metabolism in Proliferating and Quiescent Mammary Epithelial Cells. *Cell metabolism*, **23**(5), 867–80.
- CONSORTIUM, ERCC. 2005. Proposed methods for testing and selecting the ERCC external RNA controls. *Bmc genomics*, **6**(June 2004), 150.
- CRAWFORD, J., & COHEN, H. J. 1985. The essential role of L-glutamine in lymphocyte differentiation in vitro. *Journal of cellular physiology*, **124**(2), 275–82.
- DANG, CHI V. 2012. Links between metabolism and cancer. *Genes & development*, **26**(9), 877–90.
- DARZYNKIEWICZ, Z., EVENSON, D. P., STAIANO-COICO, L., SHARPLESS, T. K., & MELAMED, M. L. 1979. Correlation between cell cycle duration and RNA content. *Journal of cellular physiology*, **100**(3), 425–38.
- DAVE, S. S., FU, K., WRIGHT, G. W., *et al.* 2006. Molecular diagnosis of Burkitt’s lymphoma. *The new england journal of medicine*, **354**(23), 2431–42.
- DAVIS, R. E., BROWN, K. D., SIEBENLIST, U., & STAUDT, L. M. 2001. Constitutive nuclear factor kappaB activity is required for survival of activated b cell-like diffuse large b cell lymphoma cells. *The journal of experimental medicine*, **194**(12), 1861–74.
- DAVIS, R. E., NGO, V. N., LENZ, G., *et al.* 2010. Chronic active B-cell-receptor signalling in diffuse large B-cell lymphoma. *Nature*, **463**(7277), 88–92.
- DE ALBORAN, I. M., O’HAGAN, R. C., GÄRTNER, F., *et al.* 2001. Analysis of C-MYC function in normal cells via conditional gene-targeted mutation. *Immunity*, **14**(1), 45–55.
- DETTMER, K., NÜRNBERGER, N., KASPAR, H., *et al.* 2011. Metabolite extraction from adherently growing mammalian cells for metabolomics studies: optimization of harvesting and extraction protocols. *Analytical and bioanalytical chemistry*, **399**(3), 1127–39.
- DING, B. B., YU, J. J., YU, R. Y.-L., *et al.* 2007. Constitutively activated STAT3 promotes cell proliferation and survival in the activated B-cell subtype of diffuse large B-cell lymphomas. *Blood*, **111**(3), 1515–1523.
- DOMINGUEZ-SOLA, D., VICTORA, G. D., YING, C. Y., *et al.* 2012. The proto-oncogene MYC is required for selection in the germinal center and cyclic reentry. *Nature immunology*, **13**(11), 1083–91.
- DREHER, S. 2009. *Die Rolle von STAT3 in der TLR vermittelten Signalkaskade*. Ph.D. thesis, Technische Universität München.

-
- DUNN-WALTERS, D., THIEDE, C., ALPEN, B., & SPENCER, J. 2001. Somatic hypermutation and B-cell lymphoma. *Philosophical transactions of the royal society of london. series b, biological sciences*, **356**(1405), 73–82.
- EDLEFSEN, K. L., MARTÍNEZ-MAZA, O., MADELEINE, M. M., *et al.* 2014. Cytokines in serum in relation to future non-Hodgkin lymphoma risk: Evidence for associations by histologic subtype. *International journal of cancer. journal international du cancer*, jan.
- ELGUETA, R., BENSON, M. J., DE VRIES, V. C., *et al.* 2009. Molecular mechanism and function of CD40/CD40L engagement in the immune system. *Immunological reviews*, **229**(1), 152–72.
- EMMERICH, F., THEURICH, S., HUMMEL, M., *et al.* 2003. Inactivating I kappa B epsilon mutations in Hodgkin/Reed-Sternberg cells. *The journal of pathology*, **201**(3), 413–20.
- EWEN, M. E., SLUSS, H. K., WHITEHOUSE, L. L., & LIVINGSTON, D. M. 1993. TGF beta inhibition of Cdk4 synthesis is linked to cell cycle arrest. *Cell*, **74**(6), 1009–20.
- FAGARASAN, S., & HONJO, T. 2000. T-Independent immune response: new aspects of B cell biology. *Science (new york, n.y.)*, **290**(5489), 89–92.
- FERLAY, J., STELIAROVA-FOUCHER, E., LORTET-TIEULENT, J., *et al.* 2013. Cancer incidence and mortality patterns in Europe: estimates for 40 countries in 2012. *European journal of cancer (oxford, england : 1990)*, **49**(6), 1374–403.
- FOLLIS, A. V., HAMMOUDEH, D. I., WANG, H., PROCHOWNIK, E. V., & METALLO, S. J. 2008. Structural rationale for the coupled binding and unfolding of the c-Myc oncoprotein by small molecules. *Chemistry & biology*, **15**(11), 1149–55.
- FRIEDMAN, J., HASTIE, T., & TIBSHIRANI, R. 2010. Regularization Paths for Generalized Linear Models via Coordinate Descent. *Journal of statistical software*, **33**(1), 1–22.
- FRITZ, V., & FAJAS, L. 2010. Metabolism and proliferation share common regulatory pathways in cancer cells. *Oncogene*, **29**(31), 4369–77.
- GALIBERT, L., BURDIN, N., DE SAINT-VIS, B., *et al.* 1996. CD40 and B cell antigen receptor dual triggering of resting B lymphocytes turns on a partial germinal center phenotype. *The journal of experimental medicine*, **183**(1), 77–85.
- GAO, P., TCHERNYSHYOV, I., CHANG, T.-C., *et al.* 2009. c-Myc suppression of miR-23a/b enhances mitochondrial glutaminase expression and glutamine metabolism. *Nature*, **458**(7239), 762–5.
- GRANDORI, C., COWLEY, S. M., JAMES, L. P., & EISENMAN, R. N. 2000. The Myc/Max/Mad network and the transcriptional control of cell behavior. *Annual review of cell and developmental biology*, **16**(8), 653–99.
- GREINER, E. F., GUPPY, M., & BRAND, K. 1994. Glucose is essential for proliferation and the glycolytic enzyme induction that provokes a transition to glycolytic energy production. *The journal of biological chemistry*, **269**(50), 31484–90.

-
- GRIVENNIKOV, S. I., & KARIN, M. 2010. Dangerous liaisons: STAT3 and NF- κ B collaboration and crosstalk in cancer. *Cytokine & growth factor reviews*, **21**(1), 11–19.
- GRONWALD, W, KLEIN, M S, KASPAR, H, *et al.*. 2008. Urinary metabolite quantification employing 2D NMR spectroscopy. *Analytical chemistry*, **80**(23), 9288–97.
- GUPTA, M., HAN, J. J., STENSON, M., *et al.*. 2012. Elevated serum IL-10 levels in diffuse large B-cell lymphoma: a mechanism of aberrant JAK2 activation. *Blood*, **119**(12), 2844–53.
- HAAN, C., & BEHRMANN, I. 2007. A cost effective non-commercial ECL-solution for Western blot detections yielding strong signals and low background. *Journal of immunological methods*, **318**(1-2), 11–9.
- HAGIHARA, K., NISHIKAWA, T., SUGAMATA, Y., *et al.*. 2005. Essential role of STAT3 in cytokine-driven NF-kappaB-mediated serum amyloid A gene expression. *Genes to cells*, **10**(11), 1051–1063.
- HAN, S.-S., YUN, H., SON, D.-J., *et al.*. 2010. NF-kappaB/STAT3/PI3K signaling crosstalk in iMyc E mu B lymphoma. *Molecular cancer*, **9**(jan), 97.
- HANAHAH, D., & WEINBERG, R. A. 2011. Hallmarks of cancer: the next generation. *Cell*, **144**(5), 646–674.
- HANSON, K. D., SHICHIRI, M., FOLLANSBEE, M. R., & SEDIVY, J. M. 1994. Effects of c-myc expression on cell cycle progression. *Molecular and cellular biology*, **14**(9), 5748–5755.
- HARDEE, J., OUYANG, Z., ZHANG, Y., *et al.*. 2013. STAT3 targets suggest mechanisms of aggressive tumorigenesis in diffuse large B-cell lymphoma. *G3 (bethesda, md.)*, **3**(12), 2173–85.
- HARPER, J. W., ELLEDGE, S. J., KEYOMARSI, K., *et al.*. 1995. Inhibition of cyclin-dependent kinases by p21. *Molecular biology of the cell*, **6**(4), 387–400.
- HAYDEN, M. S., & GHOSH, S. 2012. NF- κ B, the first quarter-century: remarkable progress and outstanding questions. *Genes & development*, **26**(3), 203–34.
- HENGST, L., GÖPFERT, U., LASHUEL, H. A., & REED, S. I. 1998. Complete inhibition of Cdk/cyclin by one molecule of p21(Cip1). *Genes and development*, **12**(24), 3882–3888.
- HENSLEY, C. T., WASTI, A. T., & DEBERARDINIS, R. J. 2013. Glutamine and cancer: cell biology, physiology, and clinical opportunities. *The journal of clinical investigation*, **123**(9), 3678–84.
- HERMEKING, H., RAGO, C., SCHUHMACHER, M., *et al.*. 2000. Identification of CDK4 as a target of c-MYC. *Proceedings of the national academy of sciences of the united states of america*, **97**(5), 2229–34.
- HODGKIN. 1832. On some Morbid Appearances of the Absorbent Glands and Spleen. *Medico-chirurgical transactions*, **17**(jan), 68–114.

-
- HOLTICK, U., VOCKERODT, M., PINKERT, D., *et al.* 2005. STAT3 is essential for Hodgkin lymphoma cell proliferation and is a target of tyrphostin AG17 which confers sensitization for apoptosis. *Leukemia*, **19**(6), 936–44.
- HORN, H., ZIEPERT, M., BECHER, C., *et al.* 2013. MYC status in concert with BCL2 and BCL6 expression predicts outcome in diffuse large B-cell lymphoma. *Blood*, **121**(12), 2253–63.
- HOU, T., RAY, S., & BRASIER, A. R. 2007. The functional role of an interleukin 6-inducible CDK9/STAT3 complex in human gamma-fibrinogen gene expression. *The journal of biological chemistry*, **282**(51), 37091–102.
- HU, G., WITZIG, T. E., & GUPTA, M. 2013. A novel missense (M206K) STAT3 mutation in diffuse large B cell lymphoma deregulates STAT3 signaling. *Plos one*, **8**(7), e67851.
- HUANG, D. W., LEMPICKI, R. A., & SHERMAN, B. T. 2009. Systematic and integrative analysis of large gene lists using DAVID bioinformatics resources. *Nature protocols*, **4**(1), 44–57.
- HUANG, FANG, ZHANG, QIUYUE, MA, HONG, LV, QING, & ZHANG, TAO. 2014. Expression of glutaminase is upregulated in colorectal cancer and of clinical significance. *International journal of clinical and experimental pathology*, **7**(3), 1093–100.
- HUMMEL, M., BENTINK, S., BERGER, H., *et al.* 2006. A biologic definition of Burkitt’s lymphoma from transcriptional and genomic profiling. *The new england journal of medicine*, **354**(23), 2419–30.
- JACOBS, S. R., HERMAN, C. E., MACIVER, N. J., *et al.* 2008. Glucose Uptake Is Limiting in T Cell Activation and Requires CD28-Mediated Akt-Dependent and Independent Pathways. *The journal of immunology*, **180**(7), 4476–4486.
- JINEK, M., CHYLINSKI, K., FONFARA, I., *et al.* 2012. A programmable dual-RNA-guided DNA endonuclease in adaptive bacterial immunity. *Science (new york, n.y.)*, **337**(6096), 816–21.
- JOHNSON, D. G., & WALKER, C. L. 1999. Cyclins and cell cycle checkpoints. *Annual review of pharmacology and toxicology*, **39**, 295–312.
- JOOS, S., KÜPPER, M., OHL, S., *et al.* 2000. Genomic imbalances including amplification of the tyrosine kinase gene JAK2 in CD30+ Hodgkin cells. *Cancer research*, **60**(3), 549–52.
- JOOS, S., MENZ, C. K., WROBEL, G., *et al.* 2002. Classical Hodgkin lymphoma is characterized by recurrent copy number gains of the short arm of chromosome 2. *Blood*, **99**(4), 1381–7.
- KEMPER, J. unpublished. *Die Rolle von STAT3 und p65 in der nicht kanonischen Glutaminolyse*. MD thesis, Georg-August Universität Göttingen.
- KESANAKURTI, D., CHETTY, C., RAJASEKHAR MADDIRELA, D., GUJRATI, M., & RAO, J. S. 2013. Essential role of cooperative NF- κ B and Stat3 recruitment to ICAM-1 intronic consensus elements in the regulation of radiation-induced invasion and migration in glioma. *Oncogene*, **32**(43), 5144–55.

-
- KLEIN, M. S., OEFNER, P. J., & GRONWALD, W. 2013. Metaboquant: A tool combining individual peak calibration and outlier detection for accurate metabolite quantification in 1D1H and 1H-13C HSQC NMR spectra. *Biotechniques*, **54**(5), 251–256.
- KLEIN, U., & DALLA-FAVERA, R. 2008. Germinal centres: role in B-cell physiology and malignancy. *Nature reviews immunology*, **8**(1), 22–33.
- KLEIN, U., TU, Y., STOLOVITZKY, G. A., *et al.* 2003. Transcriptional analysis of the B cell germinal center reaction. *Proceedings of the national academy of sciences of the united states of america*, **100**(5), 2639–44.
- KORANGATH, P., TEO, W. W., SADIK, H., *et al.* 2015. Targeting Glutamine Metabolism in Breast Cancer with Aminooxyacetate. *Clinical cancer research*, **21**(14), 3263–3273.
- KUBE, D., HOLTICK, U., VOCKERODT, M, *et al.* 2001. STAT3 is constitutively activated in Hodgkin cell lines. *Blood*, **98**(3), 762–770.
- KÜPPERS, R. 2005. Mechanisms of B-cell lymphoma pathogenesis. *Nature reviews. cancer*, **5**(4), 251–62.
- KÜPPERS, R. 2009. The biology of Hodgkin’s lymphoma. *Nature reviews. cancer*, **9**(1), 15–27.
- KÜPPERS, R., ENGERT, A., & HANSMANN, M.-L. 2012. Hodgkin lymphoma. *Journal of clinical investigation*, **122**(10), 3439–3447.
- KUROSAKI, T. 2011. Regulation of BCR signaling. *Molecular immunology*, **48**(11), 1287–91.
- LA ROSA, F. A., PIERCE, J. W., & SONENSHEIN, G. E. 1994. Differential regulation of the c-myc oncogene promoter by the NF- kappa B rel family of transcription factors. *Mol.cell biol.*, **14**(2), 1039–1044.
- LAEMMLI, U. K. 1970. Cleavage of structural proteins during the assembly of the head of bacteriophage T4. *Nature*, **227**(5259), 680–5.
- LAM, L. T., WRIGHT, G., DAVIS, R. E., *et al.* 2008. Cooperative signaling through the signal transducer and activator of transcription 3 and nuclear factor-kappa B pathways in subtypes of diffuse large B-cell lymphoma. *Blood*, **111**(7), 3701–13.
- LANE, A. N., & FAN, T. W.-M. 2015. Regulation of mammalian nucleotide metabolism and biosynthesis. *Nucleic acids research*, **43**(4), 2466–85.
- LATHAM, K. M., EASTMAN, S. W., WONG, A., & HINDS, P. W. 1996. Inhibition of p53-mediated growth arrest by overexpression of cyclin-dependent kinases. *Molecular and cellular biology*, **16**(8), 4445–55.
- LE, A., LANE, A. N., HAMAKER, M., *et al.* 2012. Glucose-independent glutamine metabolism via TCA cycling for proliferation and survival in B cells. *Cell metabolism*, **15**(1), 110–21.
- LEBIEN, T. W., & TEDDER, T. F. 2008. B lymphocytes: how they develop and function. *Blood*, **112**(5), 1570–80.

-
- LECH-MARANDA, E., BIENVENU, J., MICHALLET, A.-S., *et al.* 2006. Elevated IL-10 plasma levels correlate with poor prognosis in diffuse large B-cell lymphoma. *European cytokine network*, **17**(1), 60–6.
- LEE, H., HERRMANN, A., DENG, J.-H., *et al.* 2009. Persistently Activated Stat3 Maintains Constitutive NF- κ B Activity in Tumors. *Cancer cell*, **15**(4), 283–293.
- LEE, H., DENG, J., XIN, H., *et al.* 2011. A requirement of STAT3 DNA binding precludes Th-1 immunostimulatory gene expression by NF- κ B in tumors. *Cancer research*, **71**(11), 3772–80.
- LENZ, G., WRIGHT, G., DAVE, S. S., *et al.* 2008. Stromal gene signatures in large-B-cell lymphomas. *The new england journal of medicine*, **359**(22), 2313–23.
- LEVY, Y., & BROUET, J. C. 1994. Interleukin-10 prevents spontaneous death of germinal center B cells by induction of the bcl-2 protein. *The journal of clinical investigation*, **93**(1), 424–8.
- LI, F., WANG, Y., ZELLER, K. I., *et al.* 2005. Myc stimulates nuclearly encoded mitochondrial genes and mitochondrial biogenesis. *Molecular and cellular biology*, **25**(14), 6225–34.
- LIANG, ZHENG, DIEPSTRA, ARJAN, XU, CHUANHUI, *et al.* 2014. Insulin-like growth factor 1 receptor is a prognostic factor in classical Hodgkin lymphoma. *Plos one*, **9**(1), e87474.
- LIN, C. Y., LOVÉN, J., RAHL, P. B., *et al.* 2012. Transcriptional Amplification in Tumor Cells with Elevated c-Myc. *Cell*, **151**(1), 56–67.
- LING, X., & ARLINGHAUS, R. B. 2005. Knockdown of STAT3 expression by RNA interference inhibits the induction of breast tumors in immunocompetent mice. *Cancer research*, **65**(7), 2532–6.
- LIU, B.-S., STOOP, J. N., HUIZINGA, T. W., & TOES, R. E. M. 2013. IL-21 enhances the activity of the TLR-MyD88-STAT3 pathway but not the classical TLR-MyD88-NF- κ B pathway in human B cells to boost antibody production. *Journal of immunology (baltimore, md. : 1950)*, **191**(8), 4086–94.
- LIU, W., LE, A., HANCOCK, C., *et al.* 2012. Reprogramming of proline and glutamine metabolism contributes to the proliferative and metabolic responses regulated by oncogenic transcription factor c-MYC. *Proceedings of the national academy of sciences of the united states of america*, **109**(23), 8983–8.
- LOVE, C., SUN, Z., JIMA, D., *et al.* 2012. The genetic landscape of mutations in Burkitt lymphoma. *Nature genetics*, **44**(12), 1321–5.
- LOVE, M. I., HUBER, W., & ANDERS, S. 2014. Moderated estimation of fold change and dispersion for RNA-seq data with DESeq2. *Genome biology*, **15**(12), 550.
- LOVÉN, J., ORLANDO, D. A., SIGOVA, A. A., *et al.* 2012. Revisiting global gene expression analysis. *Cell*, **151**(3), 476–82.
- MACINTYRE, A. N., & RATHMELL, J. C. 2013. Activated lymphocytes as a metabolic model for carcinogenesis. *Cancer & metabolism*, **1**(1), 5.

-
- MACLENNAN, I. C. 1994. Germinal centers. *Annual review of immunology*, **12**(jan), 117–39.
- MADDALY, R., PAI, G., BALAJI, S., *et al.* 2010. Receptors and signaling mechanisms for B-lymphocyte activation, proliferation and differentiation - Insights from both in vivo and in vitro approaches. *Febs letters*, **584**(24), 4883–4894.
- MAGRATH, I. T., PIZZO, P. A., WHANG-PENG, J., *et al.* 1980. Characterization of lymphoma-derived cell lines: comparison of cell lines positive and negative for Epstein-Barr virus nuclear antigen. I. Physical, cytogenetic, and growth characteristics. *Journal of the national cancer institute*, **64**(3), 465–76.
- MALUMBRES, M., & BARBACID, M. 2001. To cycle or not to cycle: a critical decision in cancer. *Nature reviews. cancer*, **1**(3), 222–31.
- MÅNSSON, A., ADNER, M., HÖCKERFELT, U., & CARDELL, L.-O. 2006. A distinct Toll-like receptor repertoire in human tonsillar B cells, directly activated by PamCSK, R-837 and CpG-2006 stimulation. *Immunology*, **118**(4), 539–48.
- MBULAITEYE, S. M., BIGGAR, R. J., BHATIA, K., LINET, M. S., & DEVESA, S. S. 2009. Sporadic childhood Burkitt lymphoma incidence in the United States during 1992-2005. *Pediatric blood & cancer*, **53**(3), 366–70.
- MCCARTHY, BRIAN A, YANG, LIQUN, DING, JANE, *et al.* 2012. NF- κ B2 mutation targets survival, proliferation and differentiation pathways in the pathogenesis of plasma cell tumors. *Bmc cancer*, **12**(1), 203.
- MEYER, N., & PENN, L. Z. 2008. Reflecting on 25 years with MYC. *Nature reviews. cancer*, **8**(12), 976–90.
- MOLYNEUX, E. M., ROCHFORD, R., GRIFFIN, B., *et al.* 2012. Burkitt's lymphoma. *Lancet*, **379**(9822), 1234–44.
- MORIN, R., MUNGALL, K., & PLEASANCE, E. 2013. Mutational and structural analysis of diffuse large B-cell lymphoma using whole genome sequencing. *Blood*, **122**(7), 1256–1265.
- MURN, JERNEJ, MLINARIC-RASCAN, IRENA, VAIGOT, PIERRE, *et al.* 2009. A Myc-regulated transcriptional network controls B-cell fate in response to BCR triggering. *Bmc genomics*, **10**, 323.
- MURPHY, TAYLOR A, DANG, CHI V, & YOUNG, JAMEY D. 2013. Isotopically nonstationary (¹³C) flux analysis of Myc-induced metabolic reprogramming in B-cells. *Metabolic engineering*, **15**(jan), 206–17.
- NATKUNAM, Y. 2007. The biology of the germinal center. *Hematology / the education program of the american society of hematology. american society of hematology. education program*, 210–215.
- NEWSHOLME, ERIC A, CRABTREE, B, & ARDAWI, M S. 1985. Glutamine metabolism in lymphocytes: its biochemical, physiological and clinical importance. *Quarterly journal of experimental physiology (cambridge, england)*, **70**(4), 473–89.

-
- NEWSHOLME, P. 2001. Why is L-glutamine metabolism important to cells of the immune system in health, postinjury, surgery or infection? *The journal of nutrition*, **131**(9 Suppl), 2515S–22S; discussion 2523S–4S.
- NGO, V. N., YOUNG, R. M., SCHMITZ, R., *et al.* 2011. Oncogenically active MYD88 mutations in human lymphoma. *Nature*, **470**(7332), 115–9.
- NIE, Z., HU, G., WEI, G., *et al.* 2012. c-Myc Is a Universal Amplifier of Expressed Genes in Lymphocytes and Embryonic Stem Cells. *Cell*, **151**(1), 68–79.
- NIKITIN, P. A., PRICE, A. M., MCFADDEN, K., YAN, C. M., & LUFTIG, MICAH A. 2014. Mitogen-induced B-cell proliferation activates Chk2-dependent G1/S cell cycle arrest. *Plos one*, **9**(1), e87299.
- NORBURY, C., & NURSE, P. 1992. Animal Cell Cycles and Their Control. *Annual review of biochemistry*, **61**(1), 441–468.
- NOWAK, D. E., TIAN, B., & BRASIER, A. R. 2005. Two-step cross-linking method for identification of NF-kappaB gene network by chromatin immunoprecipitation. *Biotechniques*, **39**(5), 715–25.
- O’CONNOR, J. C., MCCUSKER, R. H., STRLE, K., *et al.* 2008. Regulation of IGF-I function by proinflammatory cytokines: at the interface of immunology and endocrinology. *Cellular immunology*, **252**(1-2), 91–110.
- PAJIC, A., SPITKOVSKY, D., CHRISTOPH, B., *et al.* 2000. Cell cycle activation by c-myc in a burkitt lymphoma model cell line. *International journal of cancer. journal international du cancer*, **87**(6), 787–93.
- PAN, T., GAO, L., WU, G., *et al.* 2015. Elevated expression of glutaminase confers glucose utilization via glutaminolysis in prostate cancer. *Biochemical and biophysical research communications*, **456**(1), 452–8.
- PANTEGHINI, M. 1990. Aspartate aminotransferase isoenzymes. *Clinical biochemistry*, **23**(4), 311–9.
- PARKER, D. C. 1993. T cell-dependent B cell activation. *Annual review of immunology*, **11**(jan), 331–60.
- PENG, S. L. 2005. Signaling in B cells via Toll-like receptors. *Current opinion in immunology*, **17**(3), 230–6.
- POLACK, A., HÖRTNAGEL, K., PAJIC, A., *et al.* 1996. c-myc activation renders proliferation of Epstein-Barr virus (EBV)-transformed cells independent of EBV nuclear antigen 2 and latent membrane protein 1. *Proceedings of the national academy of sciences of the united states of america*, **93**(19), 10411–6.
- QUINTANILLA-MARTINEZ, L., DAVIES-HILL, T., FEND, F., *et al.* 2003. Sequestration of p27Kip1 protein by cyclin D1 in typical and blastic variants of mantle cell lymphoma (MCL): implications for pathogenesis. *Blood*, **101**(8), 3181–7.

-
- RAHL, P. B., LIN, C. Y., SEILA, A. C., *et al.* 2010. c-Myc regulates transcriptional pause release. *Cell*, **141**(3), 432–45.
- RAWLINGS, J. S., ROSLER, K. M., & HARRISON, D. A. 2004. The JAK/STAT signaling pathway. *Journal of cell science*, **117**(Pt 8), 1281–3.
- RENART, J., REISER, J., & STARK, G. R. 1979. Transfer of proteins from gels to diazobenzylxymethyl-paper and detection with antisera: a method for studying antibody specificity and antigen structure. *Proceedings of the national academy of sciences of the united states of america*, **76**(7), 3116–20.
- RHODES, D. R., YU, J., SHANKER, K., *et al.* 2004. ONCOMINE: a cancer microarray database and integrated data-mining platform. *Neoplasia (new york, n.y.)*, **6**(1), 1–6.
- RICHARDS, S., WATANABE, C., SANTOS, L., CRAXTON, A., & CLARK, E. A. 2008. Regulation of B-cell entry into the cell cycle. *Immunological reviews*, **224**(aug), 183–200.
- RICHTER, J., SCHLESNER, M., HOFFMANN, S., *et al.* 2012. Recurrent mutation of the ID3 gene in Burkitt lymphoma identified by integrated genome, exome and transcriptome sequencing. *Nature genetics*, **44**(12), 1316–1320.
- ROUSSET, F., GARCIA, E., DEFRANCE, T., *et al.* 1992. Interleukin 10 is a potent growth and differentiation factor for activated human B lymphocytes. *Proceedings of the national academy of sciences of the united states of america*, **89**(5), 1890–3.
- ROZOVSKI, U., GRGUREVIC, S., BUESO-RAMOS, C., *et al.* 2015. Aberrant LPL Expression, Driven by STAT3, Mediates Free Fatty Acid Metabolism in CLL Cells. *Molecular cancer research : Mcr*, **13**(5), 944–53.
- RUI, L., SCHMITZ, R., CERIBELLI, M., & STAUDT, L. M. 2011. Malignant pirates of the immune system. *Nature immunology*, **12**(10), 933–40.
- SABAT, R., GRÜTZ, G., WARSZAWSKA, K., *et al.* 2010. Biology of interleukin-10. *Cytokine & growth factor reviews*, **21**(5), 331–44.
- SABÒ, A., KRESS, T. R., PELIZZOLA, M., *et al.* 2014. Selective transcriptional regulation by Myc in cellular growth control and lymphomagenesis. *Nature*, **511**(7510), 488–92.
- SANCHEZ-IZQUIERDO, D., BUCHONNET, G., SIEBERT, R., *et al.* 2003. MALT1 is deregulated by both chromosomal translocation and amplification in B-cell non-Hodgkin lymphoma. *neoplasia*, **101**(11), 4539–4546.
- SANDER, S., CALADO, D. P., SRINIVASAN, L., *et al.* 2012. Synergy between PI3K signaling and MYC in Burkitt lymphomagenesis. *Cancer cell*, **22**(2), 167–79.
- SCHAADT, M., DIEHL, V., STEIN, H., FONATSCH, C., & KIRCHNER, H. H. 1980. Two neoplastic cell lines with unique features derived from Hodgkin’s disease. *International journal of cancer*, **26**(6), 723–31.

-
- SCHEEREN, F. A., DIEHL, S. A., SMIT, L. A., *et al.* 2008. IL-21 is expressed in Hodgkin lymphoma and activates STAT5: evidence that activated STAT5 is required for Hodgkin lymphomagenesis. *Blood*, **111**(9), 4706–15.
- SCHMITZ, ROLAND, YOUNG, RYAN M, CERIBELLI, MICHELE, *et al.* 2012. Burkitt lymphoma pathogenesis and therapeutic targets from structural and functional genomics. *Nature*, **490**(7418), 116–20.
- SCHNEIDER, I. 1972. Cell lines derived from late embryonic stages of *Drosophila melanogaster*. *Journal of embryology and experimental morphology*, **27**(2), 353–65.
- SCHRADER, A., MEYER, K., VON BONIN, F., *et al.* 2012a. Global gene expression changes of in vitro stimulated human transformed germinal centre B cells as surrogate for oncogenic pathway activation in individual aggressive B cell lymphomas. *Cell communication and signaling : Ccs*, **10**(1), 43.
- SCHRADER, A., BENTINK, S., SPANG, R., *et al.* 2012b. High Myc activity is an independent negative prognostic factor for diffuse large B cell lymphomas. *International journal of cancer. journal internationale du cancer*, **131**(4), E348–61.
- SCHUHMACHER, M., STAEGE, M. S., PAJIC, A., *et al.* 1999. Control of cell growth by c-Myc in the absence of cell division. *Current biology : Cb*, **9**(21), 1255–8.
- SCUTO, A., KUJAWSKI, M., KOWOLIK, C., *et al.* 2011. STAT3 inhibition is a therapeutic strategy for ABC-like diffuse large B-cell lymphoma. *Cancer research*, **71**(9), 3182–8.
- SEARS, R. 2000. Multiple Ras-dependent phosphorylation pathways regulate Myc protein stability. *Genes & development*, **14**(19), 2501–2514.
- SEHN, LAURIE H. 2010. A decade of R-CHOP. *Blood*, **116**(12), 2000–1.
- SLACK, GRAHAM W, & GASCOYNE, RANDY D. 2011. MYC and aggressive B-cell lymphomas. *Advances in anatomic pathology*, **18**(3), 219–28.
- SMITH, T. J. 2010. Insulin-like growth factor-I regulation of immune function: a potential therapeutic target in autoimmune diseases? *Pharmacological reviews*, **62**(2), 199–236.
- STEVENS, A. P., DETTMER, K., KIROVSKI, G., *et al.* 2010. Quantification of intermediates of the methionine and polyamine metabolism by liquid chromatography-tandem mass spectrometry in cultured tumor cells and liver biopsies. *Journal of chromatography a*, **1217**(19), 3282–3288.
- SULLIVAN, L. B., GUI, D. Y., HOSIOS, A. M., *et al.* 2015. Supporting Aspartate Biosynthesis Is an Essential Function of Respiration in Proliferating Cells. *Cell*, **162**(3), 552–63.
- SUN, M., SCHWALB, B., SCHULZ, D., *et al.* 2012. Comparative dynamic transcriptome analysis (cDTA) reveals mutual feedback between mRNA synthesis and degradation. *Genome research*, **22**(7), 1350–9.
- TORGBOR, C., AWUAH, P., DEITSCH, K., *et al.* 2014. A multifactorial role for *P. falciparum* malaria in endemic Burkitt's lymphoma pathogenesis. *Plos pathogens*, **10**(5), e1004170.

-
- TOWBIN, H., STAEBELIN, T., & GORDON, J. 1979. Electrophoretic transfer of proteins from polyacrylamide gels to nitrocellulose sheets: procedure and some applications. *Proceedings of the national academy of sciences of the united states of america*, **76**(9), 4350–4.
- TWEEDDALE, M. E., LIM, B., JAMAL, N., *et al.* 1987. The presence of clonogenic cells in high-grade malignant lymphoma: a prognostic factor. *Blood*, **69**(5), 1307–14.
- VALLABHAPURAPU, S., & KARIN, M. 2009. Regulation and function of NF- κ B transcription factors in the immune system. *Annual review of immunology*, **27**, 693–733.
- VAN DEN HEUVEL, A. P. J., JING, J., WOOSTER, R. F., & BACHMAN, K. E. 2012. Analysis of glutamine dependency in non-small cell lung cancer: GLS1 splice variant GAC is essential for cancer cell growth. *Cancer biology & therapy*, **13**(12), 1185–94.
- VAN DER GOOT, A. T., ZHU, W., VÁZQUEZ-MANRIQUE, R. P., *et al.* 2012. Delaying aging and the aging-associated decline in protein homeostasis by inhibition of tryptophan degradation. *Proceedings of the national academy of sciences of the united states of america*, **109**(37), 14912–7.
- VANDER HEIDEN, M. G., PLAS, D. R., RATHMELL, J. C., *et al.* 2001. Growth factors can influence cell growth and survival through effects on glucose metabolism. *Molecular and cellular biology*, **21**(17), 5899–912.
- VANDER HEIDEN, M. G., LUNT, S. Y., DAYTON, T. L., *et al.* 2011. Metabolic pathway alterations that support cell proliferation. *Cold spring harbor symposia on quantitative biology*, **76**(jan), 325–34.
- WANG, R., DILLON, C. P., SHI, L. Z., *et al.* 2011. The transcription factor Myc controls metabolic reprogramming upon T lymphocyte activation. *Immunity*, **35**(6), 871–82.
- WARBURG, O. 1956. On the origin of cancer cells. *Science (new york, n.y.)*, **123**(3191), 309–14.
- WEGRZYN, J., POTLA, R., CHWAE, Y.-J., *et al.* 2009. Function of mitochondrial Stat3 in cellular respiration. *Science (new york, n.y.)*, **323**(5915), 793–7.
- WENIGER, M. A., MELZNER, I., MENZ, C. K., *et al.* 2006. Mutations of the tumor suppressor gene SOCS-1 in classical Hodgkin lymphoma are frequent and associated with nuclear phospho-STAT5 accumulation. *Oncogene*, **25**(18), 2679–84.
- WHITFIELD, M. L., GEORGE, L. K., GRANT, G. D., & PEROU, C. M. 2006. Common markers of proliferation. *Nature reviews. cancer*, **6**(2), 99–106.
- WISE, D. R., DEBERARDINIS, R. J., MANCUSO, A., *et al.* 2008. Myc regulates a transcriptional program that stimulates mitochondrial glutaminolysis and leads to glutamine addiction. *Proceedings of the national academy of sciences*, **105**(48), 18782–18787.
- WOOD, K. M., ROFF, M., & HAY, R. T. 1998. Defective IkappaBalpha in Hodgkin cell lines with constitutively active NF-kappaB. *Oncogene*, **16**(16), 2131–9.

-
- WU, Z. L., SONG, Y. Q., SHI, Y. F., & ZHU, J. 2011. High nuclear expression of STAT3 is associated with unfavorable prognosis in diffuse large B-cell lymphoma. *Journal of hematology & oncology*, **4**(1), 31.
- XIANG, Y., STINE, Z. E., XIA, J., *et al.* 2015. Targeted inhibition of tumor-specific glutaminase diminishes cell-autonomous tumorigenesis. *The journal of clinical investigation*, **125**(6), 2293–306.
- YANG, J.-H., LI, J.-H., JIANG, S., ZHOU, H., & QU, LIANG-HU. 2013. ChIPBase: a database for decoding the transcriptional regulation of long non-coding RNA and microRNA genes from ChIP-Seq data. *Nucleic acids research*, **41**(Database issue), D177–87.
- YOON, S.-O., ZHANG, X., BERNER, P., & CHOI, Y. S. 2009. IL-21 and IL-10 have redundant roles but differential capacities at different stages of Plasma Cell generation from human Germinal Center B cells. *Journal of leukocyte biology*, **86**(6), 1311–8.
- YOSHIMURA, A. 2009. Regulation of cytokine signaling by the SOCS and Spred family proteins. *The keio journal of medicine*, **58**(2), 73–83.
- ZECH, L., HAGLUND, U., NILSSON, K., & KLEIN, G. 1976. Characteristic chromosomal abnormalities in biopsies and lymphoid-cell lines from patients with Burkitt and non-Burkitt lymphomas. *International journal of cancer*, **17**(1), 47–56.
- ZHAO, B., BARRERA, L. A., ERSING, I., *et al.* 2014. The NF- κ B Genomic Landscape in Lymphoblastoid B Cells. *Cell reports*, **8**(5), 1595–1606.
- ZHAO, Q., FU, W., JIANG, H., *et al.* 2015. Clinicopathological implications of nuclear factor κ B signal pathway activation in diffuse large B-cell lymphoma. *Human pathology*, **46**(4), 524–31.
- ZHU, W., STEVENS, A. P., DETTMER, K., *et al.* 2011. Quantitative profiling of tryptophan metabolites in serum, urine, and cell culture supernatants by liquid chromatography-tandem mass spectrometry. *Analytical and bioanalytical chemistry*, **401**(10), 3249–3261.
- ZIPPER, H., BRUNNER, H., BERNHAGEN, J., & VITZTHUM, F. 2004. Investigations on DNA intercalation and surface binding by SYBR Green I, its structure determination and methodological implications. *Nucleic acids research*, **32**(12), e103.

7 Appendix

Table 27: Gene Set Enrichment in KEGG Pathways of only IL10+CpG stimulation regulated genes.

Term	PValue	Genes
hsa04060: Cytokine-cytokine receptor interaction	1.59E-5	IL6, CCL3, IL2RA, IL21R, IL24, CD40, CX3CL1, CCL4, CCL17, CXCL10, ZFP91, TNFRSF9, CCL22, CCR7, CXCR5, CCL3L3, CCR2, IL12A, TNFRSF18, TNFRSF19, IL15RA, IL12B, IL13RA1, LTB
hsa04630: Jak-STAT signaling pathway	1.80E-4	IL6, IL2RA, SOCS2, SOCS3, GRB2, STAT5A, IL21R, PIM1, IL24, STAT3, ZFP91, CCND2, IL12A, IL15RA, IL12B, IL13RA1
hsa04620: Toll-like receptor signaling pathway	4.91E-4	CD86, CCL3, IL6, CD80, JUN, IL12A, NFKB1, MAPK11, IL12B, CD40, CCL4, CXCL10
hsa04062: Chemokine signaling pathway	0.0093	CCL3, BRAF, GRB2, NFKB1, CX3CL1, CCL4, STAT3, CCL17, CXCL10, CCL22, CCR7, CXCR5, CCL3L3, CCR2
hsa05221: Acute myeloid leukemia	0.0122	BRAF, GRB2, STAT5A, PIM1, NFKB1, MTOR, STAT3
hsa04514: Cell adhesion molecules (CAMs)	0.0318	ALCAM, CD86, CD80, PECAM1, CD58, VCAN, CD40, HLA-DMB, CD226, PDCD1LG2

Table 28: Gene Set Enrichment in KEGG Pathways of only Myc regulated genes.

Term	PValue	Genes
hsa03010: Ribosome	0.0061	RPS18, RPL18A, RPL6, RPL15, RPL4P5, RPS15A, RPL38, RPS4X, RPL13AP5
hsa00052: Galactose metabolism	0.0482	GALK1, B4GALT2, GALE, PFKM
hsa00250: Alanine, aspartate and glutamate metabolism	0.0444	GLUL, ASS1, ALDH5A1, GPT2

Table 29: Gene Set Enrichment in KEGG Pathways of IL10+CpG stimulation and Myc regulated genes.

Term	PValue	Genes
hsa04110: Cell cycle	3.37E-11	E2F3, DBF4, PRKDC, TTK, CHEK1, CHEK2, RBX1, CCNE1, CDC45, MCM7, BUB1, CCNA2, BUB3, TFDP1, CDC7, ANAPC1, CDC6, ANAPC5, RBL1, SKP2, CDC23, CDK6, MCM2, MCM3, CDK4, YWHAE, MCM4, CDC25A, CCNB1, YWHAG, YWHAH, CCNB2, BUB1B, ANAPC7, SMC1A
hsa00240: Pyrimidine metabolism	5.79E-7	POLR3G, POLR2G, POLR1E, POLR3K, DTYMK, POLR1A, POLA1, POLR1C, POLR3A, CTPS2, CAD, POLR1B, POLR2D, POLR3B, PNP, POLD3, NME2, POLE2, POLE3, RRM2, POLD1, DHODH, UCK1, UCK2
hsa00970: Aminoacyl-tRNA biosynthesis	1.20E-6	CARS, YARS, SARS, AARS, WARS2, QARS, DARS2, LARS2, KARS, EARS2, IARS, FARSB, MARS2, AARS2, MARS
hsa00230: Purine metabolism	1.36E-5	POLR2G, POLA1, POLR2D, PNP, PFAS, PPAT, POLE2, ATIC, POLE3, IMPDH2, POLR3G, POLR1E, POLR3K, POLR1A, AK2, POLR3A, POLR1C, POLR1B, AK7, GMPS, POLR3B, GART, POLD3, NME2, RRM2, POLD1, PAICS, PRPS2, PRPS1
hsa03040: Spliceosome	2.88E-5	DHX8, PRPF31, PPIL1, CWC15, ZMAT2, SNRPB2, SNRPD2, PRPF4, RBMX, HNRNPA1, SF3A3, PPIH, AQR, TCERG1, USP39, SNRNP200, LSM5, DHX16, SNRNP40, PHF5A, HNRNPC, THOC3, SNRPE, HSPA8, PRPF38A
hsa00010: Glycolysis / Gluconeogenesis	3.68E-5	LDHA, PFKL, ALDOC, PGAM1, HK2, PFKP, HK1, DLAT, TPI1P1, GPI, AKR1A1, ALDH1B1, PGAM4, PGM1, PDHA1, ENO1
hsa03030: DNA replication	5.61E-5	POLD3, RFC5, MCM7, POLE2, POLE3, RFC2, POLD1, POLA1, MCM2, MCM3, RNASEH2A, MCM4
hsa00030: Pentose phosphate pathway	6.37E-5	GPI, TALDO1, PFKL, ALDOC, PGM1, PGD, PFKP, RPIA, PRPS2, PRPS1

hsa03020: RNA polymerase	1.74E-4	POLR3G, POLR2G, POLR3K, POLR1E, POLR1A, POLR1C, POLR3A, POLR1B, POLR2D, POLR3B
hsa03410: Base excision repair	2.28E-4	POLD3, HMGB1, POLE2, POLE3, UNG, NEIL3, POLD1, NEIL2, NTHL1, APEX1, PARP2
hsa00020: Citrate cycle (TCA cycle)	4.12E-4	SDHA, SDHB, ACO2, ACO1, IDH2, IDH3B, ACLY, PDHA1, DLAT, IDH3A
hsa00450: Selenoamino acid metabolism	5.62E-4	CTH, SEPHS1, AHCY, MAT2A, WBSCR22, MARS2, METTL2B, MARS, CBS
hsa00670: One carbon pool by folate	8.76E-4	MTHFD1, SHMT1, DHFR, ATIC, MTR, MTHFD1L, GART
hsa03430: Mismatch repair	0.0013	POLD3, RFC5, EXO1, MSH6, RFC2, POLD1, MLH1, PMS2
hsa03420: Nucleotide excision repair	0.0016	POLD3, RFC5, GTF2H2C, POLE2, POLE3, RFC2, POLD1, CETN2, GTF2H3, ERCC3, RBX1, GTF2H2B
hsa00190: Oxidative phosphorylation	0.0023	NDUFA4, COX7A2, UQCRC1, ATP5B, NDUFB9, ATP6V1B2, ATP5G1, COX5A, NDUFA10, UQCRQ, ATP5G3, PPA1, SDHA, NDUFV3, SDHB, NDUFV1, ATP5C1, ATP5A1, NDUF3S, ATP5H, NDUF51
hsa00270: Cysteine and methionine metabolism	0.0037	GOT2, CTH, LDHA, AHCY, GOT1, MAT2A, MTR, ENOPH1, CBS
hsa00051: Fructose and mannose metabolism	0.0037	GMPPB, SORD, PFKL, ALDOC, AKR1B1, HK2, PFKP, HK1, TPI1P1
hsa00520: Amino sugar and nucleotide sugar metabolism	0.0058	GMPPB, GPI, NANS, GNE, GNPAT1, PGM1, HK2, HK1, UXS1, NANP
hsa00100: Steroid biosynthesis	0.0078	EBP, CYP27B1, SQLE, LSS, FDFT1, NSDHL
hsa00260: Glycine, serine and threonine metabolism	0.0084	SHMT1, CTH, GCAT, PHGDH, PSAT1, PSPH, CBS, GLDC
hsa03022: Basal transcription factors	0.0164	TAF2, TAF5L, GTF2H2C, TAF5, GTF2F1, GTF2A2, TAF9B, GTF2H3, GTF2H2B
hsa03010: Ribosome	0.0359	RPL7AP66, RPSAP15, RPLP0, RPL8, RPL3, RPL26L1, RPL4P4, RPL21P119, RPS10, RPL4, RPL10A, RPS6, RPS8, RPS24

Table 30: Linear regression coefficients of stimuli and stimuli interactions on number of cells in S-phase. Values are shown in percentage of total cell population.

Stimulation	S-Phase
Ctrl	4.86
CD40L	4.48
BCR	12.09
IGF	6.32
CpG	22.02
IL10	11.25
CD40L:BCR	-8.10
CD40L:IGF	10.46
CD40L:CpG	-4.97
CD40L:IL10	3.08
BCR:IGF	-8.01
BCR:CpG	3.40
BCR:IL10	-10.08
IGF:CpG	-8.89
IGF:IL10	5.92
CpG:IL10	3.38
R^2	0.98

Table 31: Distribution of cell cycle phases in BrdU labeled cells over time. Shown are percentage of total population of BrdU positive cells.

time	G0/G1				S				G2/M			
	ctrl	IL10	CpG	IL10+ CpG	ctrl	IL10	CpG	IL10+ CpG	ctrl	IL10	CpG	IL10 CpG
0h	20.68	19.26	29.3	50.8	40.09	37.81	45.18	35.83	40.3	43.29	26.02	14.2
2h	21.13	19.11	27.22	24.21	33.54	38.4	44.53	55.18	46.25	43.23	29.44	21.57
4h	23.43	22.37	16.82	22.83	32.22	33.18	49.22	55.27	45.19	44.89	35.19	22.93
6h	38.08	33.41	20.71	12.43	26.47	33.6	50.14	48.86	36.69	34.02	30.15	39.39
8h	41.23	40.04	16.38	13.93	25.15	31.91	29.72	25.35	34.8	28.66	54.88	61.68
10h	50.45	45.36	25.21	21.91	21.11	24.69	28.49	20.2	29.6	29.95	46.99	58.63
12h	57.89	50.27	29.32	44.5	20.25	20.93	27.21	9.95	22.36	29.45	44.22	45.91
24h	79.11	75.14	74.99	52.65	10.39	12.36	14.78	30.01	11.24	13.5	10.83	18.11

Table 32: Linear regression analysis of cell cycle regulator gene expression. Shown are the intercept, the regression coefficients of single stimuli and the interaction term of IL10:CpG. p-Values below 0.05 are regarded as significant effects on gene expression.

CCND2	Estimate	Std.Error	t-value	p-value
(Intercept)	1.0833	0.499	2.171	0.0617
IL10	0.7197	0.7057	1.02	0.3377
CpG	1.8497	0.7057	2.621	0.0306
IL10:CpG	1.9213	0.998	1.925	0.0904
CCND3	Estimate	Std.Error	t-value	Pr(> t)
(Intercept)	0.9003	0.2545	3.537	0.00765
IL10	0.6684	0.3599	1.857	0.10042
CpG	0.4645	0.3599	1.29	0.23296
IL10:CpG	1.5735	0.509	3.091	0.01487
CDK4	Estimate	Std.Error	t-value	Pr(> t)
(Intercept)	0.9832	0.4403	2.233	0.05605
IL10	0.7905	0.6227	1.269	0.24
CpG	2.0104	0.6227	3.228	0.01209
IL10:CpG	3.6281	0.8807	4.12	0.00335
CDK6	Estimate	Std.Error	t-value	Pr(> t)
(Intercept)	1.0705	0.505	2.12	0.0668
IL10	1.182	0.7141	1.655	0.1365
CpG	2.0624	0.7141	2.888	0.0203
IL10:CpG	2.7617	1.0099	2.734	0.0257
p21	Estimate	Std.Error	t-value	Pr(> t)
(Intercept)	1.00342	0.25785	3.891	0.0046
IL10	0.67142	0.36466	1.841	0.1029
CpG	0.53729	0.36466	1.473	0.1789
IL10:CpG	-0.08255	0.5157	-0.16	0.8768
p27	Estimate	Std.Error	t-value	Pr(> t)
(Intercept)	1.0882	0.2752	3.954	0.00421
IL10	0.3634	0.3892	0.934	0.37776
CpG	-0.2429	0.3892	-0.624	0.54989
IL10:CpG	0.5135	0.5504	0.933	0.37819

Digitally provided data:

To due their length, the following tables are provided as supplementary data on compact disc (CD):

- **Supplemental Table 1:** Linear regression coefficients of stimulation induced gene expression in Myc^{low} cells.
- **Supplemental Table 2:** Linear regression coefficients of stimulation induced metabolic changes in Myc^{low} cells.
- **Supplemental Table 3:** S-phase and metabolites of stimulated Myc^{low} cells and Myc^{high} cells.
- **Supplemental Table 4:** Log2FC gene expression of IL10, CpG, IL10+CpG stimulated Myc^{low} cells and unstimulated Myc^{high} cells relative to unstimulated Myc^{low} cells.

8 Curriculum Vitae

MAREN FEIST NÉE SCHMIDT

Personal Information

Date of birth	October 30th, 1987
Place of birth	Salzgitter-Bad (Germany)
Nationality	German
Email	maren.feist@med.uni-goettingen.de

Education

01/2013 till present	<p>Ph.D. program “Molecular Medicine“ at the University Medical Center of the Georg-August University of Göttingen Project titel of the thesis <i>“Identification of a new synergy of IL10 and TLR9 signaling on global gene expression, proliferation and metabolism in Myc depleted B cells“</i> (Clinic of Haematology and Medical Oncology, UMG Göttingen)</p>
10/2010 - 09/2012	<p>Master course “Molecular Life Science“ At the University Lübeck, Germany Titel of the master thesis: <i>“Production of monoclonal antibodies against mycobac- terial antigens for differential diagnosis of tuberculosis“</i> (Lionex Diagnostic and Therapeutics GmbH, Braun- schweig)</p>
10/2007 - 09/2010	<p>Bachelor course “Molecular Life Science “ At the University Lübeck, Germany Titel of the bachelor thesis: <i>“Development and regeneration of in vitro cultivated spontaneously contracting cardiomyogenic aggregates from rainbow trout larvae.“</i> (Fraunhofer EMB, Lübeck)</p>
09/2000 - 07/2007	<p>Abitur (A-levels) Jacobson-Gymnasium Seesen, Germany</p>

Working experience

- Since 01/2013** Scientific assistant
at the University Medical Center Göttingen
(Medical hematology and oncology, Prof. Kube)
- 10/2012 - 12/2012** Scientific assistant
at the Lionex Diagnostic and Therapeutics GmbH,
Braunschweig
- 04/2012 - 09/2012** Laboratory internship
*“Production of monoclonal antibodies against mycobac-
terial antigens“*
at the Lionex Diagnostic and Therapeutics GmbH,
Braunschweig (Prof. Singh)
- 12/2011 - 02/2012** Laboratory internship
“Analysis of cerebellar ataxia in zebrafish“
at the zoological institute, TU Braunschweig
(cellular and molecular neurobiology group, Prof.
Köster)
- 09/2011 - 11/2011** Laboratory internship
*“Regulation of differentiation in cutaneous T cell lym-
phoma“*
at the DSMZ, Braunschweig
(Human and animal cell lines team, Dr. MacLeod)
- 08/2010 - 08/2011** Student research assistant
at Fraunhofer EMB, Lübeck
(Aquatic cell technology team)
- 03/2010 - 06/2010** Laboratory internship
*“Cultivation of spontaneously contracting cardiomyo-
genic aggregates from rainbow trout larvae“*
at the Fraunhofer EMB, Lübeck
(Aquatic cell technology team, Dr. Grunow)

Additional Skills

- Language skills:** German native speaker
English fluent (spoken and written)
- EDV skills:** Microsoft Office (Word, Excel, PowerPoint), Graph Pad,
'R'

Awards and Honours

Best student of the year 2012/2013 of the “Molecular Life Science“master course at the University Lübeck.

List of publications

Original Articals

EHRENTRAUT S., SCHNEIDER B., NAGEL S., POMMERENKE C., QUENTMEIER H., GEFERS R., FEIST M., KAUFMANN M., MEYER C., KADIN M. E., DREXLER H. G., MACLEOD R.A.F. 2016. Th17 cytokine differentiation and loss of plasticity after SOCS1 inactivation in a cutaneous T-cell lymphoma. *Oncotarget*.

SCHRADER A., MEYER K., WALTHER N., STOLZ A., FEIST M., HAND E., VON BONIN F., EVER M., KOHLER C., SHIRNESHAN K., VOCKERODT M., KLAPPER W., SZCZEPANOWSKI M., MURRAY P.G., BASTIANS H., TRÜMPER L., SPANG R., KUBE D.. 2016. Identification of a new gene regulatory circuit involving B cell receptor activated signaling using a combined analysis of experimental, clinical and global gene expression data. *Oncotarget*.

FEIST M., KEMPER J., TARUTTIS F., REHBERG T. , ENGELMANN J. C., GRONWALD W., HUMMEL M., SPANG R., KUBE D. . 2016. Synergy of Interleukin 10 and Toll-like receptor 9 signaling in B cell proliferation: implications for lymphoma pathogenesis. *International Journal of Cancer: in revision*.

SCHWARZFISCHER P., REINDERS J., DETTMER K., KLEO K., DIMITROVA L., HUMMEL M., FEIST M., KUBE D., SZCZEPANOWSKI M., KLAPPER W., TARUTTIS F., ENGELMANN J., SPANG R., GRONWALD W., OEFNER P. J.. 2016. Comprehensive metabolo-proteomics of Burkitt and diffuse large B-cell lymphoma cell lines and primary tumor tissues. *Journal of Proteome Research: in revision*.

TARUTTIS F., FEIST M., SCHWARZFISCHER P., GRONWALD W., KUBE D., SPANG R., ENGELMANN J. C.. 2016. Whole cell spike-ins calibrate RNA-seq and qPCR data to an external reference point and uncover unbalanced gene expression changes. *Submitted*.

FEIST M., SCHWARZFISCHER P., HEINRICH P., TARUTTIS F., PEREZ-RUBIO P., ENGELMANN J. C., KEMPER J., DUDEK J., SPANG R., HUMMEL M., DETTMER-WILDE K., GRONWALD W., KUBE D.. 2016. Metabolic shifts toward glutamine in lymphoma: context dependent expression of GOT2 and use of metabolic derivatives. *In preparation*.

Congress participation

FEIST M., SCHWARZFISCHER P., DUDEK J., DETTMER-WILDE K., GRONWALD W., TARUTTIS F., ENGELMANN J., SPANG R., KUBE D.. 2016. Synergism of STAT3 and NF- κ B promotes cell proliferation involving glutaminolysis in B cells with low expression of the protooncogene c-Myc. Poster presentation at the Keystone Symposia “New Frontiers in Understanding Tumor Metabolism“, Calgary (Canada), February 21-25.

SCHMIDT M., TARUTTIS F., ENGELMANN J., SPANG R., KUBE D.. 2015. Global transcriptional amplification by Myc in B lymphocytes: an assay to detect selective up- and downregulation of specific Myc target genes. Poster presentation at the 13th B Cell Forum of German Society for Immunology, Hitzacker (Germany), February 19-21 .